Escuela Técnica Superior de Ingenieros de Caminos, Canales y Puertos.
UNIVERSIDAD DE CANTABRIA

INDETERMINATION ACCORDING TO EUROPEAN STANDARD REGARDING THE MEASUREMENT OF IMPACT ATTENUATION IN HIGH SPEED RAIL FASTENING SYSTEMS

TRABAJO FINAL DE GRADO

Trabajo realizado por:
Alicia Barrientos Febrero

Dirigido:
José Antonio Casado del Prado
Isidro Carrascal
Soraya Diego Cavia

Titulación:
Grado en Ingeniería Civil

Santander, junio 2018

Title: Indetermination according to the European Standard regarding the measurement of impact attenuation in high speed rail fastening systems.
Author: Alicia Barrientos Febrero.
Directors: José Antonio Casado del Prado, Isidro Alfonso Carrascal Vaquero, Soraya Diego Cavia.
Call: June 2018.
Keywords: Attenuation, impact, high speed, fastening system, railway, rail pad, elastic pad.
Abstract: This work came up when a comparison of impact attenuation for high speed railway pads results was made between Laboratorio de la División de Ciencia e Ingeniería de los Materiales (LADICIM) and another lab, both following the EN 13146-3:2012. Some of the results differed in more than 100% when obtained by different methods, both contemplated by the Standard. It was then decided to revise the methodology described in the Standard, in which impacts are performed by a mass going through a guideway by free fall in order to simulate loads originated by the traffic in the rail. The Standard presents two methods in order to test impact attenuation. In both methods, strain in the sleeper is measured by strain gauges. In the reference method, the impact is produced in a complete assembly where the sleeper is embedded in ballast. For the alternative method, a 50 kN preload is applied and maintained by means of springs, with the system over an elastomeric mat with the stiffness required. Then the free fall of the guided mass is carried out.

Figure 1. Comparison between the reference and alternative method

In this final Project, the necessary devices in order to perform tests for both methods have been designed and fabricated.
Another variable taken into account in order to perform this comparison is the rail pad, situated between the sleeper and the rail. Before the impact tests, the static and dynamic stiffness and the hardness of the material have been calculated.
The attenuation results for both methods are calculated following the same process, measuring the strain of the fibres in the sleeper in the upper and the lower part.

With this purpose, a rigid reference pad is used, and the results are compared with the ones obtained by the test pad. The result obtained is the mean attenuation between the upper and the lower gauge, as a percentage compared with the reference pad. The calculations are done following these formulas:

$$a^i_{\text{inf}} = 100\left(1 - \frac{\varepsilon^i_{mu,\text{inf}} - \varepsilon^i_{e,mu,\text{inf}}}{\varepsilon_{rf,\text{inf}} - \varepsilon_{e,rf,\text{inf}}}\right) \qquad a^i_{\text{sup}} = 100\left(1 - \frac{\varepsilon^i_{mu,\text{sup}} - \varepsilon^i_{e,mu,\text{sup}}}{\varepsilon_{rf,\text{sup}} - \varepsilon_{e,rf,\text{sup}}}\right)$$

Where:

- $\varepsilon_{\text{rf,sup/inf}}$: Mean of the maximum individual strain ($\varepsilon^{\text{i}}_{\text{rf,sup/inf}}$) in the upper/lower part of the sleeper with the reference pad.
- $\varepsilon_{\text{e,rf,sup/inf}}$: mean of the static individual strain ($\varepsilon^{\text{i}}_{\text{e,rf,sup/inf}}$) in the upper/lower part of the sleeper with the reference pad.
- $\varepsilon^{\text{i}}_{\text{mu,sup/inf}}$: Mean of the maximum individual strain in the upper/lower part of the sleeper with the reference pad.
- $\varepsilon^{\text{i}}_{\text{e,mu,sup/inf}}$: Static individual strain ($\varepsilon^{\text{i}}_{\text{e,mu,sup/inf}}$)in the upper/lower part of the sleeper with the tested pad.
-

The diagram in figure 2 shows an example of the comparison of the strain values with a reference and a test pad.

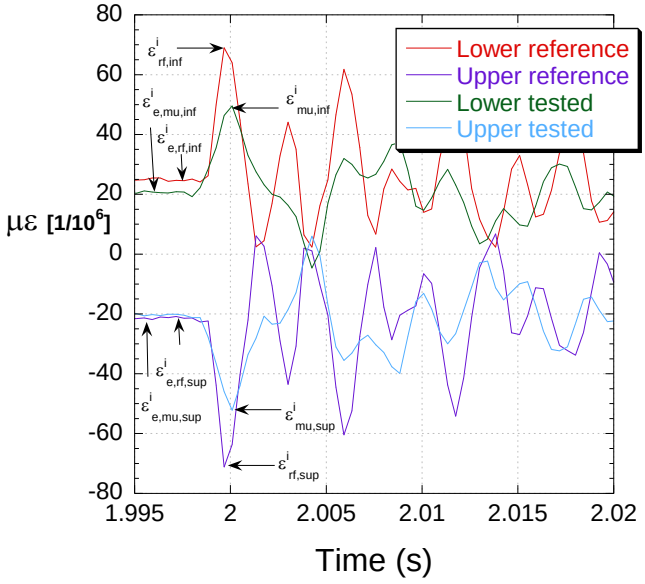

Figure 2. Evolution of the strain in the sleeper

Results and conclusions:

The table shows the stiffness results and hardness for the 7 elastic pads evaluated (identified from A to G). They differ in geometry, material and thickness.

PAD	Static stiffness, k_e (18-68 kN) [kN/mm]	Dynamic stiffness 5 Hz, $k_{d\ 5Hz}$ [kN/mm]	Dynamic rigidity 10 Hz, $k_{d\ 10Hz}$ [kN/mm]	Dynamic rigidity 20 Hz, $k_{d\ 20Hz}$ [kN/mm]	Dynamic rigidity media, k_{dm} [kN/mm]	Shore Hardness D
0 (ref)	694.4	1282.1	1362.4	1572.3	1405.6	49.8
A	53.5	106.4	116.0	134.4	118.9	7.0
B	65.8	183.8	199.2	229.4	204.1	---
C	68.5	93.1	97.3	110.6	100.3	29.8
D	35.5	90.6	94.7	106.8	97.4	22
E	126.9	162.9	169.5	188.0	173.5	44.6
F	140.8	320.5	344.8	387.6	351.0	50.1
G	284.1	490.0	515.5	588.2	531.2	27.0

Regarding impact attenuation, the reference method does not give the same results as the alternative method. However, for low preloads or no preload using the alternative method they converge, as it can be appreciated in figure 3.

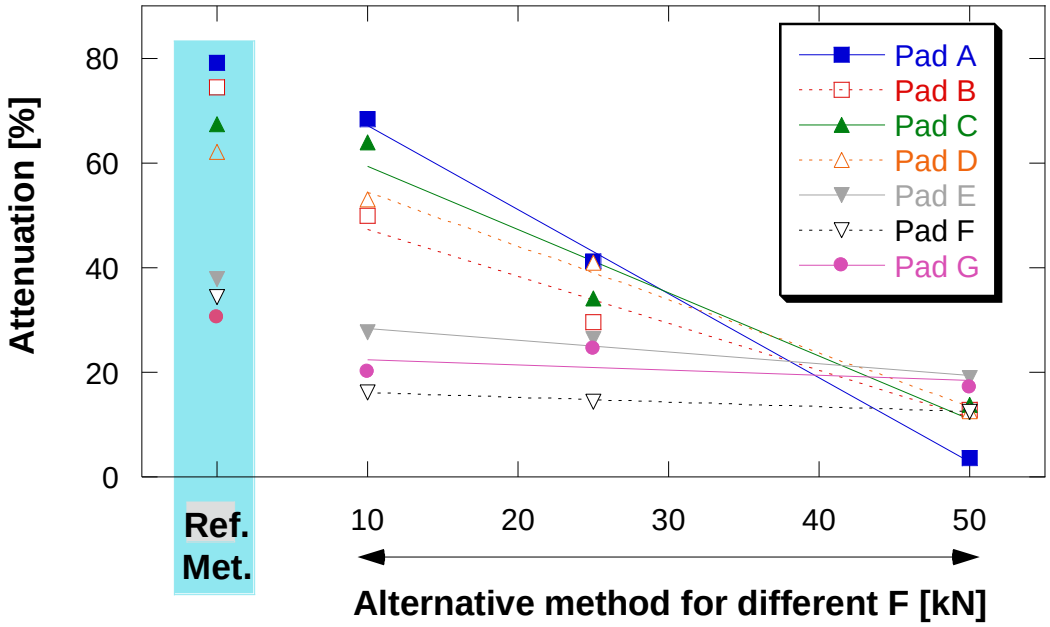

Figure 3. Comparative of attenuation

It is important to remark that the results obtained for the attenuation if the reference method is used, increase when the stiffness and hardness of the pad

decrease. However, this tendency is inverted when the alternative method is used, because of the 5-ton preload that the alternative method has.
The alternative method offers more differentiation between the pads due to the fact that the preload shortens its initial attenuation capacity.
The pad with more attenuation capacity for the reference method (pad A) is the one with the lowest attenuation for the alternative method.
Seen the results of this project, there are some proposals to be taken into account when impact attenuation is calculated according to the European Standard. If the Standard in use were maintained, it would be necessary to include, when an impact attenuation test is done, which method is being used to determine it due to the obvious difference in results. Furthermore, when EN 13481-2:2012+A1:2017 establishes a classification of the fastening systems according to its attenuation, it should be advisable to have two different criteria whether reference or alternative method is being used.

Basic bibliography:

- European Committee for Standardization, EN 13146-3: 2012. Railway applications - Track - Test methods for fastening systems - Part 3: Determination of attenuation of impact loads. (2012).
- European Committee for Standardization, EN 13146-9:2009+A1: 2011. Railway applications. Track. Test methods for fastening systems. Part 9: Determination of stiffness., n.d.
- I.A. Carrascal, J.A. Casado, J.A. Polanco, F. Gutiérrez-Solana, Dynamic behaviour of railway fastening setting pads, Eng. Fail. Anal. 14 (2007) 364–373. doi:10.1016/J.ENGFAILANAL.2006.02.003.
- I.A. Carrascal, Optimización y análisis de comportamiento de sistemas de sujección para vías de ferrocarril de alta velocidad española, PhD Thesis, Universidad de Cantabria, 2006.
- I.A. Carrascal, J.A. Casado, S. Diego, J.A. Polanco, J. Martín, A. Pérez, Placa elástica de asiento metálica para alta velocidad, in: X Jornadas Int. Ing. Para Alta Velocidad, 2016: pp. 45–62.
- López Pita, P. Teixeira, F.A. Robusté, High speed and track deterioration: the role of vertical stiffness of the track, Proc. Inst. Mech. Eng. Part F J. Rail Rapid Transit. 218 (2004) 31–40.
- ADIF, ET 03.360.570.0 Placas elásticas de asiento para sujeción VM, (2005).
- Rcmennlko, O.I. Revjew, Determination of dynamic properties of rail pads using an instrumented hammer impact technique, 33 (2005) 3–7.
- European Committee for Standardization, EN 13481-2:2012+A1:2017. Railway applications. Track. Performance requirements for fastening system. Part 2: Fastening system for concrete sleepers., n.d.

Título: Indeterminación según normativa europea en la medida de atenuación frente a impacto en sistemas de sujeción ferroviaria de alta velocidad.
Autora: Alicia Barrientos Febrero.
Directores: José Antonio Casado del Prado, Isidro Alfonso Carrascal Vaquero, Soraya Diego Cavia.
Convocatoria: Junio 2018.
Palabras clave: Atenuación, impacto, amortiguación, alta velocidad, sujeción, ferrocarril, placa asiento.
Planteamiento del problema y desarrollo de la solución adoptada: Este trabajo surge al intercomparar los resultados de atenuación de impactos para placas de asiento de carril en vías de alta velocidad obtenidos por el Laboratorio de la División de Ciencia e Ingeniería de los Materiales (LADICIM) con los obtenidos por otro laboratorio, ambos según la EN 13146-3:2012; y comprobar que los resultados difieren en más de un 100% al ser obtenidos por procedimientos diferentes, ambos aceptados por la normativa. A partir de ese momento se procede a la revisión de la metodología descrita en la norma, en la que se describe cómo sobre un carril fijado a una traviesa se deja caer una masa a modo de simulación de cargas puntuales originadas por el tráfico en la vía. La norma presenta dos métodos para llevar a cabo el ensayo de atenuación frente al impacto. En ambos se mide la deformación producida en la traviesa a través de bandas extensométricas. En el método de referencia, la masa se deja caer sobre el sistema que contempla una traviesa embebida en balasto. Sin embargo, en el método alternativo se aplica una precarga estable, a través de muelles de rigidez conocida, de 50 kN sobre el carril y simultáneamente, con el sistema apoyado sobre una superficie de caucho de rigidez prestablecida, equivalente a la del balasto, se procede a la caída libre de la masa guiada.

Figura 1. Comparación método de referencia y alternativo

En este TFG se han diseñado y fabricado dispositivos de ensayo que cubran las necesidades descritas para realizar la ejecución de las pruebas por ambos métodos. Para llevar a cabo esta comparación también se tiene en cuenta como variable la

placa de asiento, determinando previamente a los ensayos de atenuación tanto su rigidez estática y dinámica, como la dureza del material.
Los cálculos de atenuación, en ambos métodos se realizan de igual manera comparando las deformaciones medidas en la traviesa (en la fibra traccionada inferior y en la comprimida superior). Para ello se emplea una placa de referencia rígida y los resultados obtenidos se comparan con los medidos con las placas objeto de estudio, obteniéndose como resultado la atenuación media entre la banda superior e inferior como un porcentaje con respecto a la placa de referencia. Las atenuaciones se calculan siguiendo las siguientes fórmulas:

$$a^i_{\inf} = 100\left(1 - \frac{\varepsilon^i_{mu,\inf} - \varepsilon^i_{e,mu,\inf}}{\varepsilon_{rf,\inf} - \varepsilon_{e,rf,\inf}}\right) \qquad a^i_{\sup} = 100\left(1 - \frac{\varepsilon^i_{mu,\sup} - \varepsilon^i_{e,mu,\sup}}{\varepsilon_{rf,\sup} - \varepsilon_{e,rf,\sup}}\right)$$

Donde:

- $\varepsilon_{rf,\sup/\inf}$: media de las deformaciones máximas individuales ($\varepsilon^i_{rf,\sup/\inf}$) en la zona superior/inferior de la traviesa con placa de referencia
- $\varepsilon_{e,rf,\sup/\inf}$: media de las deformaciones estáticas individuales ($\varepsilon^i_{e,rf,\sup/\inf}$) en la zona superior/inferior de la traviesa con placa de referencia.
- $\varepsilon^i_{mu,\sup/\inf}$: máxima deformación individual superior/inferior con la placa elástica en estudio
- $\varepsilon^i_{e,mu,\sup/\inf}$: deformación estática individual ($\varepsilon^i_{e,mu,\sup/\inf}$) en la zona superior/inferior de la traviesa con placa de ensayo.

El diagrama de la Figura 2 muestra a modo de ejemplo tipo de la comparación de los valores de las microdeformaciones registradas con una placa de referencia y otra de ensayo.

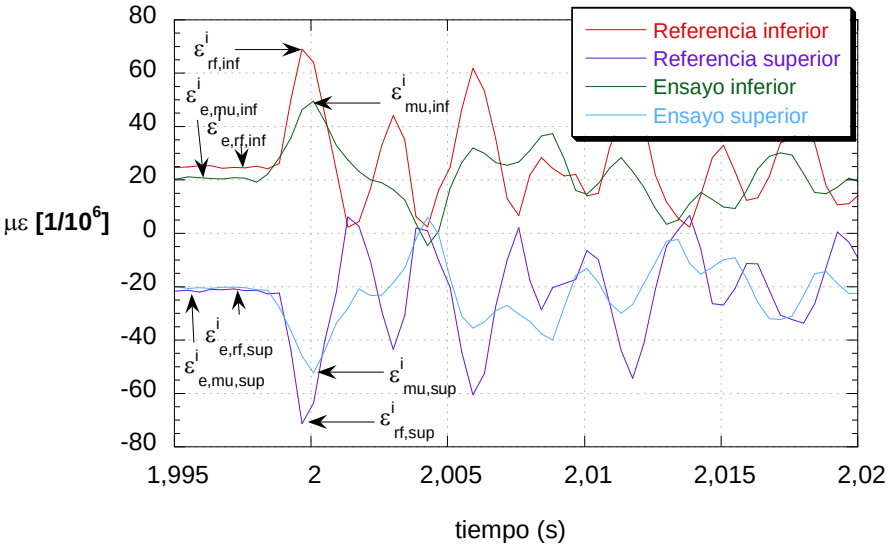

Figura 2.- Evolución de las microdeformaciones en la traviesa durante el impacto

Resultados y conclusiones:

La tabla muestra los resultados de rigideces y durezas de las 7 tipologías de placas de asiento evaluadas (identificadas desde la A hasta la G), que difieren en cuanto a geometría, espesores y material:

PLACA	Rigidez est. k_e (18-68 kN) [kN/mm]	Rigidez din. 5 Hz, $k_{d\ 5Hz}$ [kN/mm]	Rigidez din. 10 Hz, $k_{d\ 10Hz}$ [kN/mm]	Rigidez din. 20 Hz, $k_{d\ 20Hz}$ [kN/mm]	Rigidez din. media, k_{dm} [kN/mm]	Dureza Shore D
0 (ref)	694,4	1282,1	1362,4	1572,3	1405,6	49,8
A	53,5	106,4	116,0	134,4	118,9	7,0
B	65,8	183,8	199,2	229,4	204,1	---
C	68,5	93,1	97,3	110,6	100,3	29,8
D	35,5	90,6	94,7	106,8	97,4	22
E	126,9	162,9	169,5	188,0	173,5	44,6
F	140,8	320,5	344,8	387,6	351,0	50,1
G	284,1	490,0	515,5	588,2	531,2	27,0

En cuanto a la capacidad de atenuación se observa que el método de referencia no proporciona los mismos resultados que el método alternativo. No obstante, cuando se contemplan precargas bajas o inexistentes en el método alternativo ambos métodos convergen, como se puede apreciar en el gráfico de la Figura 3.

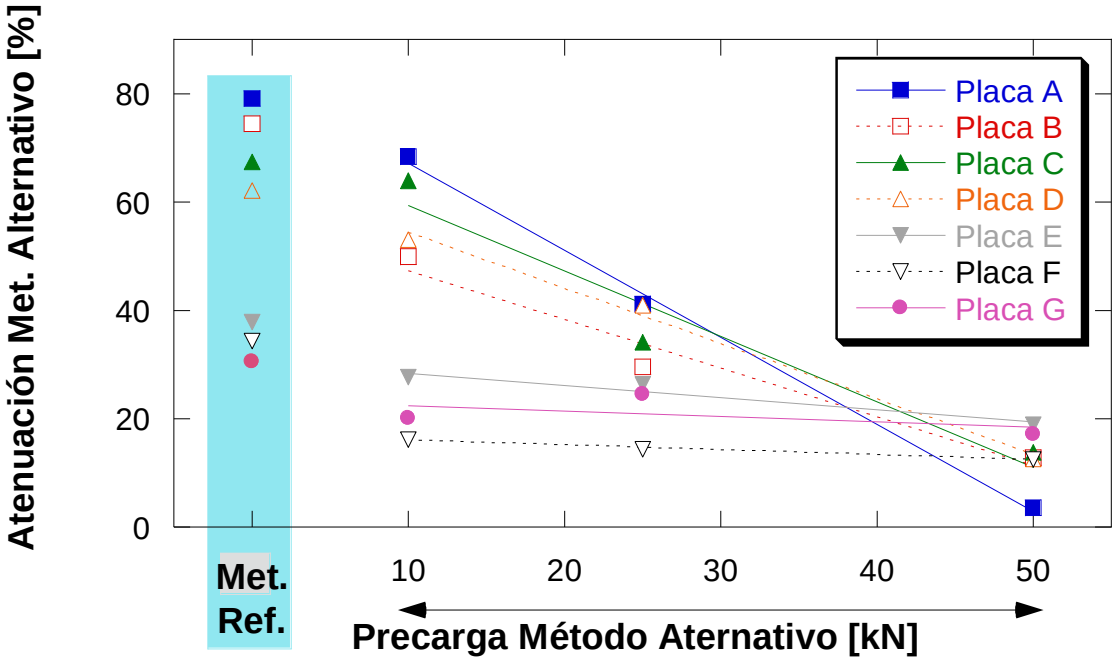

Figura 3.- Comparativa de Atenuación

Se destaca de los resultados obtenidos que la atenuación aumenta a medida que disminuye la rigidez y la dureza de la placa de asiento cuando se emplea el método de referencia. Sin embrago, esta tendencia se invierte cuando se usa el método alternativo, justificándose esta diferencia debido a la precarga de 5 toneladas que requiere éste último procedimiento.
El método alternativo ofrece menor diferenciación entre las placas de asiento dado que la precompresión coarta parte de su capacidad de amortiguamiento inicial.
La placa de mayor capacidad amortiguadora en el método de referencia (placa A) se muestra como la de menor funcionalidad atenuadora con el método alternativo.

En vista del estudio realizado en este TFG se realizan algunas propuestas a tener en cuenta de cara a futuras revisiones de la normativa. De mantenerse la versión actual, sería necesario incluir cuando se realicen ensayos de impacto el método empleado, referencia o alternativo. Además, sería recomendable que en la clasificación dada en la norma EN 13481-2:2012+A1:2017, la cual divide los sistemas de sujeción de acuerdo a su capacidad de atenuación, se establezcan dos criterios distintos según se use el método de referencia o el alternativo.

Bibliografía:

- European Committee for Standardization, EN 13146-3: 2012. Railway applications - Track - Test methods for fastening systems - Part 3: Determination of attenuation of impact loads. (2012).
- European Committee for Standardization, EN 13146-9:2009+A1: 2011. Railway applications. Track. Test methods for fastening systems. Part 9: Determination of stiffness., n.d.
- I.A. Carrascal, J.A. Casado, J.A. Polanco, F. Gutiérrez-Solana, Dynamic behaviour of railway fastening setting pads, Eng. Fail. Anal. 14 (2007) 364–373. doi:10.1016/J.ENGFAILANAL.2006.02.003.
- I.A. Carrascal, Optimización y análisis de comportamiento de sistemas de sujección para vías de ferrocarril de alta velocidad española, PhD Thesis, Universidad de Cantabria, 2006.
- I.A. Carrascal, J.A. Casado, S. Diego, J.A. Polanco, J. Martín, A. Pérez, Placa elástica de asiento metálica para alta velocidad, in: X Jornadas Int. Ing. Para Alta Velocidad, 2016: pp. 45–62.
- López Pita, P. Teixeira, F.A. Robusté, High speed and track deterioration: the role of vertical stiffness of the track, Proc. Inst. Mech. Eng. Part F J. Rail Rapid Transit. 218 (2004) 31–40.
- ADIF, ET 03.360.570.0 Placas elásticas de asiento para sujeción VM, (2005).
- Rcmennlko, O.I. Revjew, Determination of dynamic properties of rail pads using an instrumented hammer impact technique, 33 (2005) 3–7.
- European Committee for Standardization, EN 13481-2:2012+A1:2017. Railway applications. Track. Performance requirements for fastening system. Part 2: Fastening system for concrete sleepers., n.d.

Acknowledgements

What started as some attenuation tests with a hammer ended up being my final bachelor project. First, I would like to thank my three project directors, Soraya, Isidro and José. Not only for being always available to answer my questions or ask me about my future, but also for giving me the opportunity to learn while working with them. This experience has personally enrichened me and has also given me a practical understanding of engineering that I had not had before.

Besides, I would like to thank all of the people that are part of Ladicim, especially the lab staff, for being always willing to help me with my thousands of doubts about the equipment of the programs with good words. Another important person for this project has been Diego, who performed most of the tests with me during the long hours where we were not getting any good result.

My sincere thank you to the people in Ladicim who was always prepared to have coffee in the middle of the morning, as well as my officemate María, whom I hope has a brilliant future.

Finally, I would like to thank my family and friends, which are always there for me, in the next door or hundreds of kilometres away. My family has been an example of what I want for me. As Newton said, "If I have seen further it is only by standing on the shoulders of giants". I thank you all for always being there for listening to me, lifting me up or teaching me something new.

Contents

1. Objectives and terminology 12
Objectives 12
Terminology 14
2. Review of the state of the art 18
Stiffness 18
Preloading and its influence on impacts 21
The previous device 24
The acceleration of the previous device 26
Breakage of the sleeper and the new device 28
3. Test procedures 30
Stiffness Test 30
Impact testing 31
Determination of the impact attenuation 34
Alternative method 35
Alternative method using springs 38
Different preloading 42
Reference method 43
4. Equipment to carry out the tests and material employed 48
Strain gauges 49
Material used: Elastic pads 51
5. Experimental campaign: comparison between the two methods 55
Studded EPDM alternative method 55
Studded EVA alternative method 58
Microcellular rubber alternative method 60
Studded TPE alternative method 63
Solid EPDM alternative method 65
Solid reinforced rubber alternative method 66
Solid NFU alternative method 69
Solid EPDM reference method 71
Studded TPE reference method 72
Studded EPDM reference method 72
Microcellular rubber reference method 73
Solid NFU reference method 74
Solid reinforced rubber reference method 74

6. Validation: results 76
Stiffness 76
Impact attenuation 78
7. Conclusions and proposal of improvement 83
Bibliography 84
Appendix I: Photos of the sleeper breakage
Appendix II: Alternative method graphs
Appendix III: Reference method graphs
Appendix IV: Comparison between methods

1. Objectives and terminology

Objectives

A significant factor driving the growth of both economy and society of any country around the world is transportation. It is commonly believed that the best and safest solution for the transportation of either passenger or freight nowadays is the railway system.

The railway is seen as the transportation mode of the future, due to its functionality, efficiency, capacity and minimal environmental impact. However, its development has technical difficulties that need to be overcome in order to have long-lasting structures.

In the first place, generalized increase in the speed incurs higher forces on the track. Secondly, modern railway lines uses concrete sleepers which are 3 to 5 times more rigid than wood sleepers and give the track about the double of its rigidity according to D-117 [1] Committee. This extended use of concrete sleepers contributes to the need of a shock-absorbing material, the rail pad, in order to compensate for that increment in the system rigidity. With the increase in rail freight traffic and train speed, many countries have incorporated elastic elements into their railway systems [2].

Rail pads are a major component of ballasted railway tracks. Based on numerous analytical and numerical models, rail pad plays a crucial role in the dynamic behaviour of railway track. An adequate use of rail pads is essential in order to achieve solutions that are safe and have high durability too [3] as well as provide comfort to the passengers [4]. As one of the key factors regarding elastic pads is attenuation and this property has not been deeply studied, an extensive analyse is done.

In this project, the UNE-EN13146-3 [5] is analysed in order to characterize the differences existing regarding the two methods proposed by the Standard. Firstly, both methods are tested using different devices in order to fit with the Standard. Furthermore, the results are compared achieving conclusions regarding pad's properties and the method itself. The enormous influence that preloading has in

order to calculate attenuation is investigated in order to understand the sources of divergence between the methods.

The difference between both methods might generate disagreements when it comes to the classification of the fastening systems according to their parameter of impact attenuation in [6]:

- Fastening assembly with medium attenuation: 15%<attenuation<30%
- Fastening assembly with high attenuation: attenuation>30%

Besides, the rigidity of those rail pads is analysed and compared with their attenuation capacity, in order to obtain the possible correlation between them.

Terminology

Rail track is a fundamental part of railway infrastructure and its components can be classified into two main categories: superstructure and substructure. The most obvious parts of the track as the rails, rail pads, concrete sleepers, and fastening systems are referred to as the superstructure while the substructure is associated with a geotechnical system consisting of ballast, sub-ballast and subgrade (formation). Both superstructure and substructure are mutually important in ensuring the safety and comfort of passengers and quality of the ride [2].

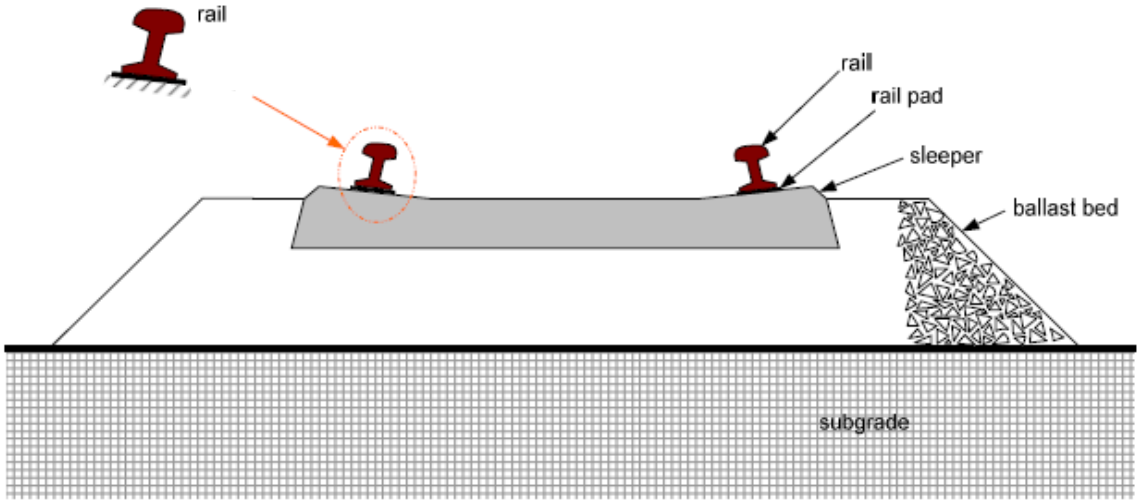

Figure 1.1. Ballast superstructure [7]

Regarding the assembly system, rail pads play an important role in the general maintenance of the state of the overall structure of a railway line because of the advantages that it gives to the whole system. They are placed between the base of the steel rails and the prestressed concrete sleepers as the following image shows.

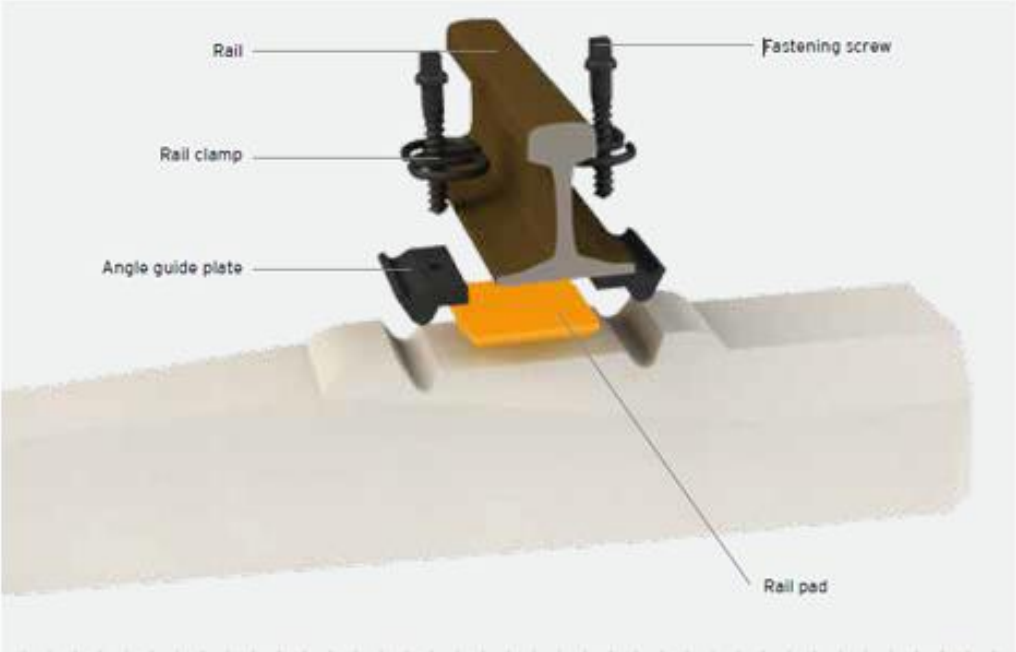

Figure 1.2. Fastening assembly [8]

The use of this component improves load distribution, eliminating load concentration and the resultant fatigue stresses, centring the load on the supporting element, reducing the wear of the rail and its support and acting as a seal between the bottom of the rail and the top of the support [8]. That means a smoother ride and a better conservation of the superstructure.

Moreover, these rail-setting pads damp the vibrations and noise that the rail transmits to the sleeper, thus avoiding the cracking of the concrete sleepers and preventing the wear and tear of the ballast or other infrastructure components. They also provide electrical insulation between the rails [9].

Rail pads present properties due to its geometry and the materials they are made of. Nevertheless, it is important to note that elasticity properties are sensitive to the level of loading, the frequency of loading, the temperature while loading and the duration and repetition of loading.

Figure 1.3. Rail pad over sleeper before installing the rail.

The two properties analysed in this project are attenuation and rigidity.

Attenuation is defined as the gradual loss of flux intensity through a medium. In our case, it means that it filters the dynamic forces from rails and fasteners transferred to the sleepers. The high dashpot value of rail pads reduces excessive high-frequency forces and provides a resiliency between rail and sleeper that helps alleviate rail seat cracking and contact attrition [7].

As it has been mentioned before, they need an adequate rigidity and also degradation resistance because of the environmental condition that it is going to face [10]. Rail pads are normally made out of rubber, high-density polyethylene (HDPE), thermoplastic polyester elastomer (TPE), and ethylene vinyl acetate (EVA) [11,12]. Nonetheless, over the last few years, new elastic elements have been developed from alternative materials, with emphasis upon those made from used tires, having positive results for being used in railway tracks [13].

Figure 1.4. Pads made out of used tires [13].

Another innovation proposed is the metallic pad fabricated from stainless steel [14]. These new pads deal with the problems derived from environmental agents like UV radiation, temperature, humidity and the damage suffered by the pads due to the continue mechanical fatigue in compression, which increments the rigidity of the rail pads [9,10].

Figure 1.5. Pads made out of stainless steel.

Generally, these pads come in various designs in order to better adapt to the railway system, and can thus range in thickness from 4.5 to 15.0 mm. With regard the horizontal geometry, rail pads are usually 180 mm long and 140 mm wide under rail type UIC 54, and 180 mm long and 148 mm wide under rail UIC 60 [15]. The pads used for this project vary between 5 mm and 11 mm, being the EVA reference pad supplemented with aluminium whenever needed.

2. Review of the state of the art

In order to characterise rail pads, the series EN-13146:2012 [5] has the following requirements:

- Determination of longitudinal rail restraint
- Determination of torsional resistance
- Determination of attenuation of impact loads
- Effect of repeated loading
- Determination of electrical resistance
- Effect of severe environmental conditions
- Determination of clamping force
- In service testing
- Determination of stiffness

The parameters analysed here, as mentioned before, are attenuation of impact loads and rigidity (determination of stiffness).

Stiffness

The existing literature has done many studies regarding rail pad stiffness; however, it does not show a clear agreement regarding how to classify the pads according to its rigidity. According to Pita [16], pads can be divided into soft (k<80 kN/mm), medium rigidity (80kN/mm < k < 150kN/mm) and rigid (k>150 kN/mm).

On the other hand, ADIF, the Spanish administrator of railway infrastructures, specifies that soft pads used for high-speed need to have a static rigidity between 80-125 kN/mm [6].

If we take a look at different countries we can notice that there are variations between countries and even in the same country, mainly depending on the use that the line is going to have.

Country	Line	Vertical rigidity of the pad (kN/mm)
France	Conventional lines	150 (or over)
	High-speed lines	90
Germany	Conventional lines	500 (or over)
Spain	Conventional lines	500
	High speed lines	100
Italy	High-speed lines	100
Belgium	Conventional lines	100
	High-speed lines	60

Table 1. Rigidities used in different European countries [17]

Even though there is no consensus regarding an exact classification of pads according to its rigidity, the change in properties is undoubtable. It is necessary to narrow down an optimum value of rigidity, both with a minimum and a maximum value [18,19]. There is a tendency to lower the rigidity in high-speed, because enormous rigidities provoke faster corrugation growth [20]. Also, a low value would lead to the sinking of the rail, with an increase in the rail stresses [21,22]. Furthermore, there are other parameters that influence the stiffness behaviour, as the following table shows.

Parameters	Stiffness increase	Stiffness reduction
Temperature (*increase*)		✓
Dynamic loads	✓	
Frequency (*increase*)	✓ Low influence	
Pre-load (increase)	✓ High influence	
Fatigue process	✓ High influence	
Pad thickness (*increase*)		✓
Mechanical deterioration	✓ High influence	
Thermal ageing	✓	

Figure 2.1. Influence of different parameters on rail pad stiffness [15]

The analysis of rail pad properties is done worldwide by different organizations, with either one or two degrees of freedom. Furthermore, each laboratory presents different preload capacity.

Place	Excitation	Method	Model	Preload Capacity
TU-Delf	Impact	Direct	SDOF	0–25 kN
VUB-Belgium	Harmonic	Direct	SDOF	0–1 kN
UNICAN-Spain	Harmonic	Direct	SDOF	20–95 kN
TNO-UK	Harmonic	Indirect	2DOF	0–80 kN
TU-Berlin	Harmonic	Indirect	2DOF	0–95 kN
UoW-Australia	Impact	Direct	SDOF	0–400 kN

Figure 2.2. Review of current rail pad testers [3]

Preloading and its influence on impacts

Every rail pad is subjected to preloading. This loading, for UIC 60 rail (60 kg/m) and a 0.6 m distance between two sleepers each rail pad is subjected to about 0.36 kN rail weight load. Thus the initial preload in the rail pad is about 20.36 kN [23].

One of the keys for our study is the analyse of preloading in the pads. A comparison between the two methods of attenuation proposed by the European Standard [5] has not been done before. However, in the analysis of harmonic loads, S. Koroma came to the conclusion that, as the preload increases, the rail pads become much stiffer than their initial linear value hence resulting in lower response amplitudes [24].

Even though the study of rail pads attenuation is not frequent, the US Department of Transportation showed some results in May 1982 [25]. Firstly, they analysed different drop heights, obtaining a linear increase in displacement with an increase in the drop height, with a similar slope in all of the pads. This is remarkable because it means that it does not matter the height that is being used to drop the hammer, the attenuation obtained, as it is a comparison between the reference and the tested pad, is going to be the same value.

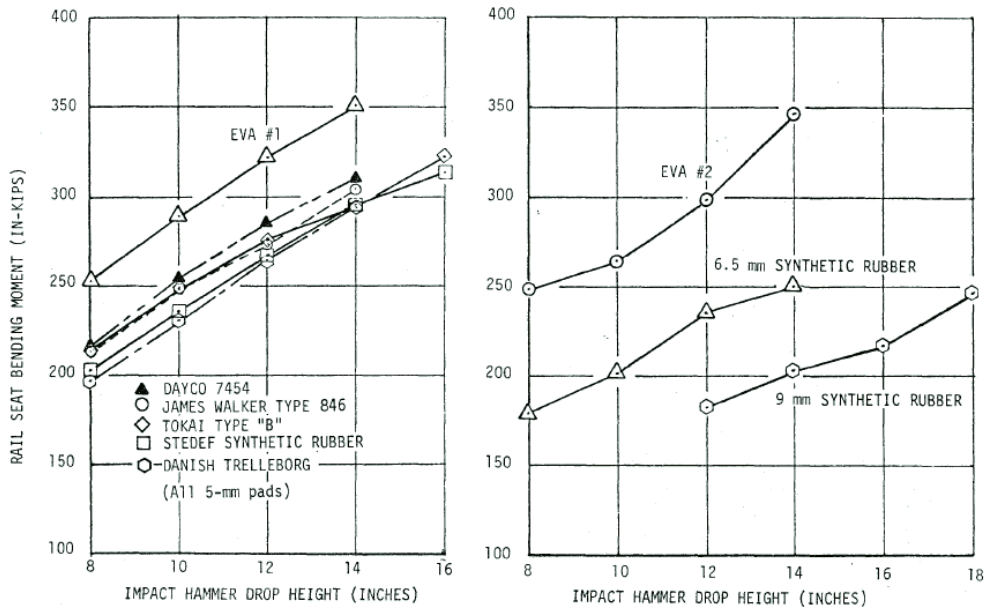

Figure 2.3. Effect of tie pad substitutions on impact bending moment at tie rail seat [25]

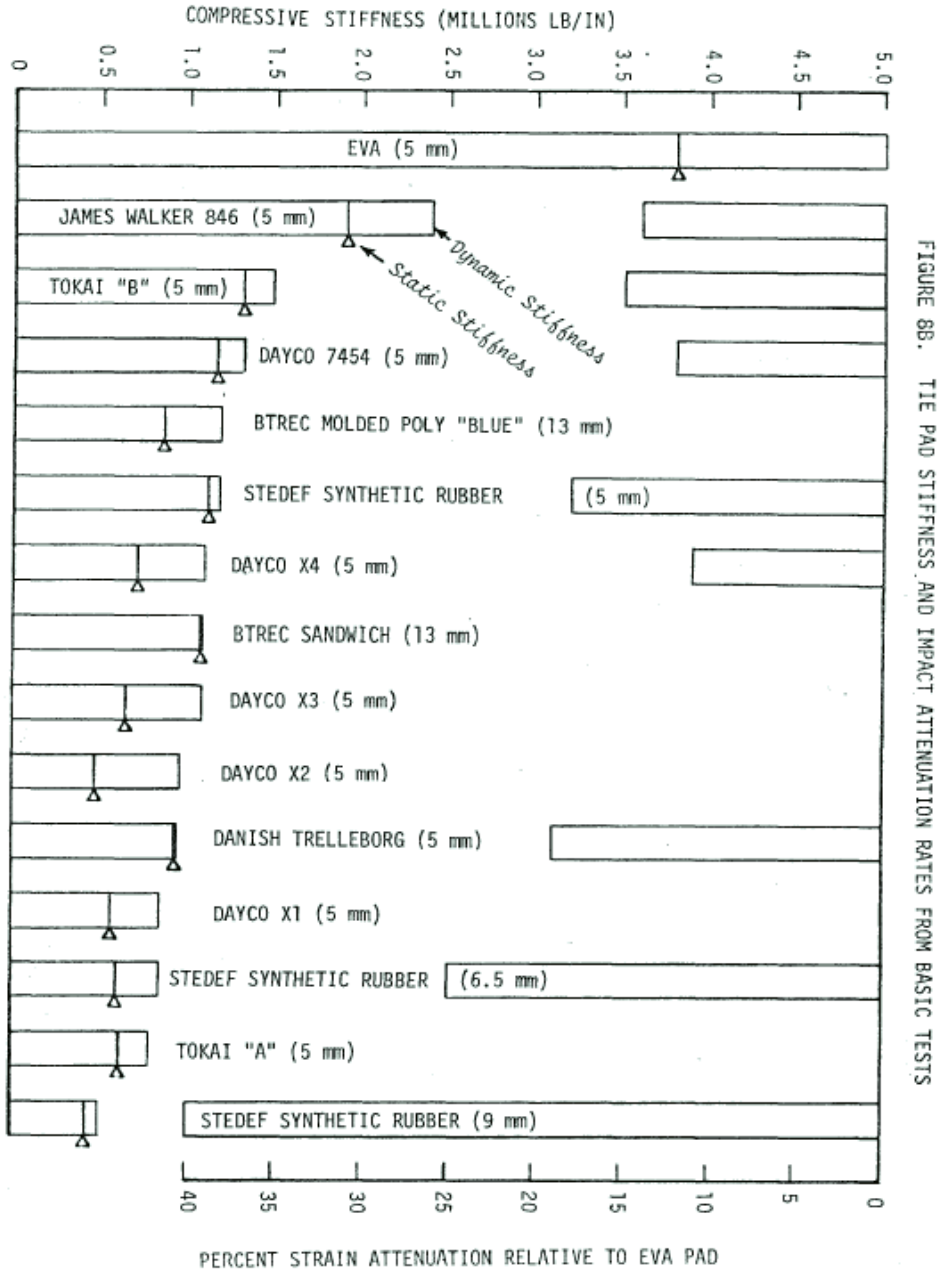

Figure 2.4. Attenuation and stiffness

Here we can see a comparison between the attenuation and the stiffness. As it can be seen, pad stiffness provides a very unreliable measure of attenuation. This means that the attenuation rate of a given pad can only be obtained by laboratory impact tests or by field measurements of impact strain. On the other hand, the stiffness measurement is valuable as a measure of the change in condition that may occur in a pad as the result of testing or service loads. Japanese National Railway results

show an increase of two-thirds in the stiffness of Takaido Shinkansen Type A pads over an expected 10-year life from 90 tons/cm to 150 tons/cm.

However, the comparison made here in order to calculate the attenuation differs from the one used by the European Standard [5]. The European Standard compares each pad with a reference pad of the same thickness, while the comparison made by the U.S. Department of Transportation does not always compare it with a reference pad of the same thickness, as it can be seen in the graph. The writer also realized that the 5.5 mm pad performed poorly relative to the 6.5 mm pads, which all had higher attenuations.

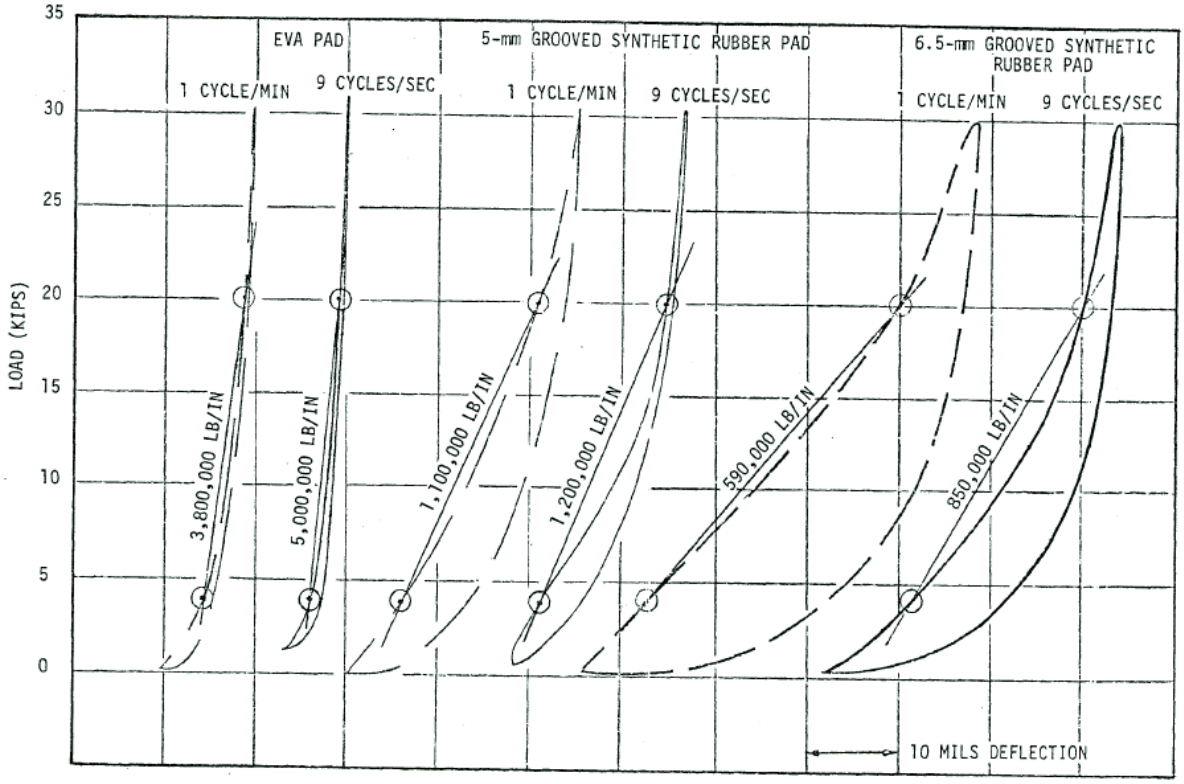

Figure 2.5. Load-deflection plots.

Regarding the dynamic stiffness of these pads, it varied widely, as it can be seen in the figure. This is not the only reference that we have regarding variation in dynamic stiffness [26]. The results obtained for stiffness in our tested pads are showed in chapter 6.

The previous device

Adif Standards[27] propose using an instrumented hammer in order to apply the impact load. Before this load, a preload of 50 kN is applied, and then maintained during the test. This coincides with the alternative method of the European Standard [5].

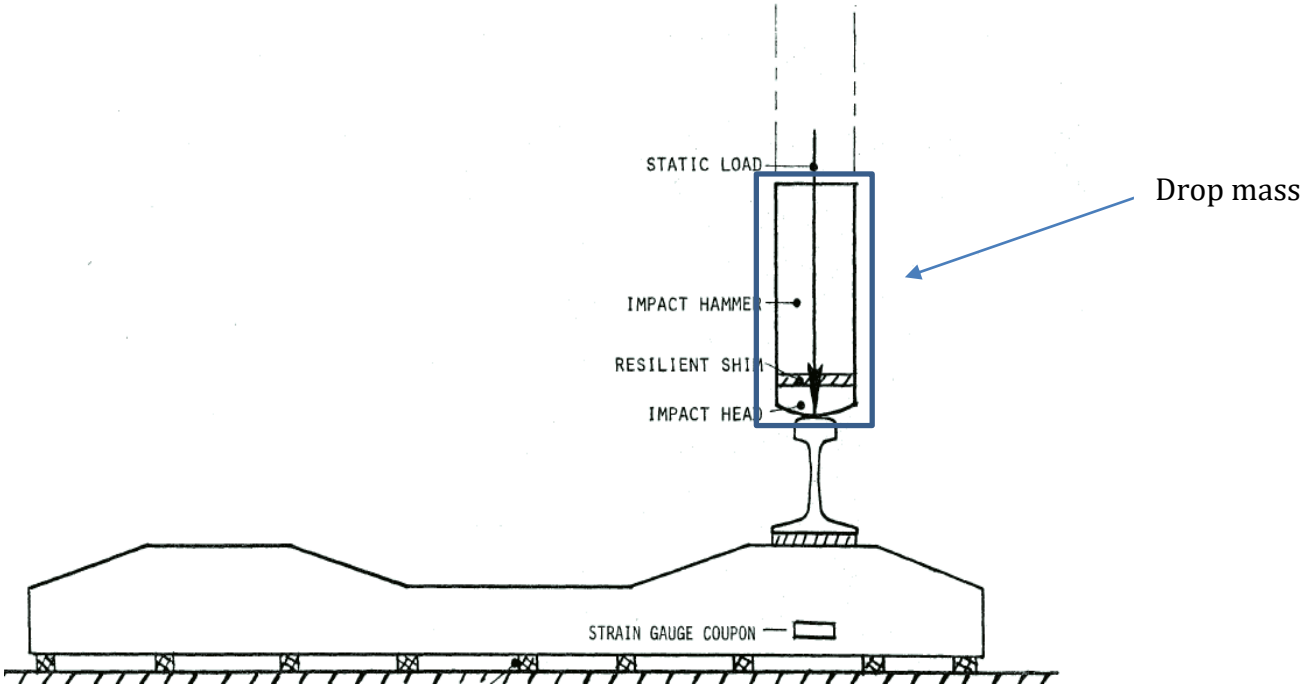

Figure 2.6. Schematic of impact test arrangement [25]

The hammer has a total length of 950 mm, with a steel bar of 850 mm and 50 mm diameter. The impact head, bullet-shaped, has a length of 270 mm and 100 mm diameter. The total weight of the hammer is 23 kg. In the join of the impact head with the bar, a corbel was welded. The 50 kN are applied by means of an actuator that stays in contact with the rail at two points equidistant to the plane of symmetry of the sleeper.

Figure 2.7. Hammer setup

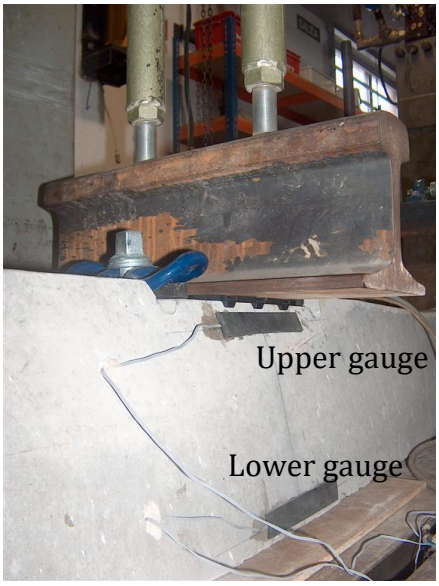

Figure 2.8. Position of the strain gauges in the sleeper

The acceleration of the previous device

The value of the impact load had been previously studied [28]. Firstly, using numerical elements by means of finite elements, showing the stress handled in different instants during the impact. The estimated value was 100 kN, which was corroborated experimentally with an accelerometer set in the back of the impact head, as shown in figure 8.

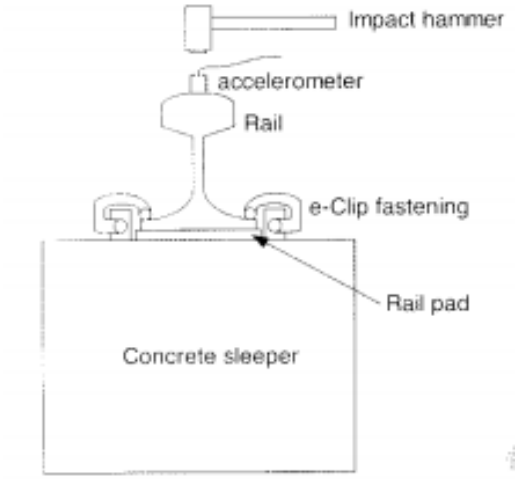

Figure 2.9. Schematic tests rig [29]

Figure 2.10. Detail of the accelerometer

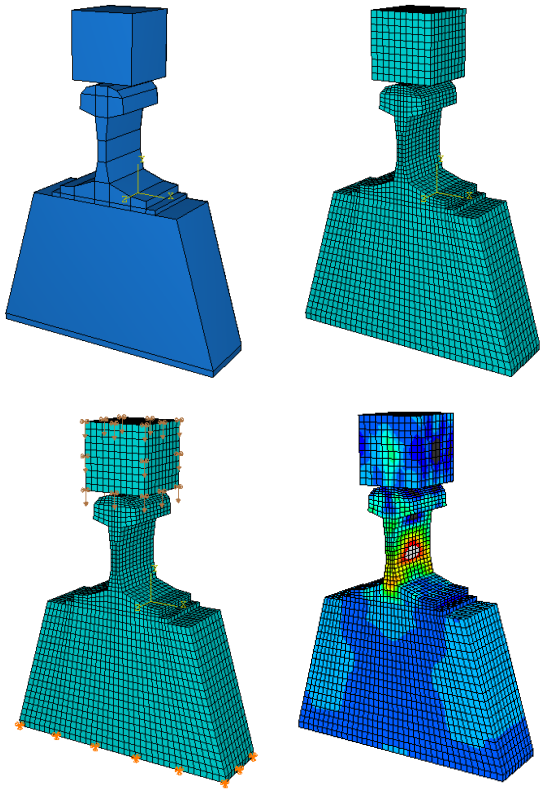

Figure 2.11. FE-Simulation sequence [28]

A similar hammer has also been used in order to tests rail pads in other places such as LabIC at Granada.

Figure 2.12. Laboratory arrangement of the tests in LabIC [30]

Breakage of the sleeper and the new device

In order to perform this attenuation tests a new sleeper. Due to the number of tests performed, the sleeper started developing small cracks that gave a mistaken strain when the impacts occurred (see figure). After visual inspection, this defect was discovered. Due to the crack, the strain recorded was huge compared with the real one. Consequently, it was decided that the technique should change to a hammer that produced lower stress and a new equipment able to give a smaller impact was then designed.

Figure 2.13. Crack developed under the sleeper. See Annex 1 for more photographs

The new hammer was no longer a pendulum, but a vertical drop mass. The mass decreased substantially so it would not have more problems regarding breakage. The drop mass goes inside a guide cylinder. The mass is taken to the upper position and it is released from there, having then free fall. The fall height is 38.5 mm. Two grabbers were added (shown in red in picture 12) so it was easier to rise the drop mass until the adequate height. It also progressed during the tests. Firstly, the load was applied through the actuator to the rail. Afterwards, it was decided to include a set of springs as the Standard requires with a total stiffness lower than 2 MN/m, as it is explained in the following chapter.

According to the Standard, the combination of mass and drop height shall be such that the strain measured at each gauge position shall be less than 80 % of the calculated cracking strain of the sleeper. For the drop mass and the sleeper used, that was shown to be covered.

Also, the sleeper was changed for a new one without any cracks in which only the new device was used.

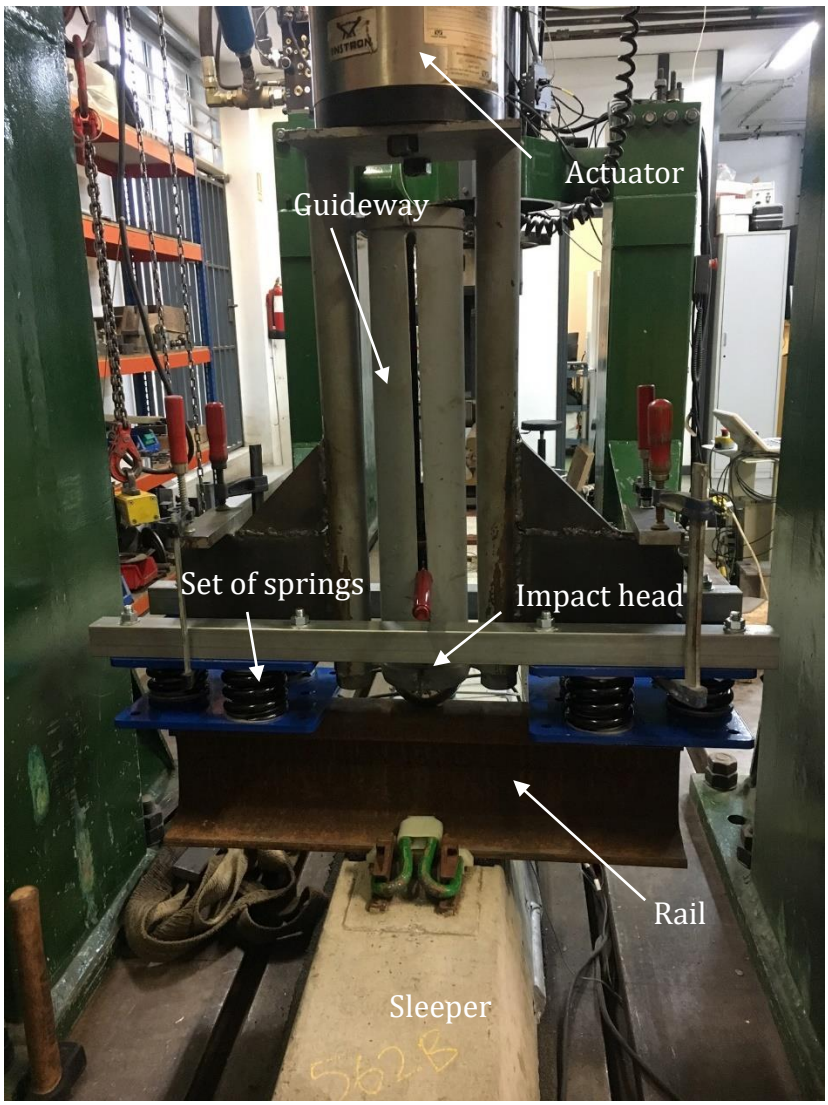

Figure 2.14. New device assembly

3. Test procedures

Stiffness Test

Before the characterization of the pads regarding impact tests, both static and dynamic stiffness was measured. In order to calculate them the UNE-EN 13146-9[6] was used, taking into account that they are considered for high speed, therefore type D [31].

With the objective of performing the static and dynamic stiffness tests, the assembly shown in figure 1 was used. The measurement of the shortening of the pad during the test is done by means of 4 LVDT situated in each of the four corners while the load was being applied by a servo-hydraulic machine, INSTRON with ±250 kN of capacity.

Figure 3.1. Assembly used for the stiffness tests

In order to perform the static stiffness tests, a load ($F_{SPmax,}$) is applied through a spherical seating in the actuator. Then the load is reduced to F_{SP1} and repeat this cycle of loading twice more with a rate of (V_e: 120 ±10 kN/min). The vertical displacement of the pad (d) was registered by LVDT and the static stiffness (k_e) was calculated during the loading in the third cycle according to expression (1) between the force values F_{sp1} and F_{SP2}=0.8·F_{SPmax}.

$$k_e = \frac{F_{SP2} - F_{SP1}}{d_{SP}} = \frac{50}{d_{SP}} \quad (1)$$

The value d_{SP} is the average displacement between the loading values F_{SP1} and F_{SP2}.

In order to perform the dynamic stiffness tests, a sinusoidal compressive load between the values F_{LFP1} y F_{LFP2}=0.8·F_{LFPmax} was applied for 1.000 cycles at the frequencies 5, 10 and 20 Hz. The testing set-up was the same as that used in the

static test. The low-frequency dynamic stiffness (k_d) was determined as the mean in the last 10 cycles according to expression (2).

$$k_d(5/10/15Hz) = \frac{F_{LFP2} - F_{LFP1}}{d_{LFP}} = \frac{50}{d_{LFP}} \quad (2)$$

The value d_{LFP} is the average displacement between the loading values F_{LFP1} and F_{LFP2}.

In table 1, we can see the parameters used in the stiffness tests, both static and dynamic.

Component	F_{SP1} F_{LFP1} [kN]	F_{SPmax} F_{LFPmax} [kN]	F_{SP2} F_{LFP2} [kN]	V_e [kN/min]
Pad	18	85	68	120±10

Table 2. Parameters for the stiffness tests

Impact testing

The proposed method in order to determine the attenuation produced by a pad in the Standard consists in measuring the strain produced over the sleeper with a test pad and compare it with the one obtained with the reference pad with low attenuation.

An impact vertical load is applied by dropping a mass onto the head of a rail fastened to a concrete sleeper. It is important to note that the test procedures apply to a complete fastening assembly.

The impact applied tries to simulate the impact loading caused by traffic or railway tracks. The effect of the impact is measured as strain in the concrete sleeper. The impact attenuation of a fastening system is assessed by comparing the strains induced with a low attenuation reference rail pad in the fastening system and with the test pad in the fastening system.

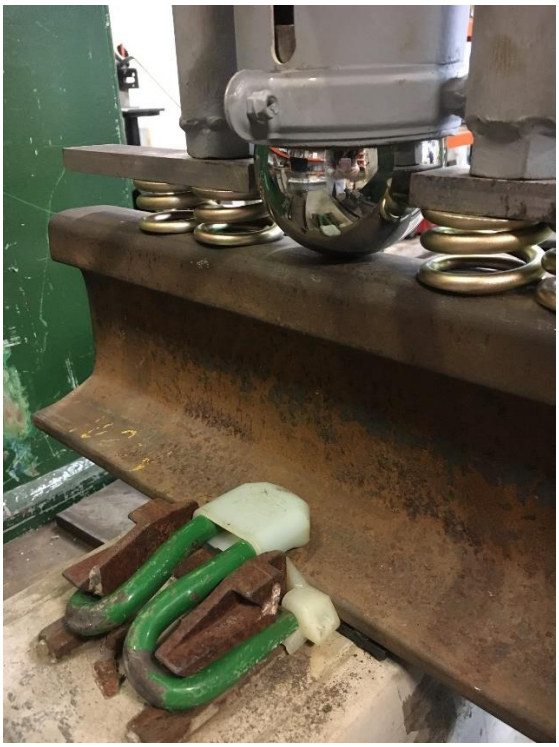

Figure 3.2. Impact testing arrangement

The procedure of the test is the following: With the reference pad in the system, the mass falls, with a strain induced by the impact load that does not exceed 80 % of the rail seat resistance moment of the sleeper (*M*dr in accordance with EN 13230-1 [32]) at the gauge positions. The drop mass, drop height and resilience of the striking head are adjusted to ensure the limit on strain is not exceeded. Without a subsequent change to the drop mass, drop height and striking head, the procedure is repeated with the test pad.

During the testing time, there has been evolution regarding the loading as it has been mentioned before. Two variables are played with: springs and preloading. The springs came out when it was seen that the Standard requires that the load is applied by a set of springs [5]. As it was a compulsory condition, different assemblies were used until getting springs able to resist the 50 kN. Regarding the preloading, different iterations have been made so they could compare with each other and perform a correlation between the two methods. The development in time of the different testing setups has been the following:

1. Preloading of 50 kN with the actuator and no set of springs
2. Preloading with small springs at 10 and 20 kN.
3. Testing with ballast.
4. Preloading with a spring arrangement such that 50 kN are able to be applied.
5. Different tests with springs and 5, 10, 25 and 50 kN.
6. A second period of ballast testing.

The fastening system and the rail were assembled with a 5 mm thick plain reference pad of EVA stacked with a 5 mm thick aluminum plate to determinate the 10 mm thick pad attenuation, with 2 mm thick aluminum plate to determine the 7 mm thick pad attenuation and with a 6 mm thick aluminum plate to determinate the 11 mm pad attenuation, respectively.

In order to perform new tests or whenever there has been a change in the ballast or the sleeper, a series of impacts are carried out and the strain recorded 10 impacts. When 5 consecutive strains have a strain pick in which scale and time interval are within del ±10 % of its mean, the preparation of the test is complete.

The tests were carried out at room temperature (23±5 ºC). All of the components of the tests are kept within this temperature range for at least 4 hours before the test starts.

For an established test rig, the magnitude and time interval of the first strain peak was compared with the mean of 10 preceding impacts, and when it did not differ by more than 10 % testing started. With the test pad in place, five impacts were carried out. The three last strains were recorded and those were the ones used in order to calculate the attenuation.

Regarding the sleeper condition, it was checked after each test. For the first sleeper used, the sleeper had a crack, as mentioned in chapter 2. Those results were discarded, and another sleeper was used in order to continue with the tests. In all the following tests, the sleeper remained uncracked.

Determination of the impact attenuation

The impact attenuation is determined as the mean of the attenuation measured in the upper part, a_{sup}, and the lower one, a_{inf}, according to expression 1, being a_{sup} and a_{inf} the mean of the individual results:

$$a = \frac{a_{sup} + a_{inf}}{2} \ (\%) \qquad (3)$$

The individual value of percentage attenuation in the upper and lower parts is obtained from the static and dynamic strains registered with the reference pad and the tested pad, according to expressions (4) and (5):

$$a_{sup}^{i} = 100\left(1 - \frac{\varepsilon_{mu,sup}^{i} - \varepsilon_{e,mu,sup}^{i}}{\varepsilon_{rf,sup} - \varepsilon_{e,rf,sup}}\right) \qquad (4)$$

$$a_{inf}^{i} = 100\left(1 - \frac{\varepsilon_{mu,inf}^{i} - \varepsilon_{e,mu,inf}^{i}}{\varepsilon_{rf,inf} - \varepsilon_{e,rf,inf}}\right) \qquad (5)$$

Where:

- $\varepsilon_{rf,sup/inf}$: Mean of the maximum individual strain ($\varepsilon_{rf,sup/inf}^{i}$) in the upper/lower part of the sleeper with the reference pad.
- $\varepsilon_{e,rf,sup/inf}$: mean of the static individual strain ($\varepsilon_{e,rf,sup/inf}^{i}$) in the upper/lower part of the sleeper with the reference pad, this means, the strain for the preload. In case of using the reference method, its value is 0.
- $\varepsilon_{mu,sup/inf}^{i}$: Mean of the maximum individual strain in the upper/lower part of the sleeper with the reference pad.
- $\varepsilon_{e,mu,sup/inf}^{i}$: Static individual strain ($\varepsilon_{e,mu,sup/inf}^{i}$)in the upper/lower part of the sleeper with the tested pad. In case of using the reference method, its value is 0.

In the next figure, it can be seen an example of a representation of the individual results for both the test pad and the reference pad. In the figure, it is represented

the evolution of the microstrain obtained by the strain gauge versus time. The upper gauge registers negative values because when the impact happens in the upper gauge of the sleeper goes to compression, while the lower zone is in tension so it registers positive values. The fact that the reference pad registers higher and narrower picks than the tested pad can be noticed in the picture.

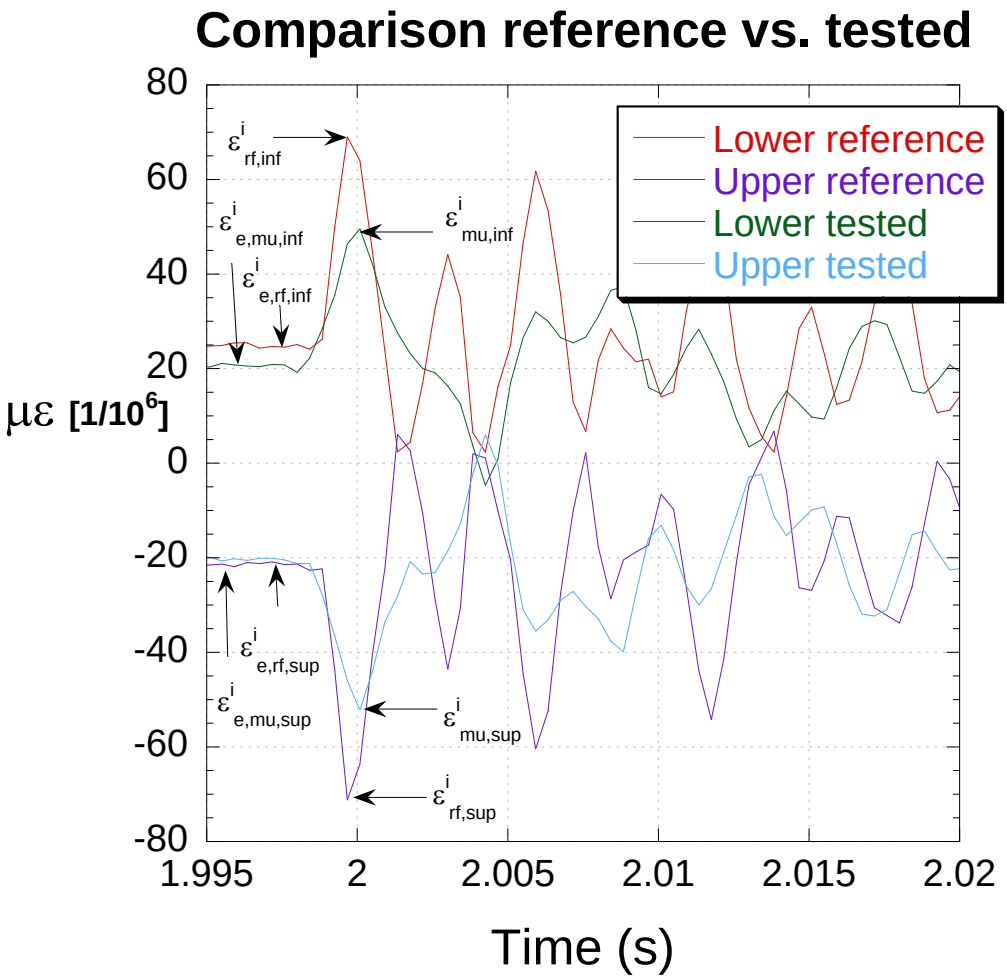

Figure 3.3. Results obtained for an individual impact test by the alternative method with the reference and the test pad

Alternative method

The sleeper support was a mat made of crushed end-of-life tires bonded with polyurethane resin that allows a vertical deflection of 0.37 mm (see Figure 5) when the G44 sleeper supported on it was subjected to an increase in static load from 50

kN to 60 kN at one rail seat. The standard requires a vertical deflection between 0.1 ≤ δ ≤ 0.5 mm. In the next figure, the assembly for the stiffness of the mat is shown.

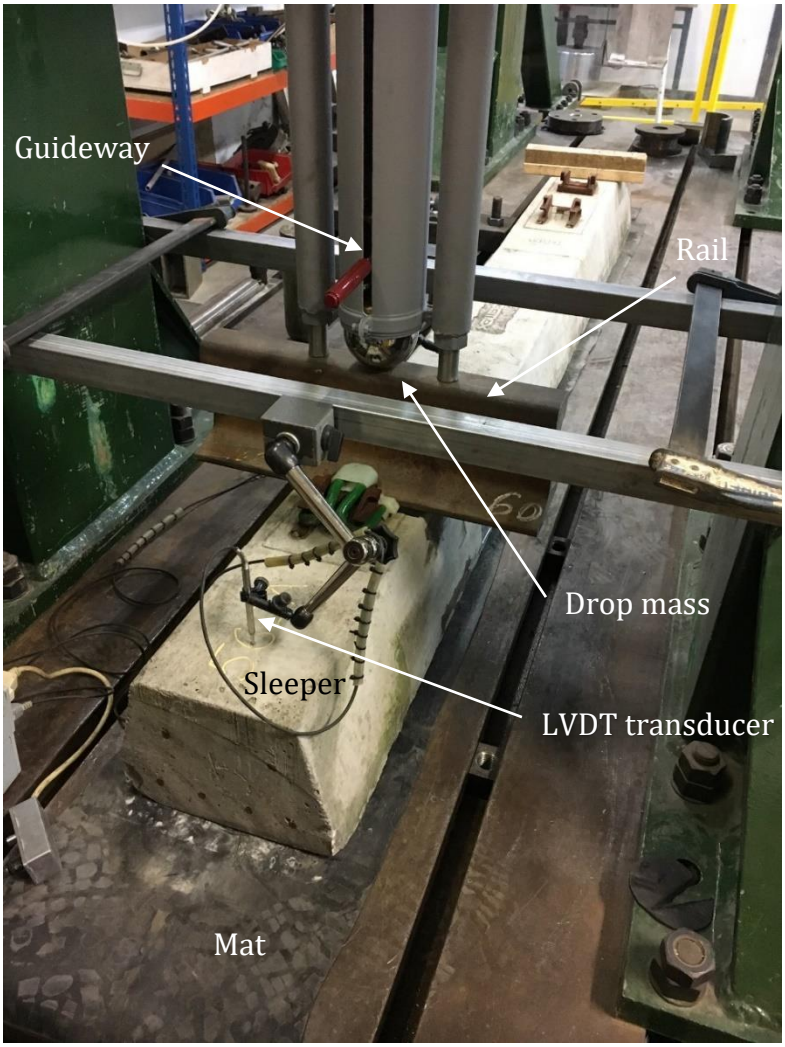

Figure 3.4. Assembly for the mat stiffness determination

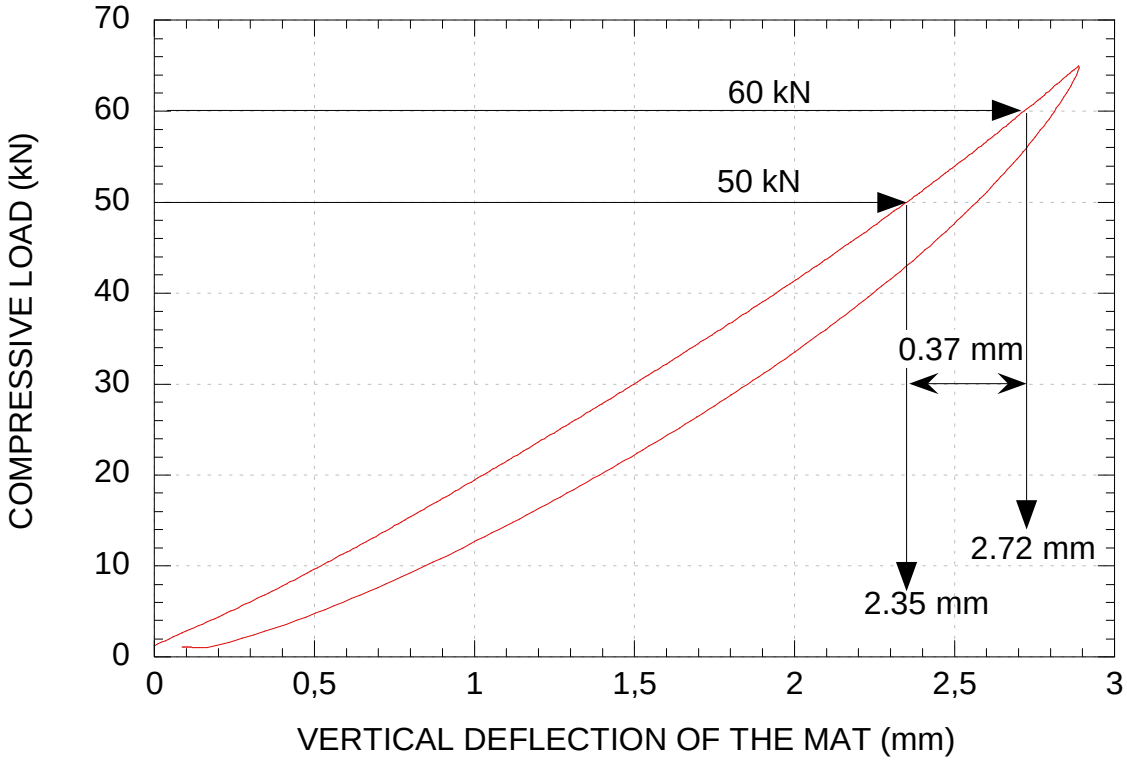

Figure 3.5. Vertical displacement of the mat

The test consisted in applying a preload of 50 kN to the rail and subsequently, an impact load to the rail by free fall of the drop mass. The combination of mass and drop height did not generate strains higher than 190 με over the upper gauge and 212 με over the lower gauge.

Alternative method using springs

Seen that the actuator could possibly not be behaving as a spring system, it was decided to perform tests using actual springs with the actuator in order to compare it with the ones using just an actuator.

In a first try, a set of four springs were arranged, having two of them at each side of the mass.

Figure 3.6. Testing using the alternative method with springs

These springs were just tested with 10 and 20 kN, due to the fact that they did not have more length to decrease if the load increased. The stiffness requirement was accomplished.

Figure 3.7. The arrangement of the springs

It was seen that the results obtained were good; however, those springs were not able to provide the 50 kN that the Standard requires. After that and several prototypes, the final set of springs, able to resist 50 kN and with the stiffness needed was designed.

Furthermore, the springs needed to have small aluminum sheets because we wanted to apply the same load on each side and without the springs the actuator touched one of the sides first and the other afterwards. With this sheet, the distribution of the load in half of the load for each side was ensured.

Figure 3.8. Final setup including springs

Figure 3.9. Detail of the springs

In order to achieve the stiffness needed, two big sets of springs that had 6 springs each one were used. After checking that they were too stiff, different assemblies

were evaluated. The final set of springs able to give a stiffness smaller than 2 MN/m was composed of two sets with 3 springs in each side.

Number of springs	Measurement equipment	Stiffness (kN/mm)
12	Actuator	2.90
8	Actuator	2.20
6	Actuator	1.72
6	LVDT	1.99

Table 3. Spring's stiffness results

Because the measurement of the actuator is not 100% accurate (the assembly of the actuator might have deformations that influence the stiffness results), the stiffness was recalculated using LVDT transducers. The stiffness obtained was 1.99MN/m, as the following graph shows. That fulfils the requirements (stiffness < 2MN/m).

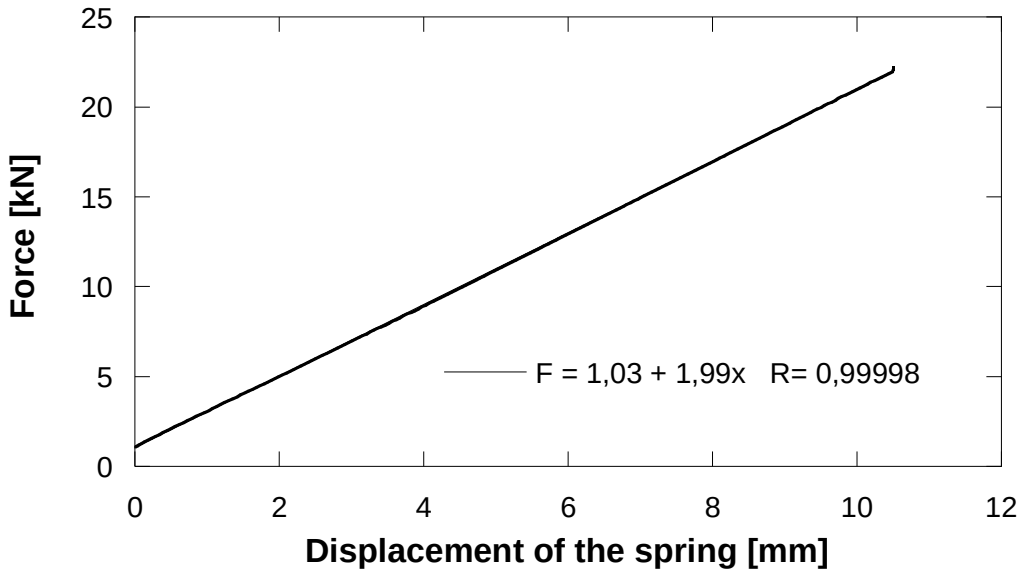

Figure 3.10. The elasticity of the spring using LVDT transducers

Different preloading

The tests carried out using the alternative method gave different results than the tests that used the reference method. Because the requirement for the ballast is the same as the requirement for the mat, the only difference between the two methods is the preloading. The preloading used in the alternative method is 50 kN. The preloading for the reference method is just due to the embedment of the sleeper in the ballast, which is a value much lower than the 50 kN. The preload given by the clips is the same in both methods because the fastening assembly does not vary between them. A more reasonable comparison between the two methods wanted to be done. In the first set of tests, preloading of 20 kN and 10 kN using the alternative method were tested. Afterwards, with a more accurate measuring device, preloading of 5, 10, 25 and 50 kN was done. Furthermore, tests without preloading were done as well. It was expected that the attenuation would increase as the load decreased. In the chapter 5, the results that compare the different preloading are shown. It is important to mention that the reference method is expected to be linear with the 25 and the 50 kN preloading. However, the preloading of 5 and the test that does not have preloading when they are performed using the alternative method there might be some moving in the general superstructure. This moving makes that the sleeper moves as well. As the displacement measured in the strain gauges is in the microstrain order, the movement in the sleeper interferes with the measurement of the strain that comes from the impact. In fact, the impact itself should cause microstrains, but not move the sleeper. Therefore, whenever there is movement in the sleeper, the resultant strain is not reliable.

Reference method

The support consists of a bed of crushed stone with a nominal particle size in the range 5 - 15 mm contained in a wood tank with an opening able to fit the sleeper. In order to obtain the stone, the sieves in that 5-15 mm interval were used.

Figure 3.11. Sieved stone

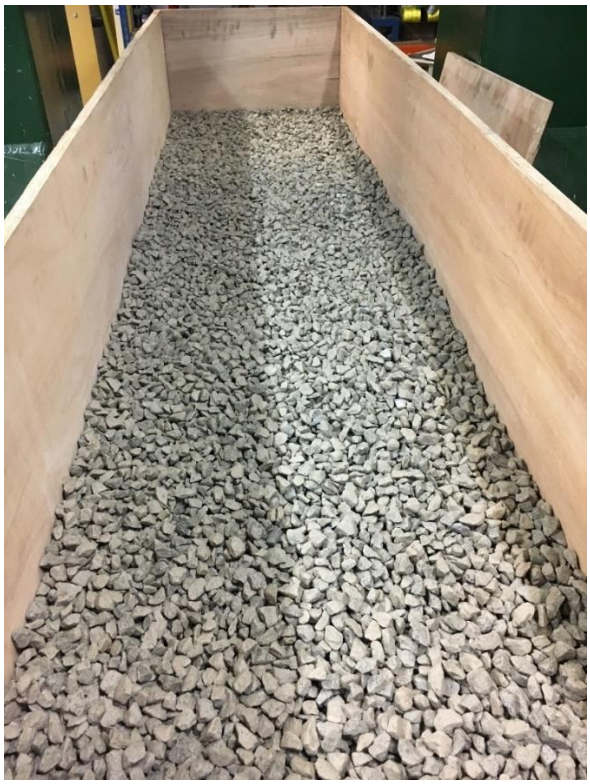

Figure 3.12. Wood tank

The bed is continuous for the full length of the sleeper, as required by the Standard. The Standard also requires a vertical deflection of the sleeper of $.1 \leq \delta \leq 0.5$ mm when a sleeper supported on it is subject to an increase in static load from 50 kN to 60 kN at one rail seat. The vertical deflection of the sleeper was 0.32 for the first series of tests (performed in February) and 0.31 for the second series of tests (performed in May). The graphs can be seen in figures 3.15 and 3.16.

The depth under the sleeper is 270 mm and the depth embedded is 100 extra millimeters. The first time that the load was applied the deflection of the sleeper was bigger than the interval required. However, with this measurement of the deflection, the stone got some settlement, which made that the deflection obtained in the second measurement was lower than in the first one. This measurement was repeated twice, achieving then results within the rank.

Figure 3.13 Verification of the deflection of the ballast

Figure 3.14. Detail of the LVDT Transducer

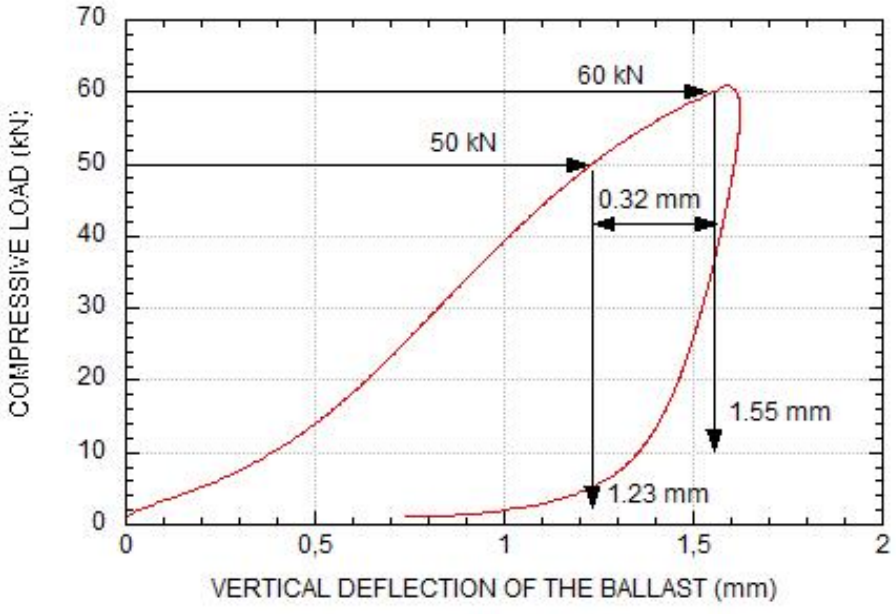

Figure 3.15. The vertical deflection of the sleeper support

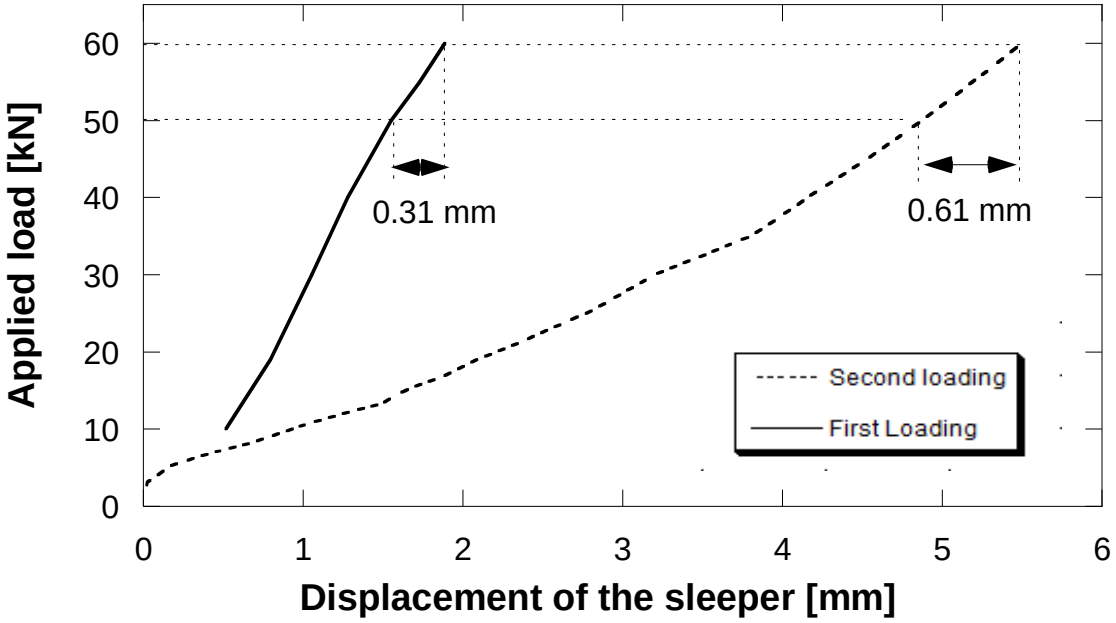

Figure 3.16. The vertical deflection of the sleeper

The test consisted in applying an impact load to the rail by free fall of the drop mass. The combination of mass and drop height did not generate strains higher than 190 με over the top gauge and 212 με over the bottom gauge. In the following figure, we can see a photo of the test.

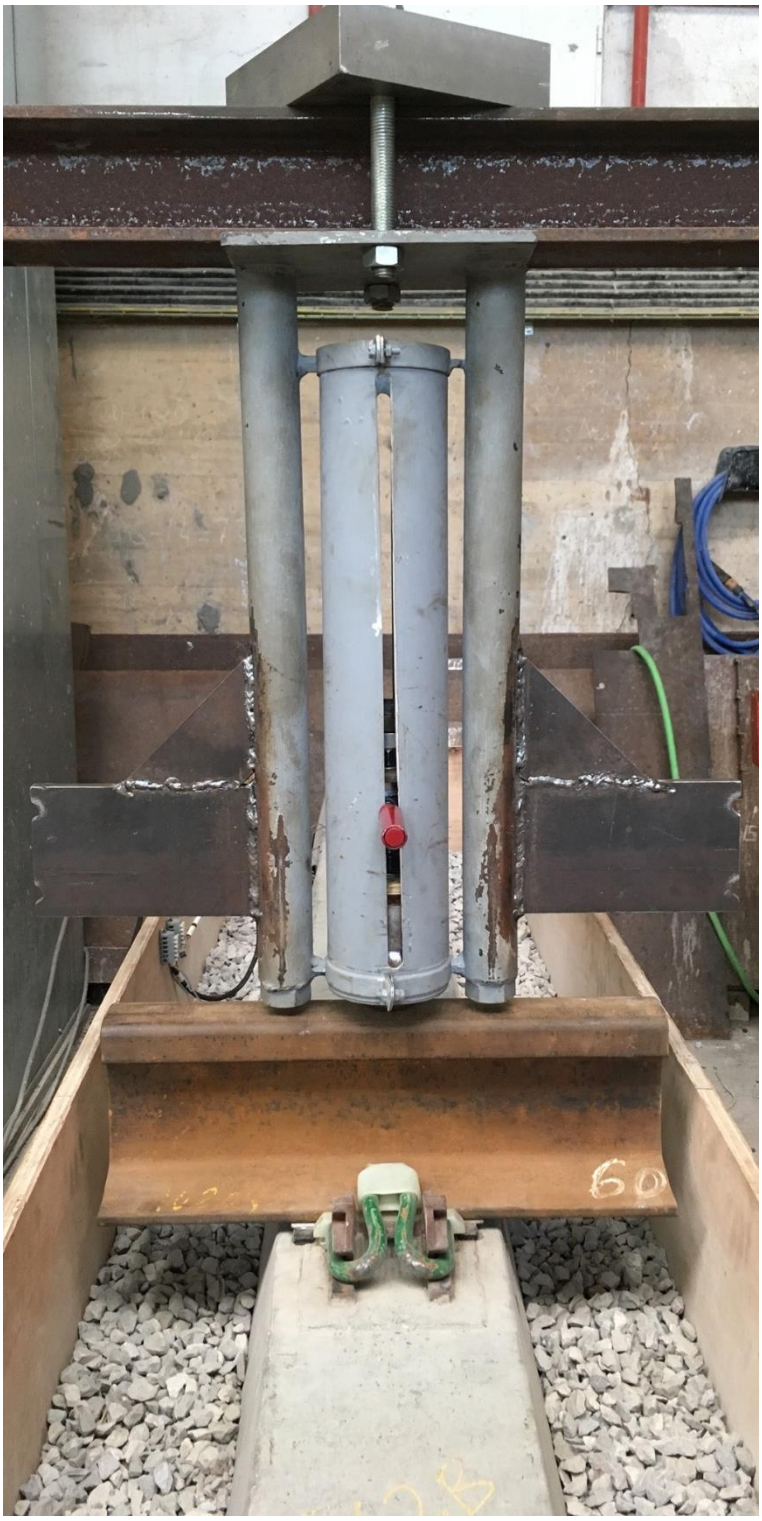

Figure 3.17. Reference method assembly

4. Equipment to carry out the tests and material employed

The tests were performed from October 2017 until May 2018. The equipment used consisted of the following:

- A bench equipped with a dynamic servo-hydraulic actuator INSTRON, class 0.5, endowed with a load cell capacity of ±100 kN in dynamic conditions.
- Equipment for the LVDT transducers, Universal High Speed Input "HBM Quantum MX410B".
- Software "HBM Catman" in order to process the data obtained.
- Two strain gauges explained afterwards in this chapter.
- Impact attenuation device and other tools to assemble the test, as explained in chapter 3.
- A wooden box filled with ballast particle size in the range 5 - 15 mm.
- A monoblock prestressed sleeper "Cemex".

Figure 4.1. Sleeper at its arrival to the lab

Figure 4.2. Detail of the reinforcement of the sleeper

- The rail fastening system, a Fast Clip, and a rail with a length of 0,5 m with the adequate section (UIC60), as it can be seen in the figure.

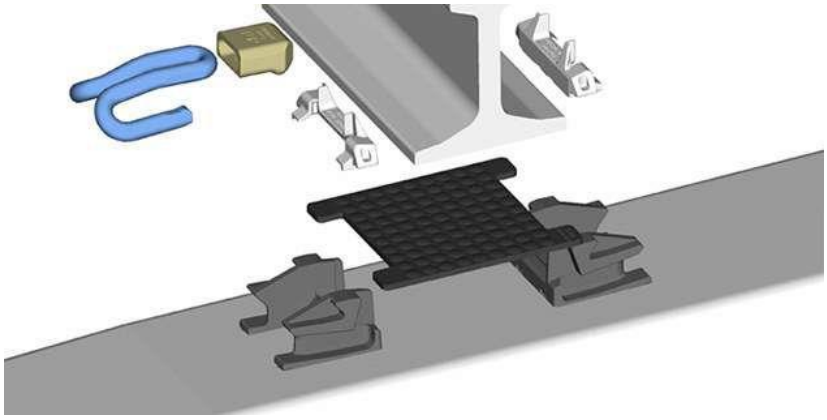

Figure 4.3. Fastening system [33]

Figure 4.4. Fastening of the rail

Strain gauges

A strain gauge is a sensor whose resistance varies with applied force; it converts strain into a change in electrical resistance, which can then be measured.

For the tests, two strain gauges of 120 mm nominal gauge length and 120 Ω nominal resistance have been used, as it can be seen in figure 4.5.

Figure 4.5. Strain gauges

Figure 6 represent the setup of the test. The lower gauge is situated between 10 and 25 mm from the bottom of the sleeper. The upper one is situated as close to the top as possible.

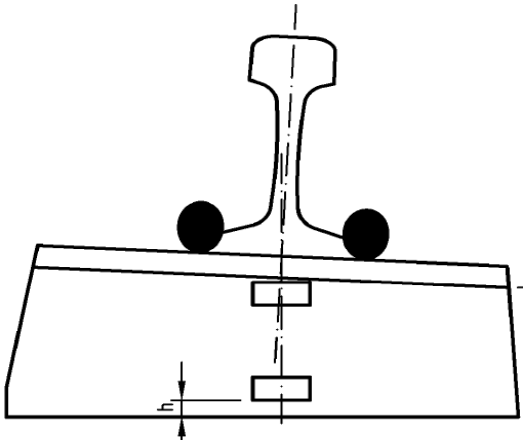

Figure 4.6. The position of the strain gauges [5]

Material used: Elastic pads

The elastic pads that are used in the tests are the following:

0. Reference pad. EVA solid PAD 5 mm thick. This pad is supplemented with aluminium pads with different thickness in order to equalise thickness with the tested pads. From now on: Solid EVA.

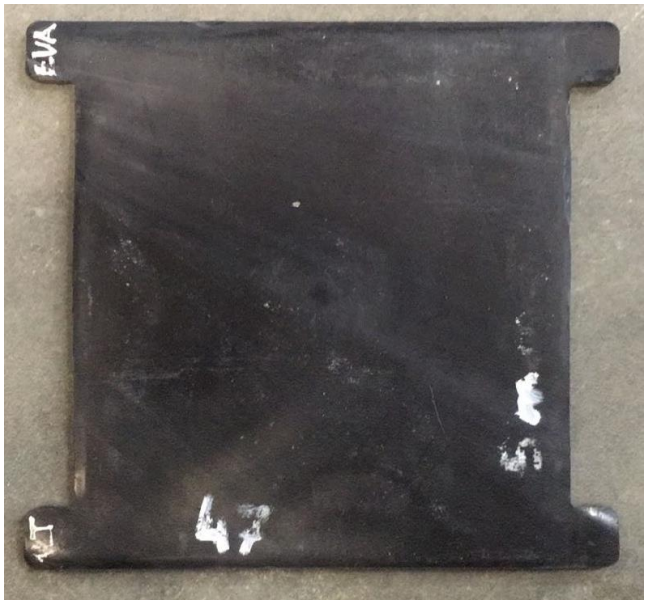

Figure 4.7. Solid EVA

A. Microcellular rubber, solid EDPM pad without studs, porous and 11 mm thick. From now on: Microcellular rubber.

Figure 4.8. Microcellular rubber

B. Solid NFU (pneumatic tyres out of use) pad with grain size lower than 4 mm, bound together with resin and 10 mm thick. From now on: Solid NFU.

Figure 4.9. Solid NFU

C. Studded EPDM pad with circular studs in both sides with 9 mm diameter, fabricated from EPDM and 11 mm thick. From now on: Studded EPDM.

Figure 4.10. Studded EPDM

D. Solid EPDM pad without studs, fabricated from EPDM and 7 mm thick. It is the pad used in Saudi Arabian high-speed trains. From now on: Solid EPDM.

Figure 4.11. Solid EPDM

E. Studded TPE (thermoplastic polyester elastomer, Hytrel) 7 mm thick. It is the pad used for Spanish high speed trains, PAE-2[27] .From now on: Studded TPE.

Figure 4.12. Studded TPE

F. Pad with 13 mm circular studs, EVA 10 mm thick. From now Studded EVA.

Figure 4.13. Studded EVA

G. Solid 11 mm rubber with textile reinforcement pad. From now on Solid reinforced rubber.

Figure 4.14. Solid reinforced rubber

Those pads are compared with EVA pads. The EVA pads need to have the same thickness as the pads tested. In order to achieve that thickness, as it has been mentioned before, EVA pads are supplemented with thin aluminium plates.

5. Experimental campaign: comparison between the two methods

The results regarding the strain values and attenuations are shown in this chapter.

Studded EPDM alternative method

REFERENCE PAD		EVA - 50kN			
		Test 1	Test 2	Test 3	Average
	$\varepsilon_{din,Upp}$	-91.75	-90.9	-90.31	-91.0
	$\varepsilon_{st,Upp}$	-42.55	-42.81	-42.5	-42.6
	$\varepsilon_{din,Low}$	87.6	87.56	86.93	87.4
	$\varepsilon_{st,Low}$	45.18	45.39	45.36	45.3

TEST PAD		Studded EPDM - 50kN			
		Test 1	Test 2	Test 3	Average
	$\varepsilon_{din,Upp}$	-82.37	-82.13	-82.45	-82.3
	$\varepsilon_{st,Upp}$	-40.9	-40.9	-40.83	-40.9
	$\varepsilon_{din,Low}$	77.69	78.35	79.53	78.5
	$\varepsilon_{st,Low}$	41.97	41.92	42.1	42.0

Attenuation		1	2	3
	a_{Upp}	14.26	14.76	13.95
	a_{Low}	15.06	13.37	10.99
	Σ_{Upp}	14.32		
	Σ_{Low}	13.14		
	a	13.73		

REFERENCE PAD		EVA - 25kN			
		Test 1	Test 2	Test 3	Average
	$\varepsilon_{din,Upp}$	-69.54	-70.22	-71.25	-70.3
	$\varepsilon_{st,Upp}$	-21.25	-21.65	-21.53	-21.5
	$\varepsilon_{din,Low}$	69.83	67.75	69.09	68.9
	$\varepsilon_{st,Low}$	25.42	25.15	25.13	25.2

TEST PAD		Studded EPDM - 25kN			
		Test 1	Test 2	Test 3	Average
	$\varepsilon_{din,Upp}$	-50.9	-52.24	-51.04	-51.4
	$\varepsilon_{st,Upp}$	-20.47	-20.36	-20.11	-20.3
	$\varepsilon_{din,Low}$	50.21	49.54	51.12	50.3
	$\varepsilon_{st,Low}$	20.7	20.42	20.63	20.6

Attenuation		1	2	3
	a_{Upp}	37.72	34.75	36.70
	a_{Low}	32.40	33.30	30.16
	Σ_{Upp}	36.39		
	Σ_{Low}	31.95		
	a	34.17		

REFERENCE PAD		EVA - 10kN			
		Test 1	Test 2	Test 3	Average
	$\varepsilon_{din,Upp}$	-60.03	-53.07	-57.06	-56.7
	$\varepsilon_{st,Upp}$	-8.83	-9.03	-8.95	-8.9
	$\varepsilon_{din,Low}$	56.29	53.2	55.46	55.0
	$\varepsilon_{st,Low}$	12.59	12.77	12.66	12.7

TEST PAD		Studded EPDM - 10kN			
		Test 1	Test 2	Test 3	Average
	$\varepsilon_{din,Upp}$	-25.7	-24.89	-24.74	-25.1
	$\varepsilon_{st,Upp}$	-7.63	-7.53	-7.84	-7.7
	$\varepsilon_{din,Low}$	24.33	23.21	24.43	24.0
	$\varepsilon_{st,Low}$	8.74	8.73	9.18	8.9

Attenuation		1	2	3
	a_{Upp}	62.18	63.67	64.63
	a_{Low}	63.15	65.78	63.96
	Σ_{Upp}	63.49		
	Σ_{Low}	64.30		
	a	63.90		

REFERENCE PAD		EVA - 5kN			
		Test 1	Test 2	Test 3	Average
	$\varepsilon_{din,Upp}$	-50.58	-53.47	-51.82	-52.0
	$\varepsilon_{st,Upp}$	-4.23	-4.05	-4.11	-4.1
	$\varepsilon_{din,Low}$	50.29	52.34	51.6	51.4
	$\varepsilon_{st,Low}$	7.78	7.94	7.94	7.9

TEST PAD		Studded EPDM - 5kN			
		Test 1	Test 2	Test 3	Average
	ε din, Upp	-22.56	-21.3	-23.25	-22.4
	ε st, Upp	-4.08	-4.12	-4.64	-4.3
	ε din, Low	21.41	20.56	19.16	20.4
	ε st, Low	4.61	4.05	3.78	4.1

Attenuation		1	2	3
	a Upp	61.36	64.08	61.09
	a Low	61.40	62.07	64.66
	Σ Upp	62.18		
	Σ Low	62.71		
	a	62.44		

REFERENCE PAD		EVA - 0kN			
		Test 1	Test 2	Test 3	Average
	ε din, Upp	-52.21	-53.71	-51.02	-52.3
	ε st, Upp	0	0	0	0.0
	ε din, Low	47.28	50.2	46.77	48.1
	ε st, Low	0	0	0	0.0

TEST PAD		Studded EPDM - 0kN			
		Test 1	Test 2	Test 3	Average
	ε din, Upp	-19.92	-18.37	-18.72	-19.0
	ε st, Upp	0	0	0	0.0
	ε din, Low	18.94	19.55	20.25	19.6
	ε st, Low	0	0	0	0.0

Attenuation		1	2	3
	a Upp	61.92	64.88	64.22
	a Low	60.61	59.34	57.89
	Σ Upp	63.67		
	Σ Low	59.28		
	a	61.48		

Studded EVA alternative method

REFERENCE PAD		EVA - 50kN			
		Test 1	Test 2	Test 3	MEAN
με	ε din, Upp	-87.46	-88.65	-87.66	-87.9
	ε st, Upp	-42.3	-41.88	-41.84	-42.0
	ε din, Low	85.99	84.97	85.82	85.6
	ε st, Low	42.63	42.85	42.88	42.8

TESTED PAD		Studded EVA - 50kN			
		Test 1	Test 2	Test 3	MEAN
με	ε din, Upp	-80.15	-79.7	-78.93	-79.6
	ε st, Upp	-38.81	-39.59	-39.39	-39.3
	ε din, Low	76.18	75.26	75.02	75.5
	ε st, Low	37.64	38.43	38.52	38.2

Results		1	2	3
	a upper	9.97	12.65	13.89
	a lower	9.97	13.96	14.73
	Σ upper	12.17		
	Σ lower	12.89		
	a(%)	12.53		

REFERENCE PAD		EVA - 25kN			
		Test 1	Test 2	Test 3	MEAN
με	ε din, Upp	-68.4	-73.57	-68.61	-70.2
	ε st, Upp	-21.82	-21.61	-21.43	-21.6
	ε din, Low	64.94	68.15	66.01	66.4
	ε st, Low	22.27	22.08	22.24	22.2

TESTED PAD		Studded EVA - 25kN			
		Test 1	Test 2	Test 3	MEAN
με	ε din, Upp	-59.47	-58.43	-60.53	-59.5
	ε st, Upp	-19.61	-18.55	-18.96	-19.0
	ε din, Low	58.82	59.86	58.69	59.1
	ε st, Low	17.62	21.67	21.57	20.3

Results		1	2	3
	a upper	17.94	17.90	14.42
	a lower	6.72	13.54	15.96
	Σ upper	16.75		
	Σ lower	12.07		
	a(%)	14.41		

REFERENCE PAD		EVA - 10kN			
		Test 1	Test 2	Test 3	MEAN
με	ε din, Upp	-56.2	-57.64	-58.78	-57.5
	ε st, Upp	-9.23	-8.94	-8.89	-9.0
	ε din, Low	52.48	54.97	54.29	53.9
	ε st, Low	10.22	9.88	9.95	10.0

TESTED PAD		Studded EVA - 10kN			
		Test 1	Test 2	Test 3	MEAN
με	ε din, Upp	-47.77	-45.88	-48.66	-47.4
	ε st, Upp	-6.88	-6.69	-6.59	-6.7
	ε din, Low	45.84	45.4	46.5	45.9
	ε st, Low	9.05	9.44	9.09	9.2

Results		1	2	3
	a upper	15.73	19.23	13.29
	a lower	16.19	18.08	14.78
	Σ upper	16.08		
	Σ lower	16.35		
	a(%)	16.22		

REFERENCE PAD		EVA - 5kN			
		Test 1	Test 2	Test 3	MEAN
με	ε din, Upp	-50.49	-52.36	-53.61	-52.2
	ε st, Upp	-4.38	-4.46	-4.38	-4.4
	ε din, Low	47.51	49.64	49.94	49.0
	ε st, Low	5.22	5.37	5.21	5.3

TESTED PAD		Studded EVA - 5kN			
		Test 1	Test 2	Test 3	MEAN
με	ε din, Upp	-44.13	-44.27	-43.76	-44.1
	ε st, Upp	-2.21	-1.88	-1.97	-2.0
	ε din, Low	42.84	42.85	43.09	42.9
	ε st, Low	4.99	5.91	4.92	5.3

Results		1	2	3
	a upper	12.20	11.22	12.48
	a lower	13.51	15.59	12.78
	Σ upper	11.97		
	Σ lower	13.96		
	a(%)	12.96		

REFERENCE PAD		EVA - 0kN			
		Test 1	Test 2	Test 3	MEAN
με	$\varepsilon_{din,Upp}$	-52.15	-50.08	-49.61	-50.6
	$\varepsilon_{st,Upp}$	1	0.5	0.6	0.7
	$\varepsilon_{din,Low}$	52.42	46.91	49.34	49.6
	$\varepsilon_{st,Low}$	0.4	0.8	0.75	0.7

TESTED PAD		Studded EVA - 0kN			
		Test 1	Test 2	Test 3	MEAN
με	$\varepsilon_{din,Upp}$	-48.3	-46.02	-50.58	-48.3
	$\varepsilon_{st,Upp}$	0	0	0	0.0
	$\varepsilon_{din,Low}$	39.35	40.76	37.38	39.2
	$\varepsilon_{st,Low}$	0	0	0	0.0

Results		1	2	3
	a_{upper}	5.87	10.32	1.43
	a_{lower}	19.54	16.66	23.57
	Σ_{upper}	5.87		
	Σ_{lower}	19.92		
	a(%)	12.90		

Microcellular rubber alternative method

REFERENCE PAD		EVA - 50kN			
		Ensayo 1	Ensayo 2	Ensayo 3	MEDIA
	$\varepsilon_{din,Upp}$	-91.75	-90.9	-90.31	-91.0
	$\varepsilon_{st,Upp}$	-42.55	-42.81	-42.5	-42.6
	$\varepsilon_{din,Low}$	87.6	87.56	86.93	87.4
	$\varepsilon_{st,Low}$	45.18	45.39	45.36	45.3

TESTED PAD		Microcellular rubber - 50kN			
		Ensayo 1	Ensayo 2	Ensayo 3	
	$\varepsilon_{din,Upp}$	-86.2	-87.66	-87.98	-87.3
	$\varepsilon_{st,Upp}$	-40.39	-40.56	-40.55	-40.5
	$\varepsilon_{din,Low}$	81.47	81.63	81.5	81.5
	$\varepsilon_{st,Low}$	41.01	41.21	41.19	41.1

Results		1	2	3
	a_{upper}	5.29	2.62	1.94
	a_{lower}	3.79	3.88	4.15
	Σ_{upper}	3.28		

	Σ lower	3.94
	a(%)	3.61

REFERENCE PAD		EVA - 25kN			
		Ensayo 1	Ensayo 2	Ensayo 3	MEDIA
	$\varepsilon_{din,\ Upp}$	-69.54	-70.22	-71.25	-70.3
	$\varepsilon_{st,\ Upp}$	-21.25	-21.65	-21.53	-21.5
	$\varepsilon_{din,\ Low}$	69.83	67.75	69.09	68.9
	$\varepsilon_{st,\ Low}$	25.42	25.15	25.13	25.2

TESTED PAD		Microcellular rubber - 25kN			
		Ensayo 1	Ensayo 2	Ensayo 3	
	$\varepsilon_{din,\ Upp}$	-48.47	-48.19	-49.03	-48.6
	$\varepsilon_{st,\ Upp}$	-20.58	-20.6	-20.59	-20.6
	$\varepsilon_{din,\ Low}$	48.29	47.75	48.02	48.0
	$\varepsilon_{st,\ Low}$	21.83	21.49	21.53	21.6

Results				
		1	2	3
	a_{upper}	42.92	43.53	41.79
	a_{lower}	39.39	39.85	39.32
	Σ_{upper}	42.75		
	Σ_{lower}	39.52		
	a(%)	41.13		

REFERENCE PAD		EVA - 10kN			
		Ensayo 1	Ensayo 2	Ensayo 3	MEDIA
	$\varepsilon_{din,\ Upp}$	-60.03	-53.07	-57.06	-56.7
	$\varepsilon_{st,\ Upp}$	-8.83	-9.03	-8.95	-8.9
	$\varepsilon_{din,\ Low}$	56.29	53.2	55.46	55.0
	$\varepsilon_{st,\ Low}$	12.59	12.77	12.66	12.7

TESTED PAD		Microcellular rubber - 10kN			
		Ensayo 1	Ensayo 2	Ensayo 3	
	$\varepsilon_{din,\ Upp}$	-25.78	-24.15	-25.43	-25.1
	$\varepsilon_{st,\ Upp}$	-9.09	-8.62	-8.54	-8.8
	$\varepsilon_{din,\ Low}$	22.44	22.05	22.41	22.3
	$\varepsilon_{st,\ Low}$	9.6	10.32	10.12	10.0

Results		1	2	3
	a upper	65.07	67.50	64.65
	a lower	69.65	72.28	70.95
	Σ upper	65.74		
	Σ lower	70.96		
	a(%)	68.35		

REFERENCE PAD		EVA - 5kN			
		Ensayo 1	Ensayo 2	Ensayo 3	MEDIA
	ε din, Upp	-50.58	-53.47	-51.82	-52.0
	ε st, Upp	-4.23	-4.05	-4.11	-4.1
	ε din, Low	50.29	52.34	51.6	51.4
	ε st, Low	7.78	7.94	7.94	7.9

TESTED PAD		Microcellular rubber - 5kN			
		Ensayo 1	Ensayo 2	Ensayo 3	
	ε din, Upp	-17.61	-20.14	-19.6	-19.1
	ε st, Upp	-3.13	-3.4	-3.82	-3.5
	ε din, Low	14.8	17.59	17.24	16.5
	ε st, Low	5.16	5.43	5.22	5.3

Results		1	2	3
	a upper	69.72	65.00	67.01
	a lower	77.85	72.06	72.38
	Σ upper	67.24		
	Σ lower	74.10		
	a(%)	70.67		

REFERENCE PAD		EVA - 0kN			
		Ensayo 1	Ensayo 2	Ensayo 3	MEDIA
	ε din, Upp	-52.21	-53.71	-51.02	-52.3
	ε st, Upp	0	0	0	0.0
	ε din, Low	47.28	50.2	46.77	48.1
	ε st, Low	0	0	0	0.0

TESTED PAD		Microcellular rubber - 0kN			
		Ensayo 1	Ensayo 2	Ensayo 3	
	ε din, Upp	-19.47	-11.73	-10.44	-13.9
	ε st, Upp	0	0	0	0.0
	ε din, Low	24.09	12.13	14.44	16.9
	ε st, Low	0	0	0	0.0

Results		1	2	3
	a upper	62.78	77.58	80.04
	a lower	49.90	74.77	69.97
	Σ upper	73.47		
	Σ lower	64.88		
	a(%)	69.17		

Studded TPE alternative method

REFERENCE PAD		EVA - 50kN			
		Ensayo 1	Ensayo 2	Ensayo 3	MEDIA
	ε din, Upp	-92.81	-93.04	-92.61	-92.8
	ε st, Upp	-45.26	-45.25	-44.94	-45.2
	ε din, Low	82.84	84.86	88.07	85.3
	ε st, Low	41.99	42.23	42.23	42.2

TESTED PAD		Studded TPE - 50kN			
		Ensayo 1	Ensayo 2	Ensayo 3	
	ε din, Upp	-80.5	-80.73	-80.97	-80.7
	ε st, Upp	-42.6	-41.91	-42.35	-42.3
	ε din, Low	77.86	79.42	78.2	78.5
	ε st, Low	43.47	43.51	43.1	43.4

Results		1	2	3
	a upper	20.50	18.57	18.98
	a lower	20.22	16.70	18.57
	Σ upper	19.35		
	Σ lower	18.50		
	a(%)	18.92		

REFERENCE PAD		EVA - 25kN			
		Ensayo 1	Ensayo 2	Ensayo 3	MEDIA
	ε din, Upp	-72.23	-70.27	-71.67	-71.4
	ε st, Upp	-23.41	-23.59	-23.71	-23.6
	ε din, Low	65.91	66.2	63.77	65.3
	ε st, Low	21.23	21.25	21.34	21.3

TESTED PAD		Studded TPE - 25kN			
		Ensayo 1	Ensayo 2	Ensayo 3	
	ε din, Upp	-56.7	-57.25	-56.22	-56.7
	ε st, Upp	-21.32	-21.37	-21.82	-21.5
	ε din, Low	54.69	55.08	54.03	54.6
	ε st, Low	22.26	22.22	22.04	22.2

Results		1	2	3
	a upper	26.01	24.97	28.06
	a lower	26.33	25.35	27.33
	Σ upper	26.35		
	Σ lower	26.34		
	a(%)	26.34		

REFERENCE PAD		EVA - 10kN			
		Ensayo 1	Ensayo 2	Ensayo 3	MEDIA
	ε din, Upp	-59.22	-59.2	-59.12	-59.2
	ε st, Upp	-10.79	-10.74	-10.97	-10.8
	ε din, Low	50.21	50.53	53.12	51.3
	ε st, Low	8.51	8.51	8.59	8.5

TESTED PAD		Studded TPE - 10kN			
		Ensayo 1	Ensayo 2	Ensayo 3	
	ε din, Upp	-44.38	-44.5	-44.76	-44.5
	ε st, Upp	-9.28	-9.15	-9.26	-9.2
	ε din, Low	41.4	39.97	39.43	40.3
	ε st, Low	9.73	9.64	9.57	9.6

Results		1	2	3
	a upper	27.40	26.88	26.57
	a lower	25.92	29.05	30.15
	Σ upper	26.95		
	Σ lower	28.37		

	a(%)	27.66

Solid EPDM alternative method

REFERENCE PAD		EVA - 50kN			
		Ensayo 1	Ensayo 2	Ensayo 3	MEDIA
	$\varepsilon_{din,Upp}$	-92.81	-93.04	-92.61	-92.8
	$\varepsilon_{st,Upp}$	-45.26	-45.25	-44.94	-45.2
	$\varepsilon_{din,Low}$	82.84	84.86	88.07	85.3
	$\varepsilon_{st,Low}$	41.99	42.23	42.23	42.2

TESTED PAD		Solid EPDM - 50kN			
		Ensayo 1	Ensayo 2	Ensayo 3	
	$\varepsilon_{din,Upp}$	-84.9	-84.59	-87.9	-85.8
	$\varepsilon_{st,Upp}$	-44.42	-44.02	-44.16	-44.2
	$\varepsilon_{din,Low}$	78.59	76.97	79.35	78.3
	$\varepsilon_{st,Low}$	40.36	40.89	40.59	40.6

Results		1	2	3
	a_{upper}	15.08	14.89	8.24
	a_{lower}	11.31	16.30	10.08
	Σ_{upper}	12.74		
	Σ_{lower}	12.57		
	a(%)	12.65		

REFERENCE PAD		EVA - 25kN			
		Ensayo 1	Ensayo 2	Ensayo 3	MEDIA
	$\varepsilon_{din,Upp}$	-72.23	-70.27	-71.67	-71.4
	$\varepsilon_{st,Upp}$	-23.41	-23.59	-23.71	-23.6
	$\varepsilon_{din,Low}$	65.91	66.2	63.77	65.3
	$\varepsilon_{st,Low}$	21.23	21.25	21.34	21.3

TESTED PAD		Solid EPDM - 25kN			
		Ensayo 1	Ensayo 2	Ensayo 3	
	$\varepsilon_{din,Upp}$	-53.43	-53.39	-53.24	-53.4
	$\varepsilon_{st,Upp}$	-24.46	-24.35	-23.59	-24.1
	$\varepsilon_{din,Low}$	44.86	45.37	45.52	45.3
	$\varepsilon_{st,Low}$	20.05	20.51	20.02	20.2

Results		1	2	3
	a_{upper}	39.42	39.27	38.00
	a_{lower}	43.64	43.53	42.07
	Σ_{upper}	38.90		
	Σ_{lower}	43.08		
	a(%)	40.99		

REFERENCE PAD		EVA - 10kN			
		Ensayo 1	Ensayo 2	Ensayo 3	MEDIA
	$\varepsilon_{din,\ Upp}$	-59.22	-59.2	-59.12	-59.2
	$\varepsilon_{st,\ Upp}$	-10.79	-10.74	-10.97	-10.8
	$\varepsilon_{din,\ Low}$	50.21	50.53	53.12	51.3
	$\varepsilon_{st,\ Low}$	8.51	8.51	8.59	8.5

TESTED PAD		Solid EPDM - 10kN			
		Ensayo 1	Ensayo 2	Ensayo 3	
	$\varepsilon_{din,\ Upp}$	-35.07	-32.52	-31.63	-33.1
	$\varepsilon_{st,\ Upp}$	-11.13	-11.2	-10.1	-10.8
	$\varepsilon_{din,\ Low}$	29.61	28.55	27.56	28.6
	$\varepsilon_{st,\ Low}$	8.24	8.05	8.15	8.1

Results		1	2	3
	a_{upper}	50.48	55.90	55.47
	a_{lower}	50.01	52.05	54.60
	Σ_{upper}	53.95		
	Σ_{lower}	52.22		
	a(%)	53.08		

Solid reinforced rubber alternative method

REFERENCE PAD		EVA - 50kN			
		Ensayo 1	Ensayo 2	Ensayo 3	MEDIA
	$\varepsilon_{din,\ Upp}$	-91.75	-90.9	-90.31	-91.0
	$\varepsilon_{st,\ Upp}$	-42.55	-42.81	-42.5	-42.6
	$\varepsilon_{din,\ Low}$	87.6	87.56	86.93	87.4
	$\varepsilon_{st,\ Low}$	45.18	45.39	45.36	45.3

TESTED PAD		Solid reinforced rubber - 50kN			
		Ensayo 1	Ensayo 2	Ensayo 3	
	$\varepsilon_{din,\ Upp}$	-79.45	-82.04	-82.01	-81.2
	$\varepsilon_{st,\ Upp}$	-42.54	-43.42	-43.86	-43.3
	$\varepsilon_{din,\ Low}$	80.63	81.31	81.61	81.2
	$\varepsilon_{st,\ Low}$	44.76	43.98	44.38	44.4

Results				
		1	2	3
	a_{upper}	23.69	20.15	21.12
	a_{lower}	14.70	11.23	11.47
	Σ_{upper}	21.65		
	Σ_{lower}	12.47		
	a(%)	17.06		

REFERENCE PAD		EVA - 25kN			
		Ensayo 1	Ensayo 2	Ensayo 3	MEDIA
	$\varepsilon_{din,\ Upp}$	-69.54	-70.22	-71.25	-70.3
	$\varepsilon_{st,\ Upp}$	-21.25	-21.65	-21.53	-21.5
	$\varepsilon_{din,\ Low}$	69.83	67.75	69.09	68.9
	$\varepsilon_{st,\ Low}$	25.42	25.15	25.13	25.2

TESTED PAD		Solid reinforced rubber - 25kN			
		Ensayo 1	Ensayo 2	Ensayo 3	
	$\varepsilon_{din,\ Upp}$	-54.97	-54.83	-55.23	-55.0
	$\varepsilon_{st,\ Upp}$	-18.59	-19.4	-19.52	-19.2
	$\varepsilon_{din,\ Low}$	55.7	56.05	56.58	56.1
	$\varepsilon_{st,\ Low}$	21.94	22.54	22.4	22.3

Results				
		1	2	3
	a_{upper}	25.54	27.49	26.91
	a_{lower}	22.67	23.24	21.71
	Σ_{upper}	26.65		
	Σ_{lower}	22.54		
	a(%)	24.59		

REFERENCE PAD		EVA - 10kN			
		Ensayo 1	Ensayo 2	Ensayo 3	MEDIA
	$\varepsilon_{din,\ Upp}$	-60.03	-53.07	-57.06	-56.7
	$\varepsilon_{st,\ Upp}$	-8.83	-9.03	-8.95	-8.9
	$\varepsilon_{din,\ Low}$	56.29	53.2	55.46	55.0
	$\varepsilon_{st,\ Low}$	12.59	12.77	12.66	12.7

TESTED PAD		Solid reinforced rubber - 10kN			
		Ensayo 1	Ensayo 2	Ensayo 3	
	ε din, Upp	-44.5	-46.69	-45.56	-45.6
	ε st, Upp	-9.4	-9.4	-9.41	-9.4
	ε din, Low	43.34	43.82	44.17	43.8
	ε st, Low	8.4	8.11	8.01	8.2

Results				
		1	2	3
	a upper	26.54	21.96	24.35
	a lower	17.42	15.60	14.54
	Σ upper	24.28		
	Σ lower	15.85		
	a(%)	20.07		

REFERENCE PAD		EVA - 5kN			
		Ensayo 1	Ensayo 2	Ensayo 3	MEDIA
	ε din, Upp	-50.58	-53.47	-51.82	-52.0
	ε st, Upp	-4.23	-4.05	-4.11	-4.1
	ε din, Low	50.29	52.34	51.6	51.4
	ε st, Low	7.78	7.94	7.94	7.9

TESTED PAD		Solid reinforced rubber - 5kN			
		Ensayo 1	Ensayo 2	Ensayo 3	
	ε din, Upp	-40.3	-41.58	-45.65	-42.5
	ε st, Upp	-4.55	-4.72	-4.8	-4.7
	ε din, Low	39.76	39.05	41.47	40.1
	ε st, Low	4.67	4.3	4.42	4.5

Results				
		1	2	3
	a upper	25.25	22.93	14.59
	a lower	19.38	20.16	14.87
	Σ upper	20.92		
	Σ lower	18.14		
	a(%)	19.53		

REFERENCE PAD		EVA - 0kN			
		Ensayo 1	Ensayo 2	Ensayo 3	MEDIA
	$\varepsilon_{din,\ Upp}$	-52.21	-53.71	-51.02	-52.3
	$\varepsilon_{st,\ Upp}$	0	0	0	0.0
	$\varepsilon_{din,\ Low}$	47.28	50.2	46.77	48.1
	$\varepsilon_{st,\ Low}$	0	0	0	0.0

TESTED PAD		Solid reinforced rubber - 0kN			
		Ensayo 1	Ensayo 2	Ensayo 3	
	$\varepsilon_{din,\ Upp}$	-39.26	-39.92	-43.11	-40.8
	$\varepsilon_{st,\ Upp}$	-1.38	-1.36	-0.95	-1.2
	$\varepsilon_{din,\ Low}$	39.48	38.33	39.12	39.0
	$\varepsilon_{st,\ Low}$	0.4	0.22	0.22	0.3

Results				
		1	2	3
	a_{upper}	27.59	26.29	19.41
	a_{lower}	18.72	20.74	19.10
	Σ_{upper}	24.43		
	Σ_{lower}	19.52		
	a(%)	21.98		

Solid NFU alternative method

REFERENCE PAD		EVA - 50kN			
		Ensayo 1	Ensayo 2	Ensayo 3	MEDIA
	$\varepsilon_{din,\ Upp}$	-91.75	-90.9	-90.31	-91.0
	$\varepsilon_{st,\ Upp}$	-42.55	-42.81	-42.5	-42.6
	$\varepsilon_{din,\ Low}$	87.6	87.56	86.93	87.4
	$\varepsilon_{st,\ Low}$	45.18	45.39	45.36	45.3

TESTED PAD		Solid NFU - 50kN			
		Ensayo 1	Ensayo 2	Ensayo 3	
	$\varepsilon_{din,\ Upp}$	-82.34	-84.65	-83.96	-83.7
	$\varepsilon_{st,\ Upp}$	-42.2	-42.05	-43.45	-42.6
	$\varepsilon_{din,\ Low}$	83.12	86.01	84.39	84.5
	$\varepsilon_{st,\ Low}$	46.43	46.52	47.91	47.0

Results		1	2	3
	a upper	17.01	11.92	16.24
	a lower	12.75	6.10	13.25
	Σ upper	15.06		
	Σ lower	10.70		
	a(%)	12.88		

REFERENCE PAD		EVA - 25kN			
		Ensayo 1	Ensayo 2	Ensayo 3	MEDIA
	ε din, Upp	-69.54	-70.22	-71.25	-70.3
	ε st, Upp	-21.25	-21.65	-21.53	-21.5
	ε din, Low	69.83	67.75	69.09	68.9
	ε st, Low	25.42	25.15	25.13	25.2

TESTED PAD		Solid NFU - 25kN			
		Ensayo 1	Ensayo 2	Ensayo 3	
	ε din, Upp	-53.06	-53.08	-51.92	-52.7
	ε st, Upp	-18.65	-19.17	-18.84	-18.9
	ε din, Low	52.25	52.63	51.15	52.0
	ε st, Low	21.03	20.69	20.59	20.8

Results		1	2	3
	a upper	29.57	30.60	32.30
	a lower	28.49	26.84	30.00
	Σ upper	30.82		
	Σ lower	28.44		
	a(%)	29.63		

REFERENCE PAD		EVA - 10kN			
		Ensayo 1	Ensayo 2	Ensayo 3	MEDIA
	ε din, Upp	-60.03	-53.07	-57.06	-56.7
	ε st, Upp	-8.83	-9.03	-8.95	-8.9
	ε din, Low	56.29	53.2	55.46	55.0
	ε st, Low	12.59	12.77	12.66	12.7

TESTED PAD		Solid NFU - 10kN			
		Ensayo 1	Ensayo 2	Ensayo 3	
	ε din, Upp	-29.93	-30.68	-29.94	-30.2
	ε st, Upp	-6.95	-6.69	-7.28	-7.0
	ε din, Low	32.01	30.75	31.05	31.3
	ε st, Low	9.57	9.52	9.14	9.4

Results		1	2	3
	a upper	51.91	49.79	52.58
	a lower	46.96	49.82	48.22
	Σ upper	51.43		
	Σ lower	48.33		
	a(%)	49.88		

Solid EPDM reference method

REFERENCE PAD		EVA 7mm - 96000Hz			
		Ensayo 1	Ensayo 2	Ensayo 3	MEDIA
	ε din, Upp	-85.09	-78.3	-84.39	-82.6
	ε st, Upp	0	0	0	0.0
	ε din, Low	56.55	55.73	53.93	55.4
	ε st, Low	0	0	0	0.0

TESTED PAD		Solid EPDM- 7mm			
		Ensayo 1	Ensayo 2	Ensayo 3	
	ε din, Upp	-34.11	-37.46	-36.22	-35.9
	ε st, Upp	0	0	0	0.0
	ε din, Low	19.07	16.27	18.34	17.9
	ε st, Low	0	0	0	0.0

Results		1	2	3
	a upper	58.70	54.65	56.15
	a lower	65.58	70.63	66.90
	Σ upper	56.50		
	Σ lower	67.70		
	a(%)	62.10		

Studded TPE reference method

REFERENCE PAD		EVA 7mm - 96000Hz			
		Ensayo 1	Ensayo 2	Ensayo 3	MEDIA
	ε din, Upp	-85.09	-78.3	-84.39	-82.6
	ε st, Upp	0	0	0	0.0
	ε din, Low	56.55	55.73	53.93	55.4
	ε st, Low	0	0	0	0.0

TESTED PAD		Studded TPE- 7mm			
		Ensayo 1	Ensayo 2	Ensayo 3	
	ε din, Upp	-53.14	-57.73	-55.79	-55.6
	ε st, Upp	0	0	0	0.0
	ε din, Low	33.62	31.08	30.14	31.6
	ε st, Low	0	0	0	0.0

Results		1	2	3
	a upper	35.66	30.10	32.45
	a lower	39.32	43.90	45.60
	Σ upper	32.74		
	Σ lower	42.94		
	a(%)	37.84		

Studded EPDM reference method

REFERENCE PAD		EVA-11mm 96000Hz			
		Ensayo 1	Ensayo 2	Ensayo 3	MEDIA
	ε din, Upp	-84.59	-79.92	-82.72	-82.4
	ε st, Upp	0	0	0	0.0
	ε din, Low	48.64	50.74	56.26	51.9
	ε st, Low	0	0	0	0.0

TESTED PAD		Studded EPDM-11mm 96000 Hz			
		Ensayo 1	Ensayo 2	Ensayo 3	
	ε din, Upp	-31.97	-15.35	-40	-29.1
	ε st, Upp	0	0	0	0.0
	ε din, Low	14.88	16.42	15.37	15.6
	ε st, Low	0	0	0	0.0

Results				
		1	2	3
	a upper	61.21	81.37	51.46
	a lower	71.32	68.35	70.37
	Σ upper	64.68		
	Σ lower	70.01		
	a(%)	67.35		

Microcellular rubber reference method

REFERENCE PAD		EVA-11mm 96000Hz			
		Ensayo 1	Ensayo 2	Ensayo 3	MEDIA
	ε din, Upp	-84.59	-79.92	-82.72	-82.4
	ε st, Upp	0	0	0	0.0
	ε din, Low	48.64	50.74	56.26	51.9
	ε st, Low	0	0	0	0.0

TESTED PAD		Microcellular rubber 11 mm			
		Ensayo 1	Ensayo 2	Ensayo 3	
	ε din, Upp	-16.09	-15.35	-15.16	-15.5
	ε st, Upp	0	0	0	0.0
	ε din, Low	11.88	12.1	9.97	11.3
	ε st, Low	0	0	0	0.0

Results				
		1	2	3
	a upper	80.48	81.37	81.60
	a lower	77.10	76.68	80.78
	Σ upper	81.15		
	Σ lower	78.19		
	a(%)	79.67		

Solid NFU reference method

REFERENCE PAD		EVA-11mm 96000Hz			
		Ensayo 1	Ensayo 2	Ensayo 3	MEDIA
	$\varepsilon_{din,Upp}$	-84.59	-79.92	-82.72	-82.4
	$\varepsilon_{st,Upp}$	0	0	0	0.0
	$\varepsilon_{din,Low}$	48.64	50.74	56.26	51.9
	$\varepsilon_{st,Low}$	0	0	0	0.0

TESTED PAD		Solid NFU 11mm			
		Ensayo 1	Ensayo 2	Ensayo 3	
	$\varepsilon_{din,Upp}$	-23.48	-24	-26.6	-24.7
	$\varepsilon_{st,Upp}$	0	0	0	0.0
	$\varepsilon_{din,Low}$	11.4	10.41	10.92	10.9
	$\varepsilon_{st,Low}$	0	0	0	0.0

Results		1	2	3
	a_{upper}	71.51	70.88	67.72
	a_{lower}	78.03	79.93	78.95
	Σ_{upper}	70.04		
	Σ_{lower}	78.97		
	a(%)	74.50		

Solid reinforced rubber reference method

REFERENCE PAD		EVA-11mm 96000Hz			
		Ensayo 1	Ensayo 2	Ensayo 3	MEDIA
	$\varepsilon_{din,Upp}$	-84.59	-79.92	-82.72	-82.4
	$\varepsilon_{st,Upp}$	0	0	0	0.0
	$\varepsilon_{din,Low}$	48.64	50.74	56.26	51.9
	$\varepsilon_{st,Low}$	0	0	0	0.0

TESTED PAD		Solid reinforced rubber			
		Ensayo 1	Ensayo 2	Ensayo 3	
	$\varepsilon_{din,Upp}$	-54.71	-51.8	-58.59	-55.0
	$\varepsilon_{st,Upp}$	0	0	0	0.0
	$\varepsilon_{din,Low}$	36.26	37.35	38.64	37.4
	$\varepsilon_{st,Low}$	0	0	0	0.0

Results		1	2	3
	a_{upper}	33.61	37.14	28.90
	a_{lower}	30.11	28.01	25.52
	Σ_{upper}	33.22		
	Σ_{lower}	27.88		
	a(%)	30.55		

6. Validation: results

Stiffness

In the following table we can see the results regarding stiffness. There are two different values of static stiffness shown: the first one is the one stablished by the Standard[6] (k_e: 18–68 kN) and the other one gathers up the behaviour due to low loads ($k_{e'}$: 1-68 kN). In figure 1 and 2 it is shown a comparison between static and dynamic behaviours at 10 Hz for the pads employed for the study.

PAD	Static stiffness, k_e (18-68 kN) [kN/mm]	Static stiffness, k'_e (1-68 kN) [kN/mm]	Dynamic stiffness 5 Hz, $k_{d\ 5Hz}$ [kN/mm]	Dynamic rigidity 10 Hz, $k_{d\ 10Hz}$ [kN/mm]	Dynamic rigidity 20 Hz, $k_{d\ 20Hz}$ [kN/mm]	Dynamic rigidity media, k_{dm} [kN/mm]	Shore Hardness D
0 (ref)	694.4	349.6	1282.1	1362.4	1572.3	1405.6	49.8
A	53.5	10.0	106.4	116.0	134.4	118.9	7.0
B	65.8	17.3	183.8	199.2	229.4	204.1	---
C	68.5	30.0	93.1	97.3	110.6	100.3	29.8
D	35.5	43.6	90.6	94.7	106.8	97.4	22
E	126.9	85.0	162.9	169.5	188.0	173.5	44.6
F	140.8	88.7	320.5	344.8	387.6	351.0	50.1
G	284.1	152.9	490.0	515.5	588.2	531.2	27.0

Table 4. Summary of dynamic and static stiffness and hardness.

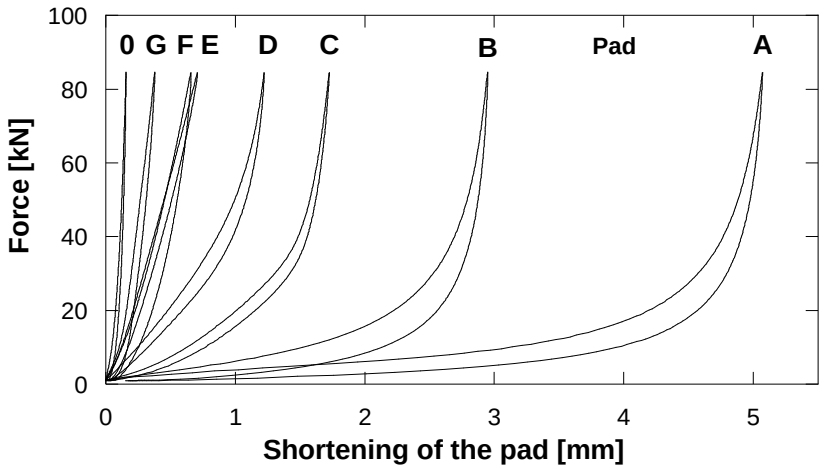

Figure 6.1. Static behaviour of the pads

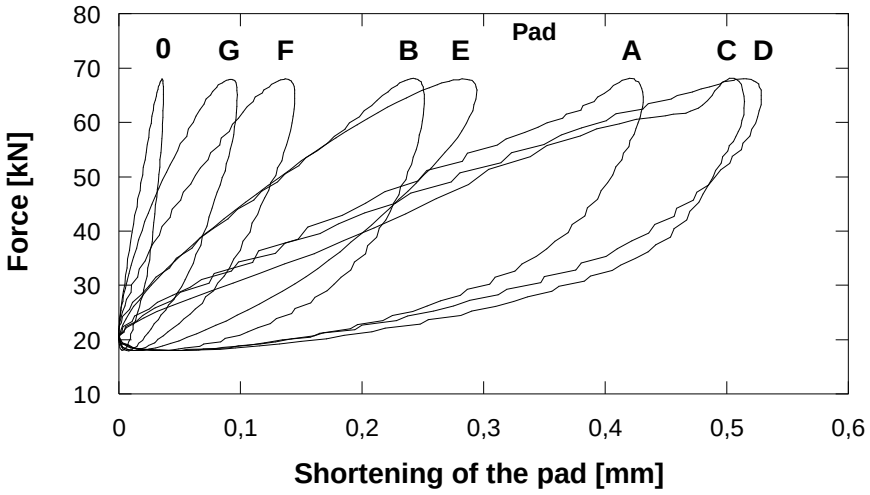

Figure 6.2. Dynamic behaviour of the pads at 10 Hz

Impact attenuation

In the following figure, we can observe the results obtained for the attenuation tests with both tests as percentages. It is verified that the results obtained by the two methods are disparate, the values obtained by the reference method are higher than the values obtained by the alternative method, and the variations between methods reach 97%. Figure 6.3 shows the relationship existing between the results of both methods and it is confirm that the relationship between them is inverse, this means, the pad that obtains higher values using one of the methods obtains the lowest values using the other method.

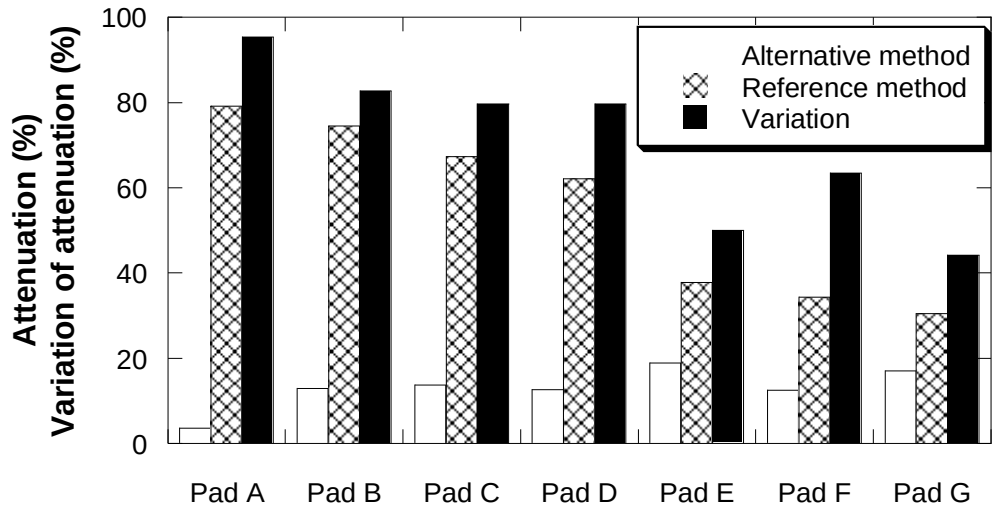

Figure 6.3. Results obtained for the impact attenuation tests

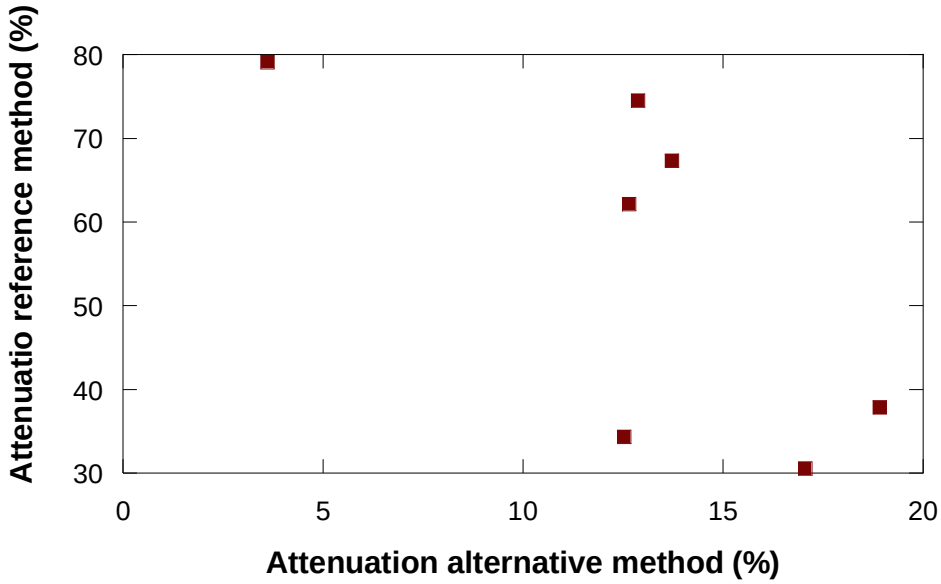

Figure 6.4. Relationship between the results obtained by both methods

Previous studies [34] have shown the existing relationship between impact attenuation and the mechanical properties of the pads. In figure 6.5 it can be checked that there is a tendency to reduce the difference between both methods when the static rigidity increases, both the one stablished in the Standard, k_e, as the one defined including low loads, k_e'. This tendency is vaguer if the correlation is made with dynamic rigidity. In figure 6.5 the evolution of the attenuation measured by both methods against static rigidity is represented and the tendency to reduce attenuation with the increase of the rigidity of the pad if reference method is used, but an inverse tendency if alternative method is used, is validated.

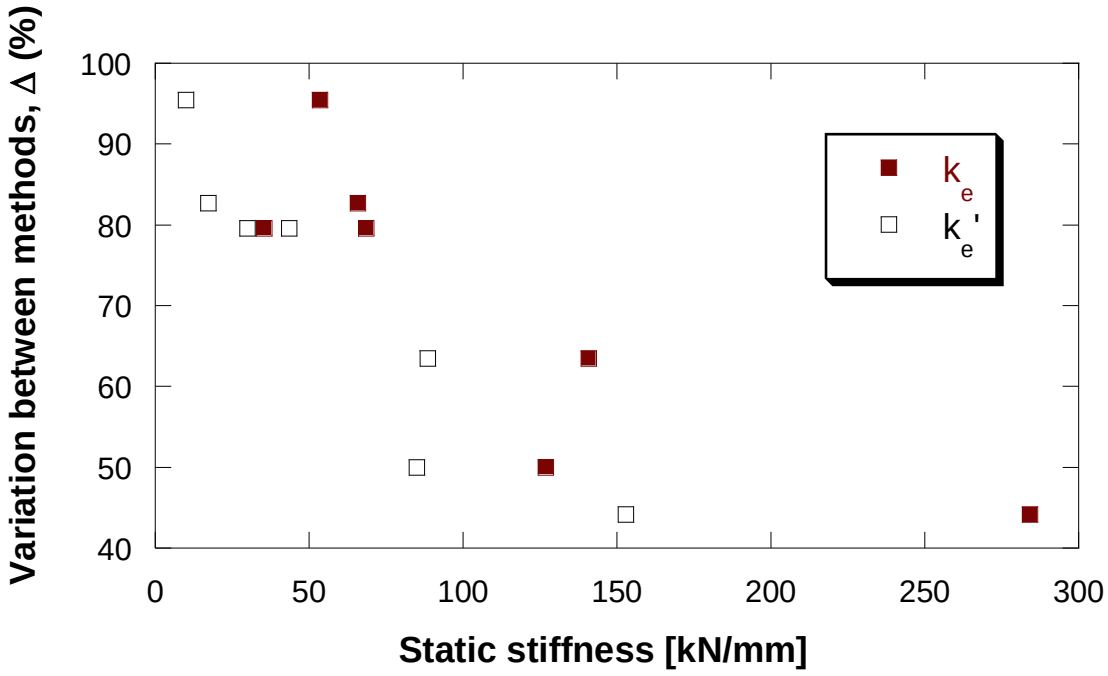

Figure 6.5. Relationship between the variation between methods and static stiffness

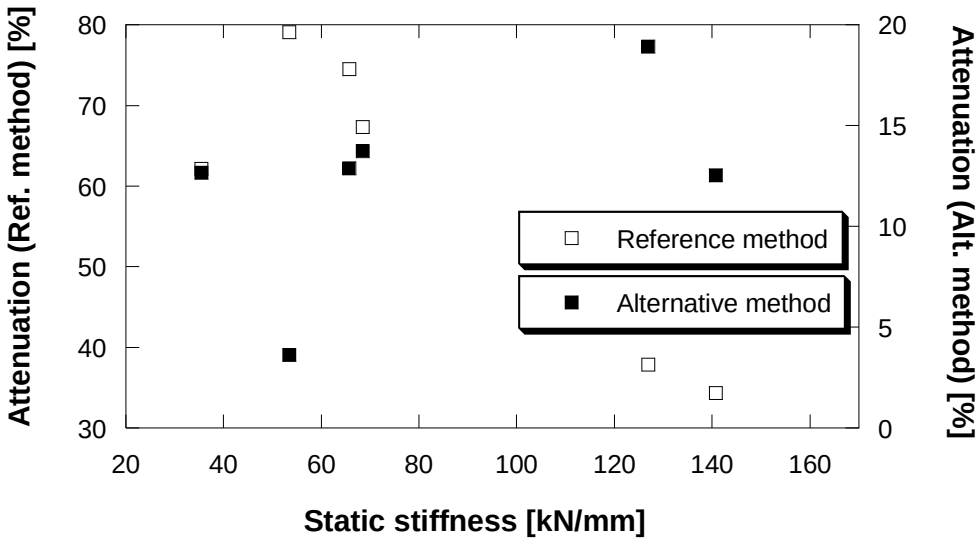

Figure 6.6. Relationship between attenuation results and stiffness

If we do not take into account the geometry of the pad and we analyse the hardness of the pads themselves, as it is shown in figure 7 there is a reduction in attenuation for the reference method when the hardness of the pad increases. Regarding the

alternative method, the opposite happens, attenuation increases with the increase in hardness of the pad, nevertheless it happens in lower absolute values.

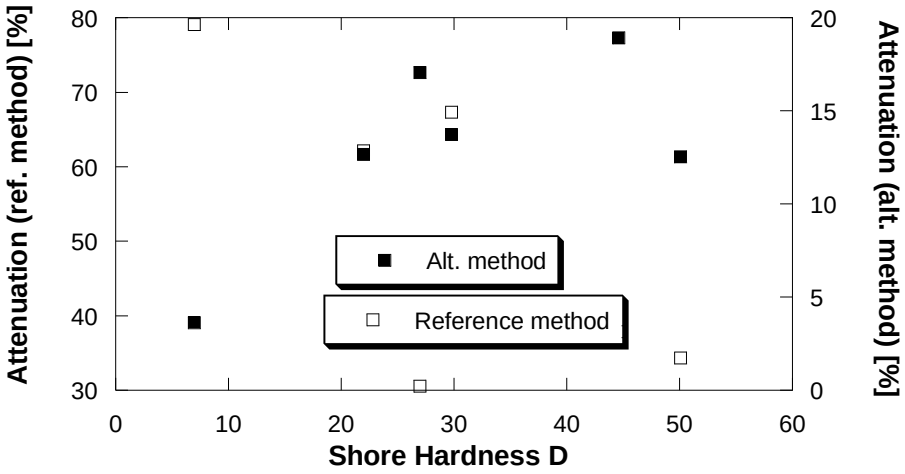

Figure 6.7. Relationship between attenuation results and hardness of the pad

This difference between the two methods, taking into account that the impact device is the same (height and mass) and the rigidity under the sleeper is the same (they both have the same criteria regarding strain even though there are different materials), leads to think that the conflicting element is preload. In the next figure, we can see a graph similar to the one presented in appendix 4. When preload decreases attenuation increases, getting closer to the values obtained by the reference method. As it was mentioned before as a hypothesis, now it is proved that under 5 kN the attenuation values loose the tendency. This is probably due to the lack of restraint of the sleeper, because it just stands on the elastomeric mat and this can lead to slight movements and distort results in the strain gauges.

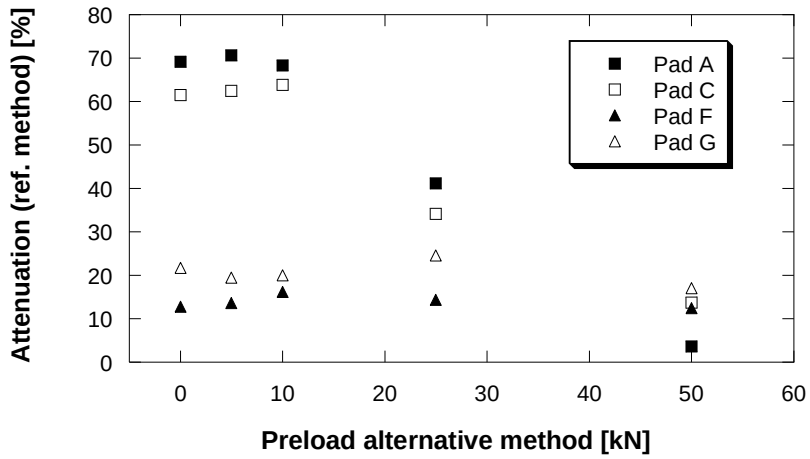

Figure 6.8. Influence of the value of the preload (alternative method) in the measurement of attenuation

In the next figure the results obtained for different preloads with the reference and the alternative method are compared, showing how reference values are in the same tendency that attenuation obtained from the alternative method it this method had no preload. This graph is just a reduced version of the one shown in annex IV.

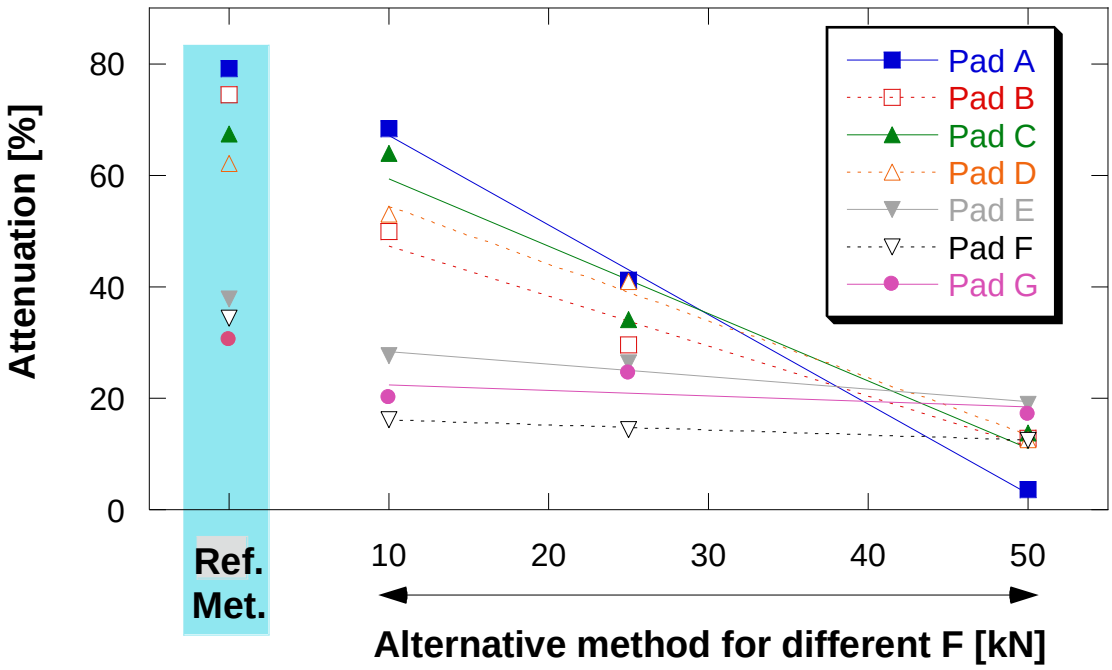

Figure 6.9. Comparison between reference and alternative method using different preloads

7. Conclusions and proposal of improvement

After all the tests performed and the analysis of the results, the following conclusions have been obtained regarding pad behaviour:

- The distribution of static rigidities does not correspond with the distribution of dynamic rigidities.
- The existing relationship between the stiffness defined by the Standard and the stiffness taking into account the behaviour due to low loads is linear.
- The methods defined in EN 13146-3:2012 [5] give impact attenuation results that are different. The variation between the two methods increases when the rigidity of the pad is reduced.
- The attenuation measured by the reference method is more variable than the attenuation measured by the alternative method, for the pads tested.
- The attenuation values measured with the reference method tend to lower when the static stiffness of the pad and hardness increases, while for the alternative method the opposite happens.
- For the analysed pads, the relationship between the results obtained by both methods is linear and inverse.
- Using the alternative method, the increase of the preload generates linearly increasing attenuation values, except for preloads under 5 kN, where the sleeper can have movement.
- If both methods are compared, the values obtained with the reference method tend to be the ones obtained with the alternative method for a preload of 0 kN (no preload).

Seen these results, there are some proposals to be taken into account when impact attenuation is calculated according to the European Standard [5]. Firstly, it would be necessary to include, when an impact attenuation test is done, which method is being used to determine it due to the obvious difference in results. Furthermore, when EN 13481-2:2012+A1:2017 [31] establishes a classification of the fastening systems according to its attenuation, there should be two different criteria whether reference or alternative method is being used.

Bibliography

[1] ORE, 117 Committee, 1974.

[2] S. Kaewunruen, A.M. Remennikov, Dynamic properties of railway track and its components: Recent findings and future research direction, Insight Non-Destructive Test. Cond. Monit. 52 (2008) 20–22. doi:10.1784/insi.2010.52.1.20.

[3] S. Kaewunruen, A.M. Remennikov, An alternative rail pad tester for measuring dynamic properties of rail pads under large preloads, Exp. Mech. 48 (2008) 55–64. doi:10.1007/s11340-007-9059-3.

[4] T. Manescu, C. Petre, N. Zaharia, T. Manesco, M. Bayer, Dynamic tests for fastening rubber plates to determine attenuation of impact loads, Mater. Plast. 46 (2009) 448–451.

[5] European Committee for Standardization, EN 13146-3: 2012. Railway applications - Track - Test methods for fastening systems - Part 3: Determination of attenuation of impact loads., (2012).

[6] European Committee for Standardization, EN 13146-9:2009+A1: 2011. Railway applications. Track. Test methods for fastening systems. Part 9: Determination of stiffness., n.d.

[7] S. Kaewunruen, A.M. Remennikov, Response and prediciton of dynamic characteristics of worn rail pads under static preloads, Proc. 14th Int. Congr. Sound Vib. (2007) 9–12.

[8] Agico Group, http://www.railway-fasteners.com/rail-rubber-plate-and-rail-pad.html, (n.d.).

[9] I.A. Carrascal, J.A. Casado, J.A. Polanco, F. Gutiérrez-Solana, Dynamic behaviour of railway fastening setting pads, Eng. Fail. Anal. 14 (2007) 364–373. doi:10.1016/J.ENGFAILANAL.2006.02.003.

[10] I.A. Carrascal, J.A. Casado, J.A. Polanco, F. Gutiérrez-Solana, Comportamiento dinámico de placas de asiento de sujeción de vía de ferrocarril, Análisis Mecánica La Fract. 22 (2005) 372–377.

[11] I.A. Carrascal, Optimización y análisis de comportamiento de sistemas de sujección para vías de ferrocarril de alta velocidad española, PhD Thesis,

Universidad de Cantabria, 2006.

[12] P.B. Lindley, Natural rubber in civil engineering, Rubber World. 161 (n.d.) 56–61. doi:10.1163/_q3_SIM_00374.

[13] M. Sol-Sánchez, F. Moreno-Navarro, M.C. Rubio-Gámez, Viability analysis of deconstructed tires as material for rail pads in high-speed railways, Mater. Des. 64 (2014) 407–414. doi:10.1016/j.matdes.2014.07.071.

[14] I.A. Carrascal, J.A. Casado, S. Diego, J.A. Polanco, J. Martín, A. Pérez, Placa elástica de asiento metálica para alta velocidad, in: X Jornadas Int. Ing. Para Alta Velocidad, 2016: pp. 45–62.

[15] M. Sol-Sánchez, F. Moreno-Navarro, M.C. Rubio-Gámez, The use of elastic elements in railway tracks: A state of the art review, Constr. Build. Mater. 75 (2015) 293–305. doi:10.1016/j.conbuildmat.2014.11.027.

[16] A.L. Pita, Infraestructuras ferroviarias, Edicions UPC, 2006. https://books.google.es/books?id=t0tpBgAAQBAJ.

[17] P. Teixeira, Contribution to the reduction of track maintenance costs by optimizing its vertical stiffness, PhD, UPC, Barcelona. (2003).

[18] A. López Pita, P. Teixeira, F.A. Robusté, High speed and track deterioration: the role of vertical stiffness of the track, Proc. Inst. Mech. Eng. Part F J. Rail Rapid Transit. 218 (2004) 31–40.

[19] B. Rajaram, Dynamic response of elastic fastenings, Rail Int. 17 (1986) 29–36.

[20] H. Ilias, The influence of railpad stiffness on wheelset/track interaction and corrugation growth, J. Sound Vib. 227 (1999) 935–948. doi:10.1006/jsvi.1999.2059.

[21] A. Lopez Pita, The vertical stiffness of the track and the deterioration of high speed lines, Rev. Obras Publicas. 148 (n.d.) 7–26.

[22] T. Dahlberg, Railway Track Stiffness Variations – Consequences and Countermeasures, Int. J. Civ. Eng. 8 (2010) 1–12. http://ijce.iust.ac.ir/article-1-420-en.html (accessed June 6, 2018).

[23] T.X. Wu, D.J. Thompson, The effects of local preload on the foundation stiffness and vertical vibration of railway track, J. Sound Vib. 219 (1999) 881–904. doi:10.1006/jsvi.1998.1939.

[24] S.G. Koroma, M.F.M. Hussein, J.S. Owen, The effects of preload and nonlinearity on the vibration of railway tracks under harmonic load, (2013) 9–12.

[25] U.S. Department of Transportation, Laboratory study to determine the effects of tie pad stiffness on the attenuation of impact loads in concrete railway ties, (n.d.).

[26] Y. Luo, Y. Liu, H.P. Yin, Numerical investigation of nonlinear properties of a rubber absorber in rail fastening systems, Int. J. Mech. Sci. 69 (2013) 107–113. doi:10.1016/j.ijmecsci.2013.01.034.

[27] ADIF, ET 03.360.570.0 Placas elásticas de asiento para sujeción VM, (2005).

[28] J.A.A. Casado, I.A. Carrascal, S. Diego, J.A.A. Polanco, Determinación experimental de la atenuación de las cargas de impacto en sistemas de fijación ferroviaria, in: Congr. Innovación Ferrov. Málaga, 2001.

[29] A. Rcmennlko, O.I. Revjew, Determination of dynamic properties of rail pads using an instrumented hammer impact technique, 33 (2005) 3–7.

[30] M. Del Sol Sánchez, Development of elastic elements from end-of-life tire layers to be applied in raliway tracks, 2014.

[31] European Committee for Standardization, EN 13481-2:2012+A1:2017. Railway applications. Track. Performance requirements for fastening system. Part 2: Fastening system for concrete sleepers., n.d.

[32] European Committee for Standardization, EN 13230-1:2016. Railway applications - Track - Concrete sleepers and bearers - Part 1: General requirements., n.d.

[33] Pandrol, (n.d.). http://www.pandrol.com/.

[34] I.A. Carrascal, J.A. Casado, S. Diego, J.A. Polanco, Atenuacion frente a impacto en sistemas de sujecion ferroviaria de alta velocidad, An. Mecánica Fract. 28 (2011) 713–728.

APPENDIX I: PHOTOS OF THE SLEEPER BREAKAGE

APPENDIX II: ALTERNATIVE METHOD GRAPHS

Studded EVA 10 mm- 50 kN

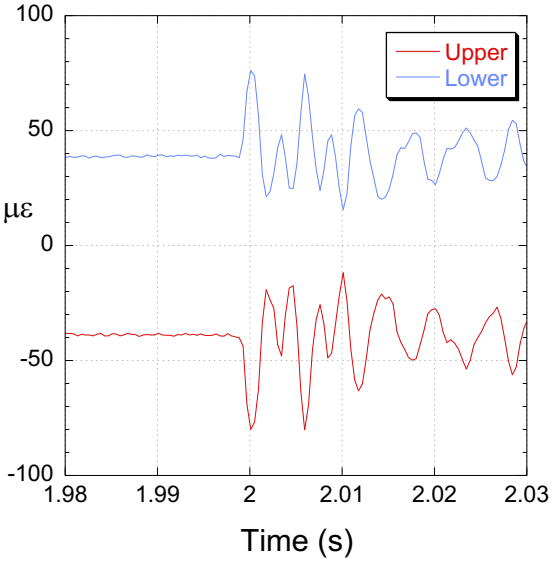

EVA REF 10 mm- 50 kN

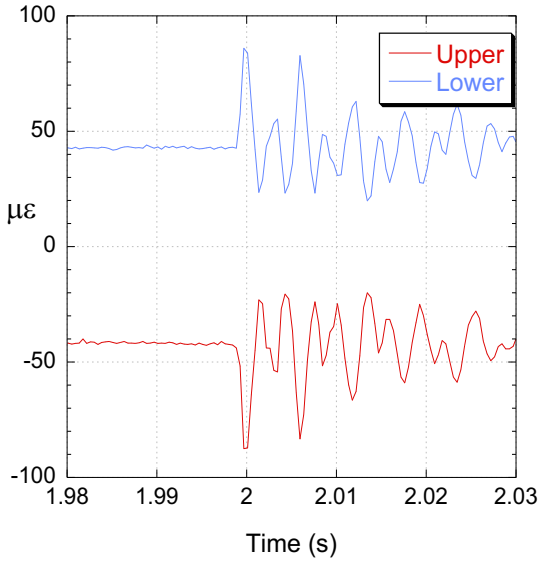

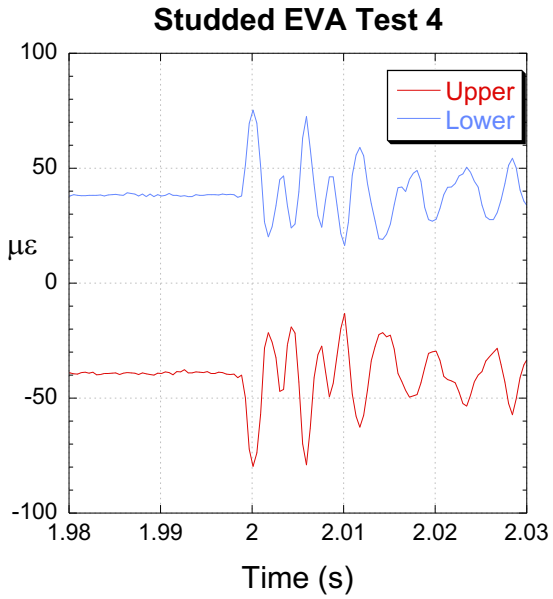

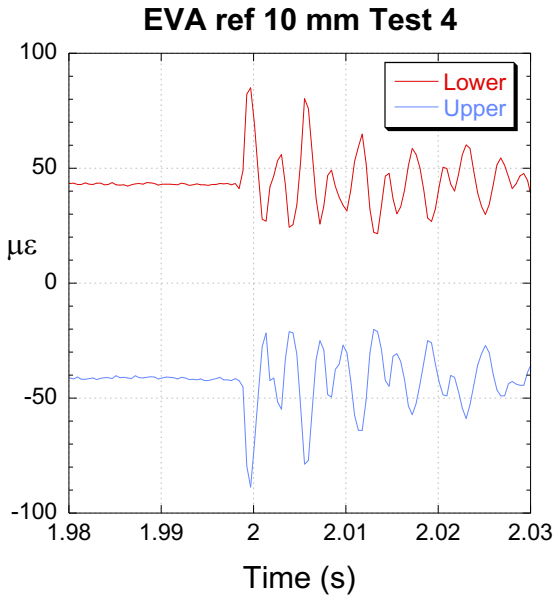

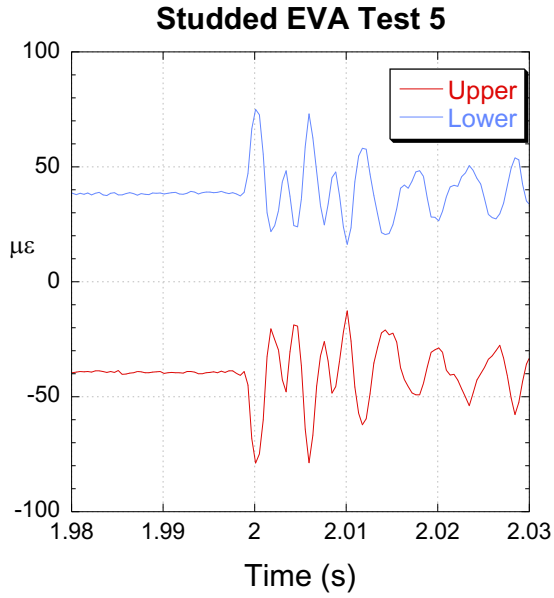

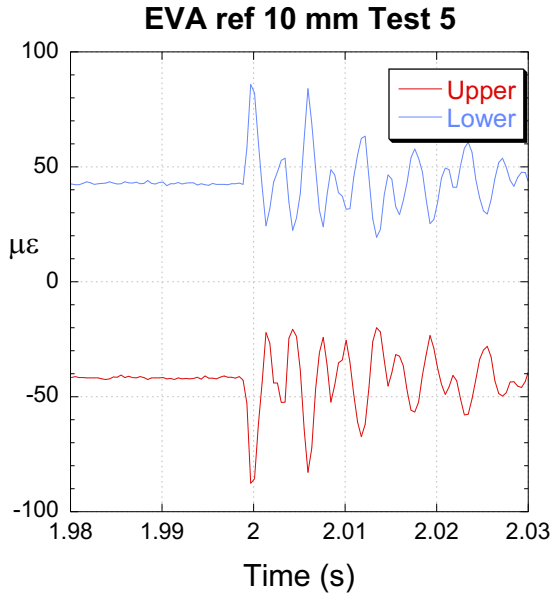

Studded EVA 10 mm- 25 kN

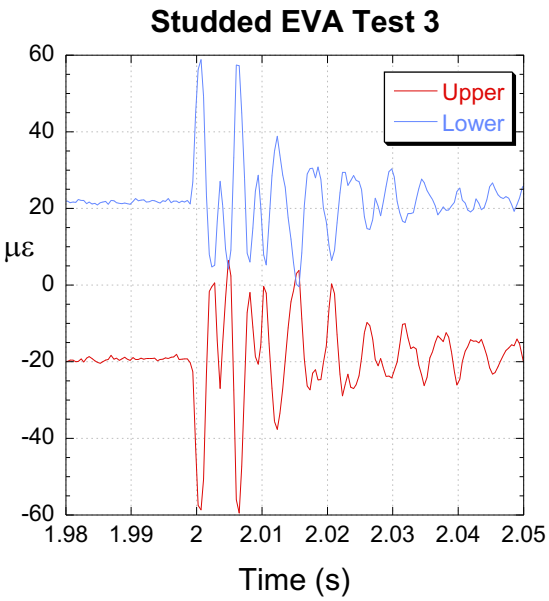

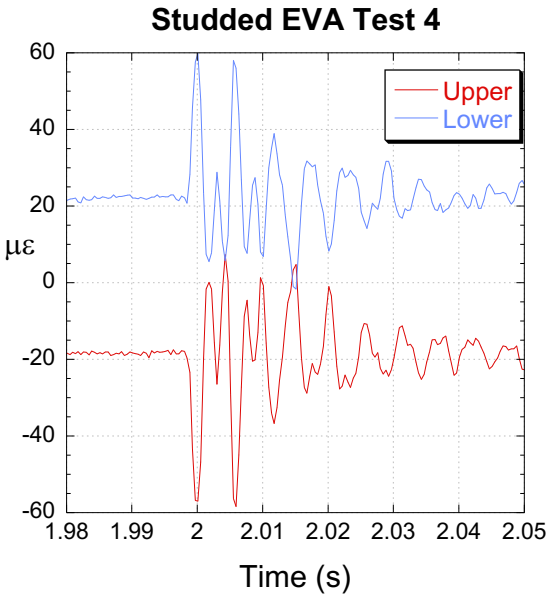

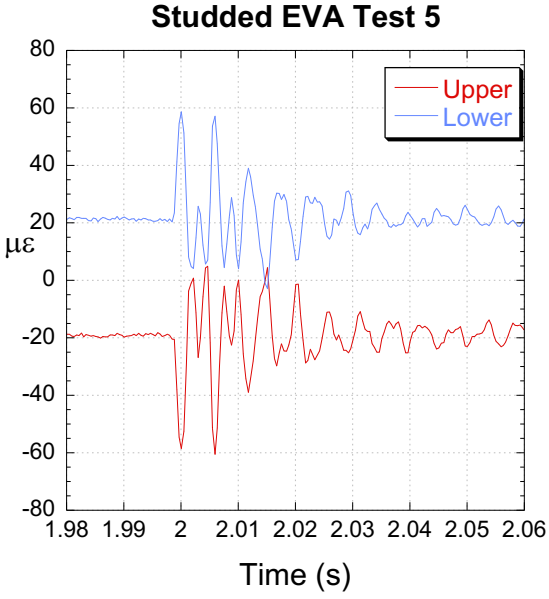

EVA REF 10 mm- 25 kN

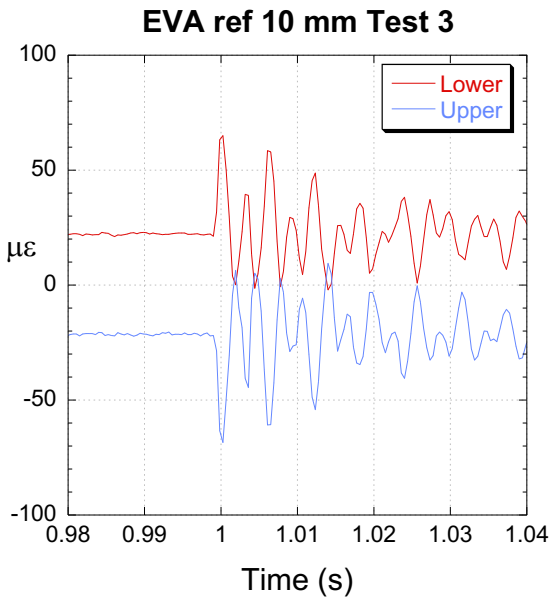

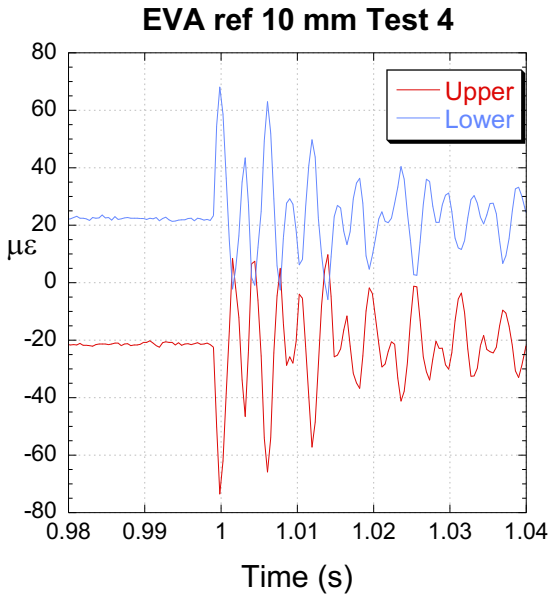

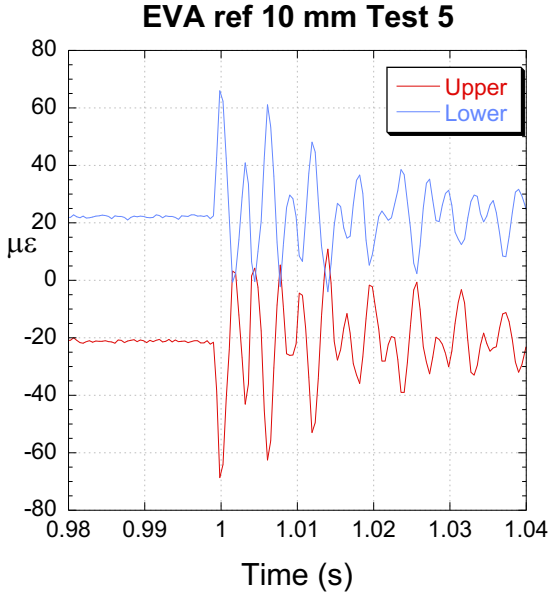

Studded EVA 10 mm- 10 kN

EVA REF 10 mm- 10 kN

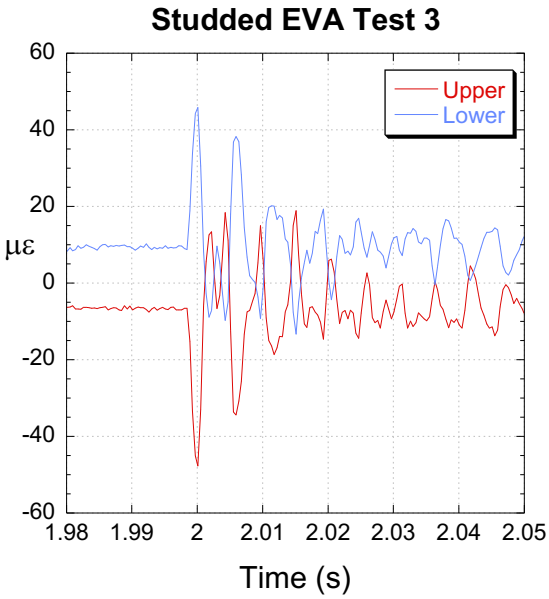

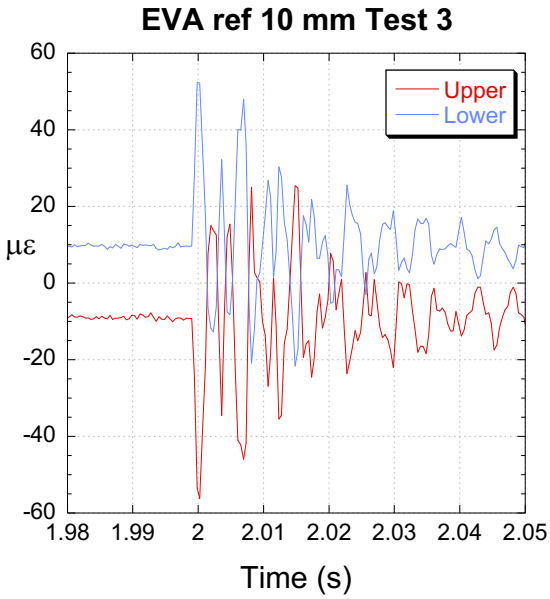

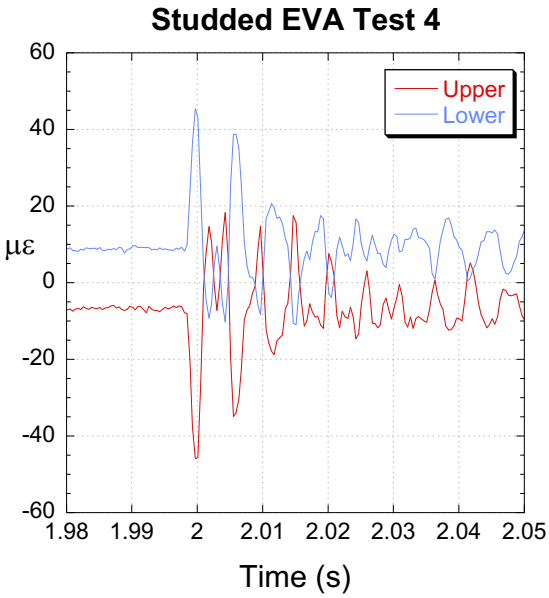

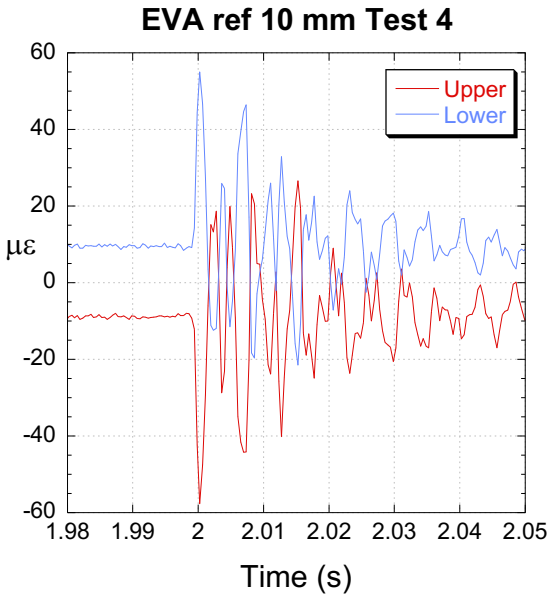

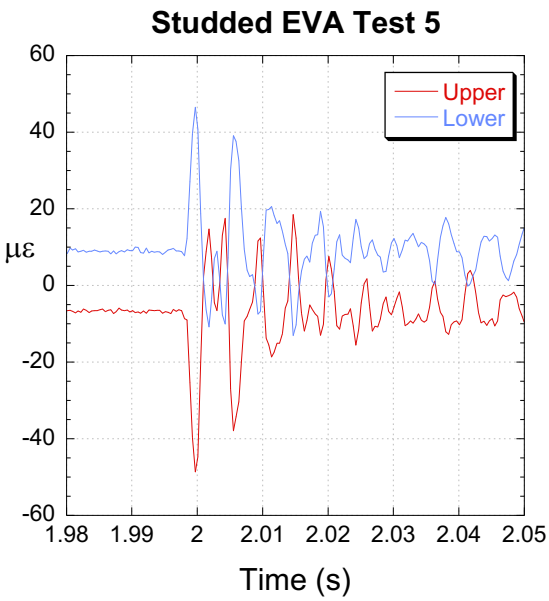

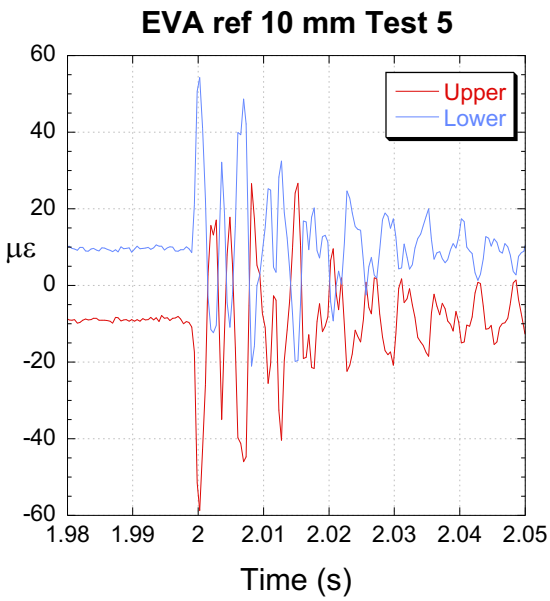

Studded EVA 10 mm- 5 kN

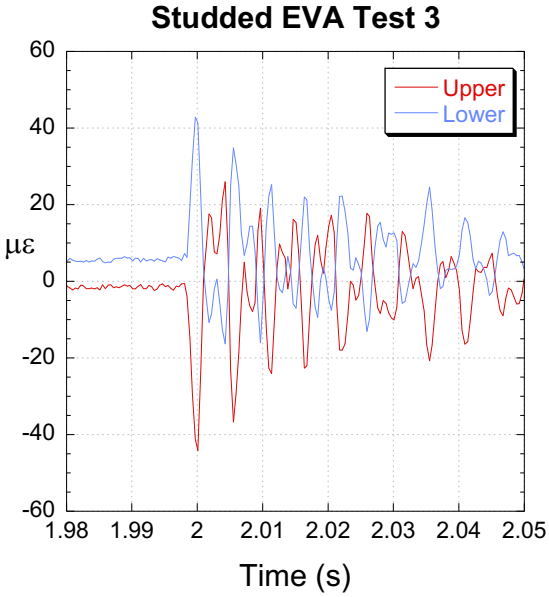

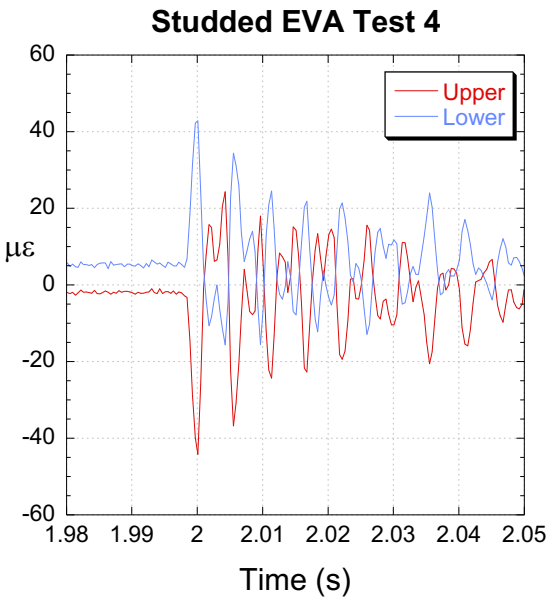

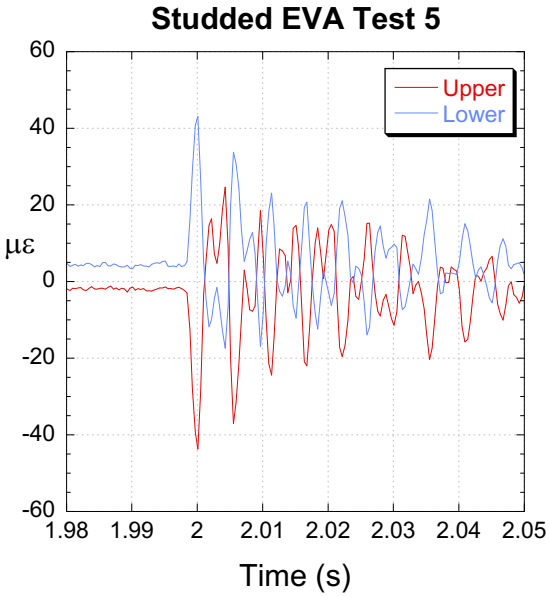

EVA REF 10 mm- 5 kN

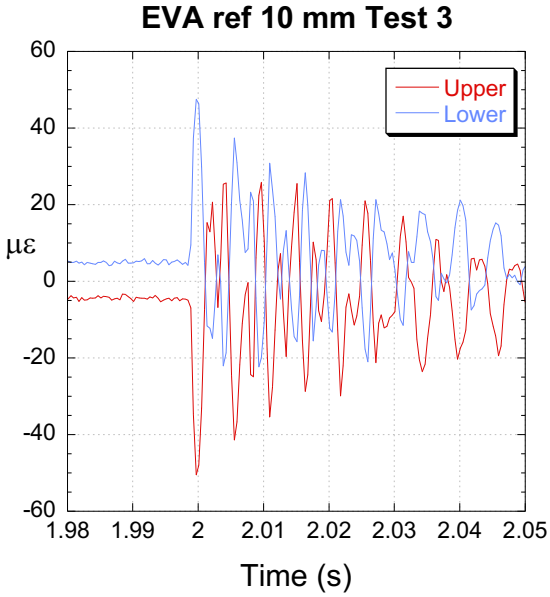

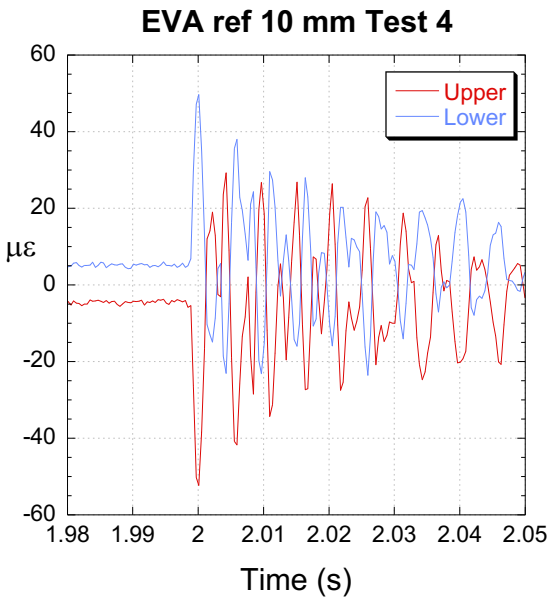

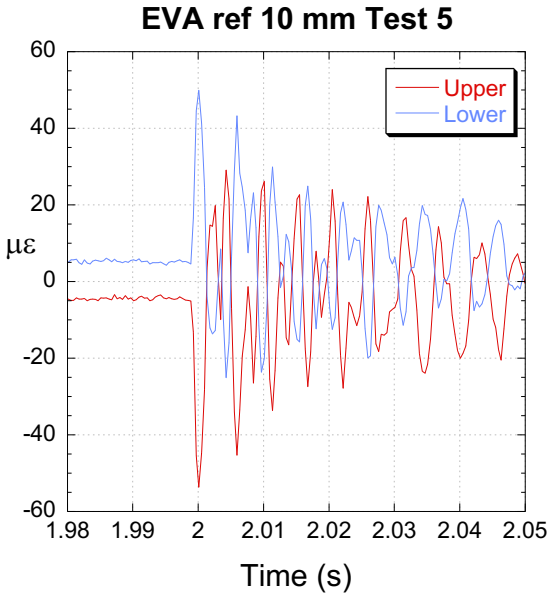

Studded EVA 10 mm- 0 kN

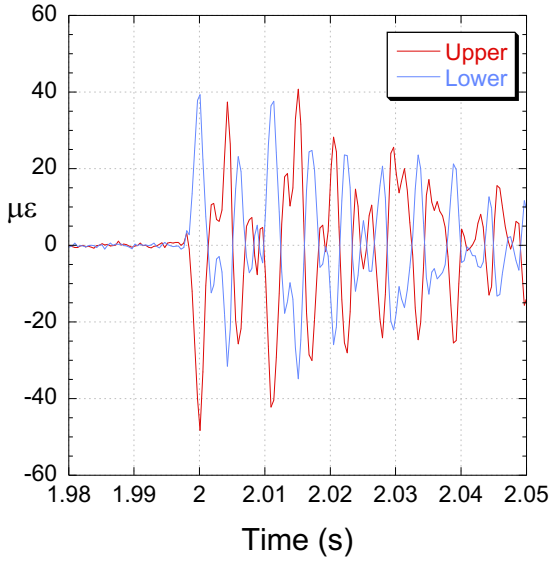

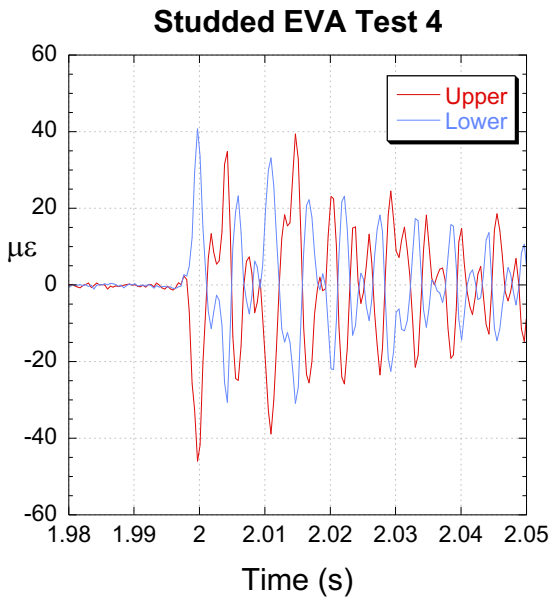

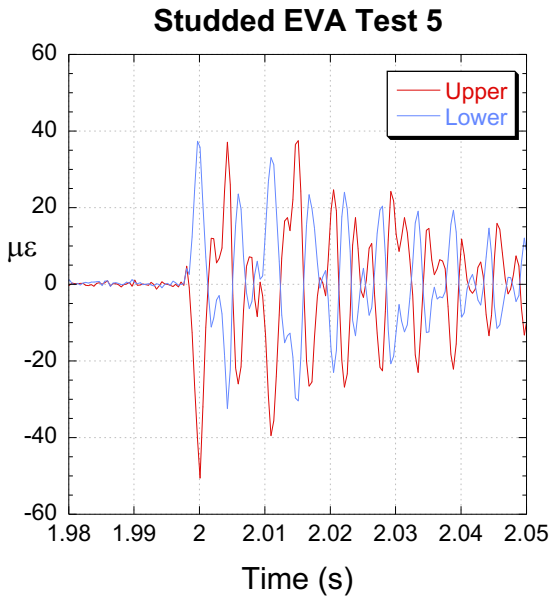

EVA REF 10 mm- 0 kN

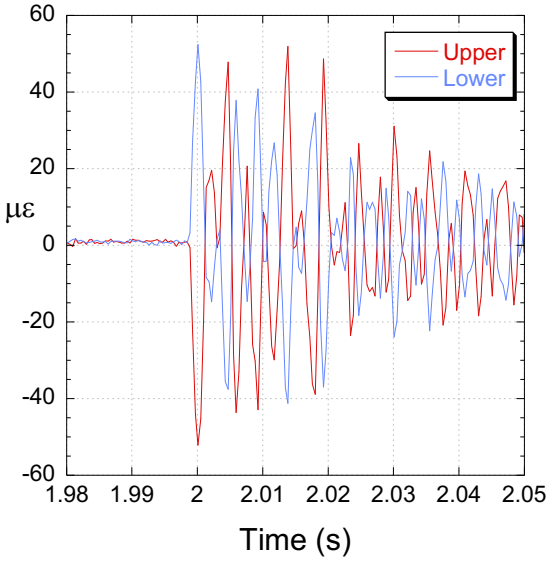

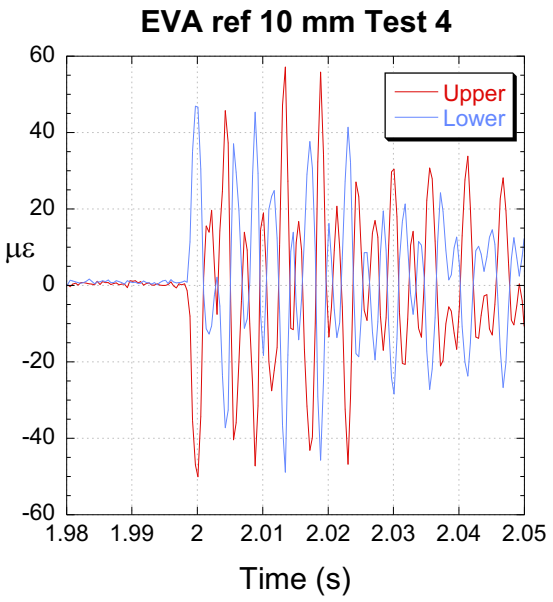

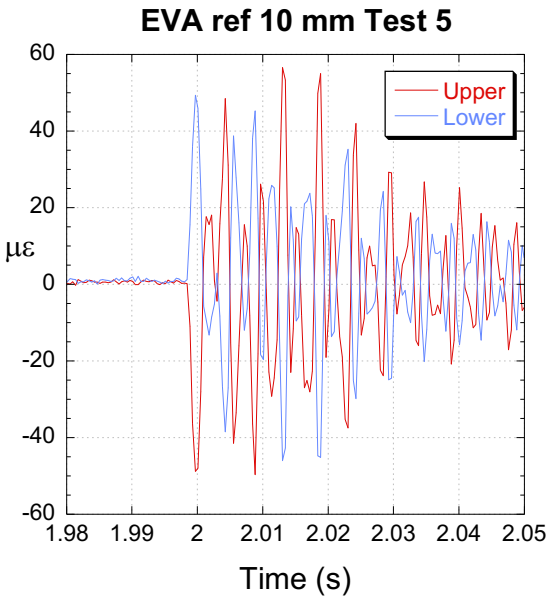

Studded EPDM 11 mm- 50 kN

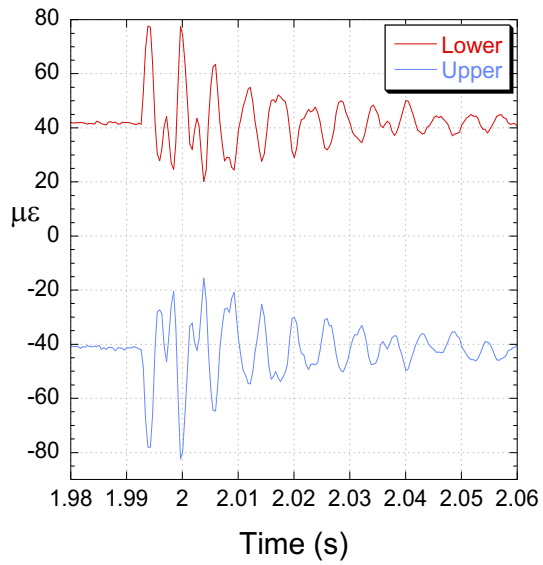

EVA REF 11 mm- 50 kN

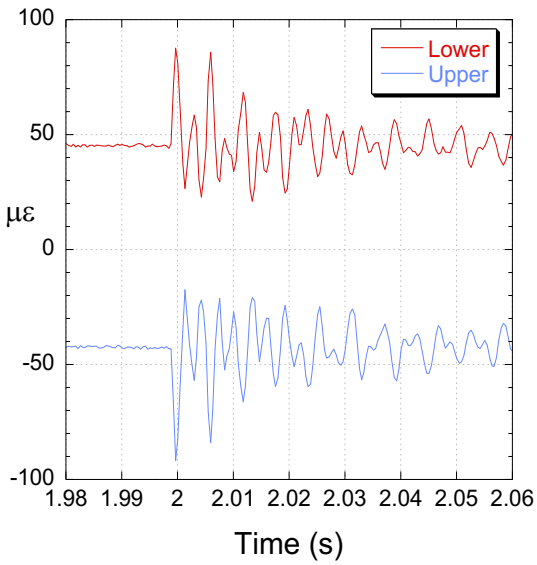

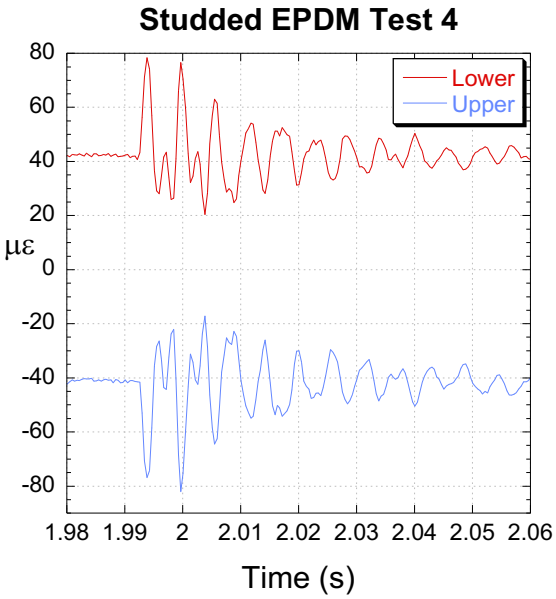

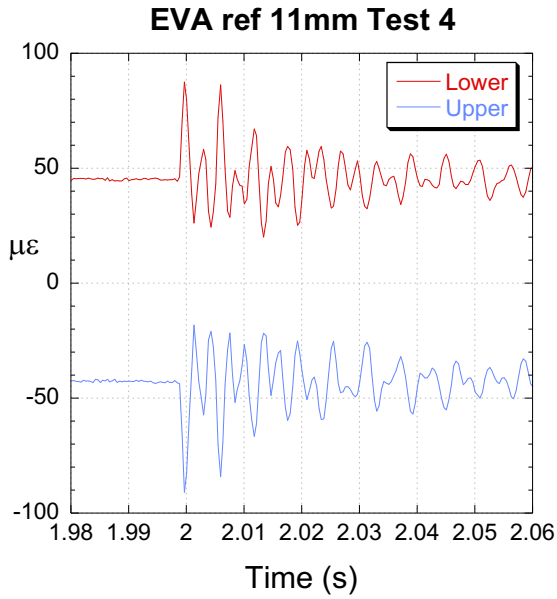

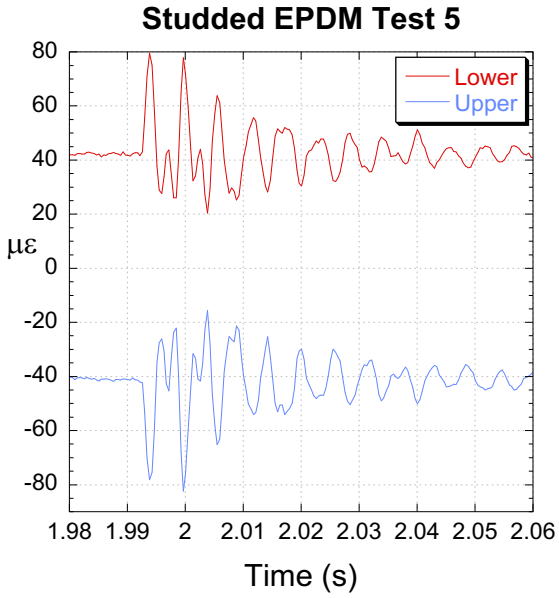

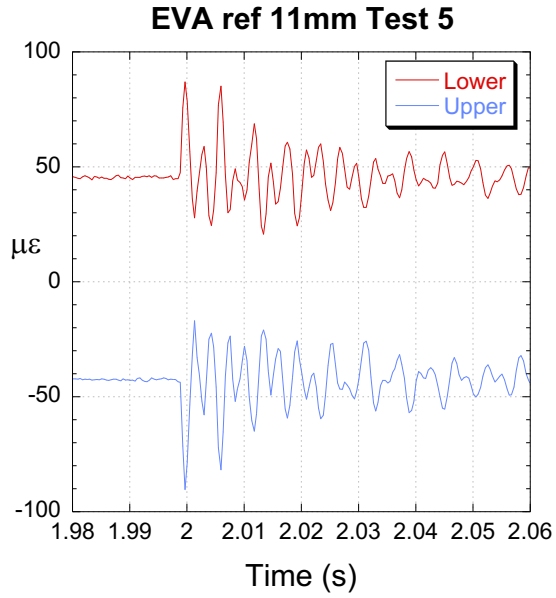

Studded EPDM 11 mm- 25 kN

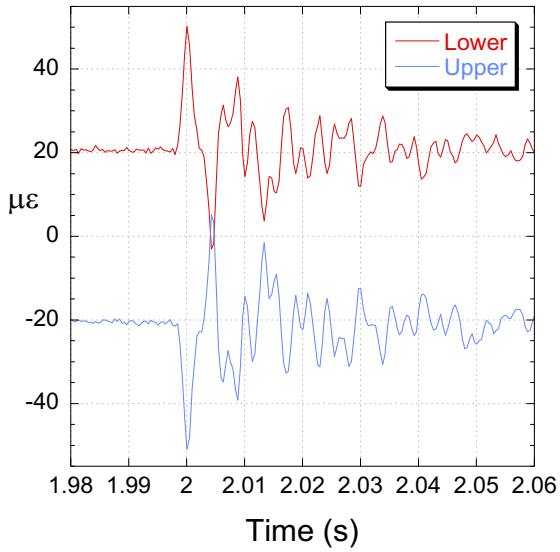

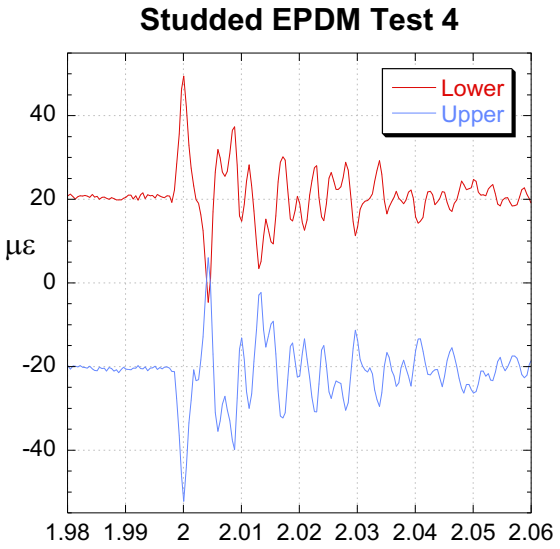

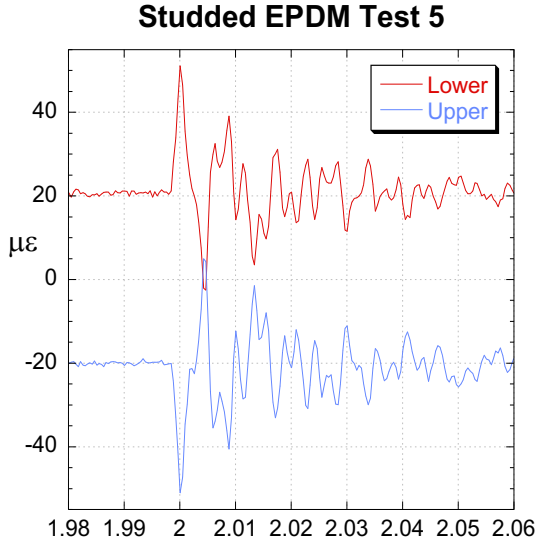

EVA REF 11 mm- 25 kN

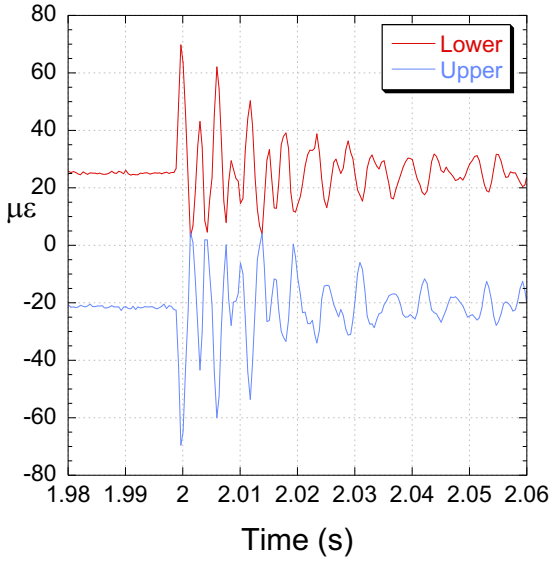

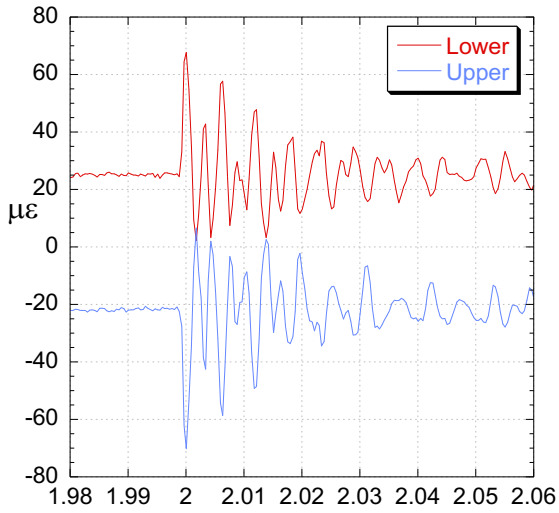

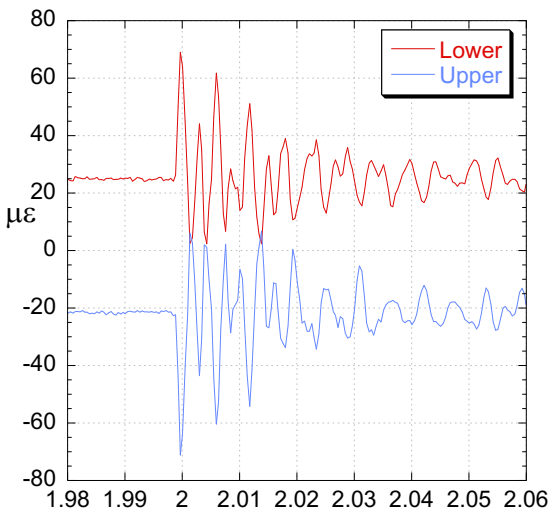

Studded EPDM 11 mm- 10 kN

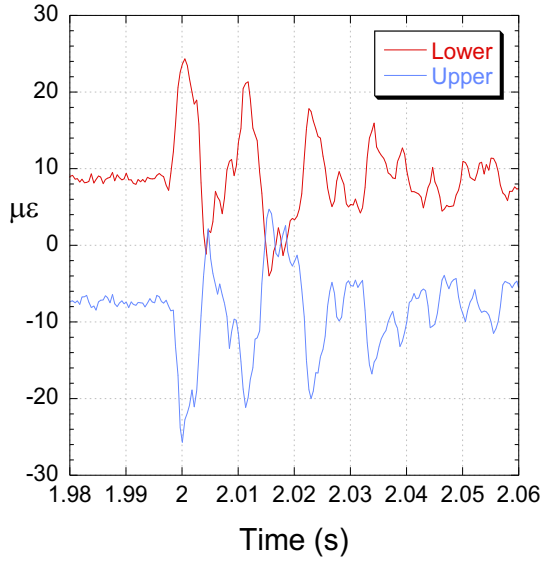

EVA REF 11 mm- 10 kN

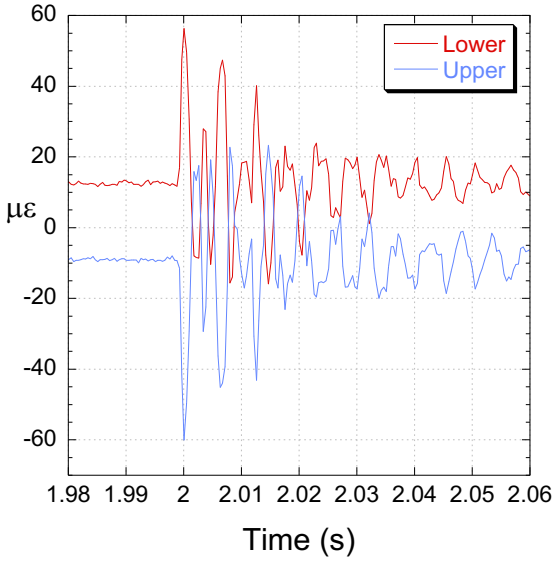

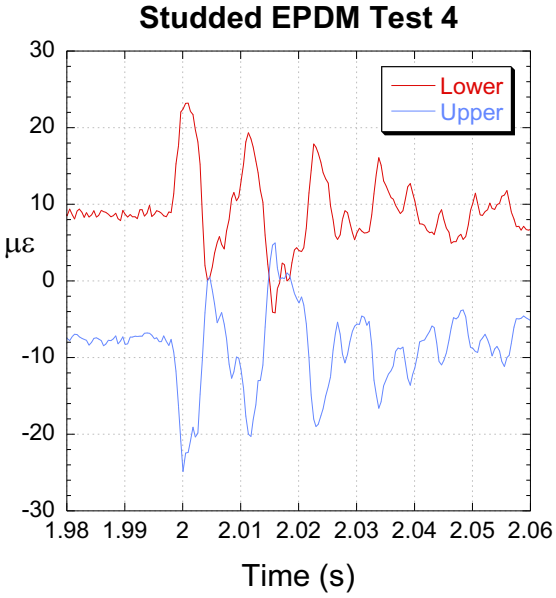

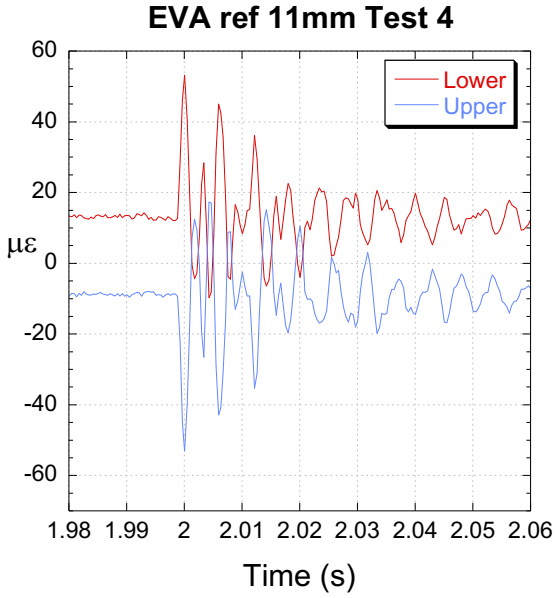

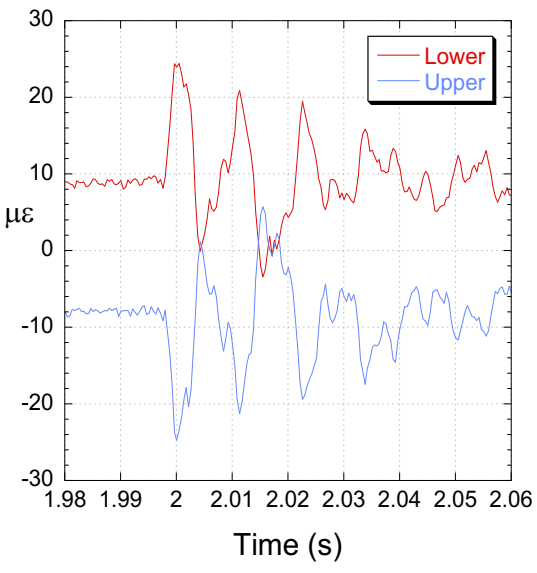

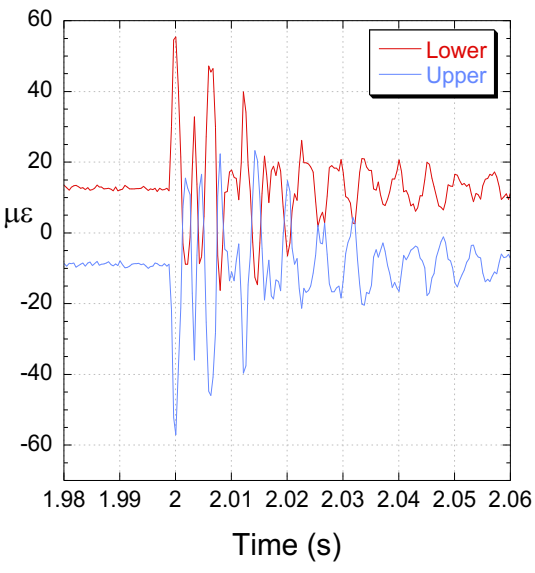

Studded EPDM 11 mm- 5 kN

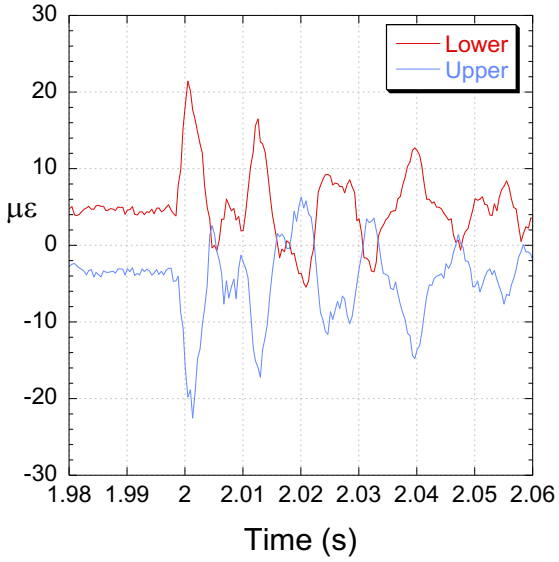

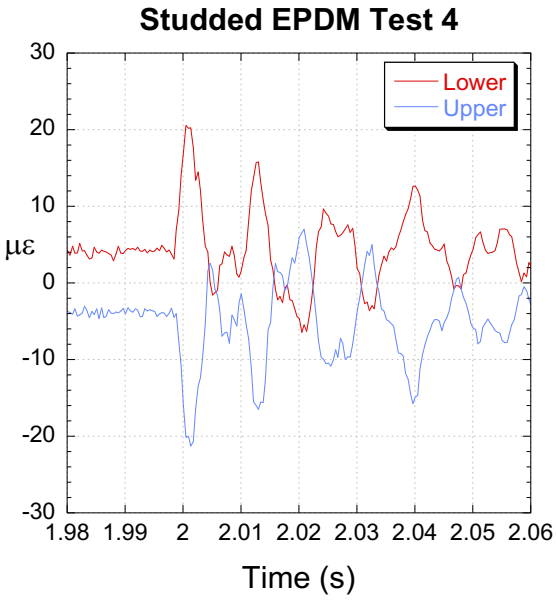

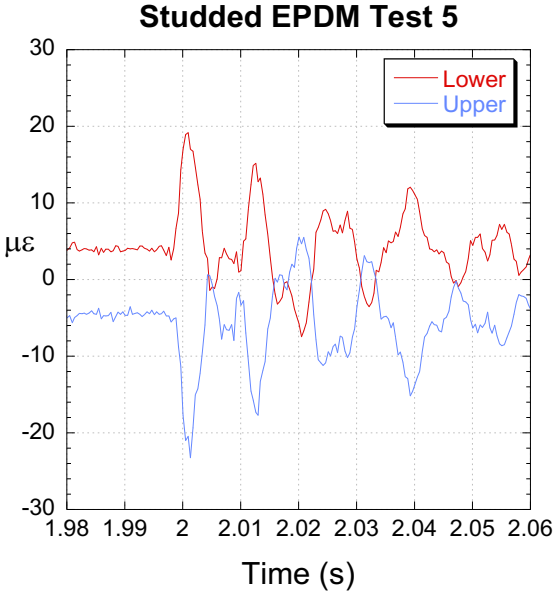

EVA REF 11 mm- 5 kN

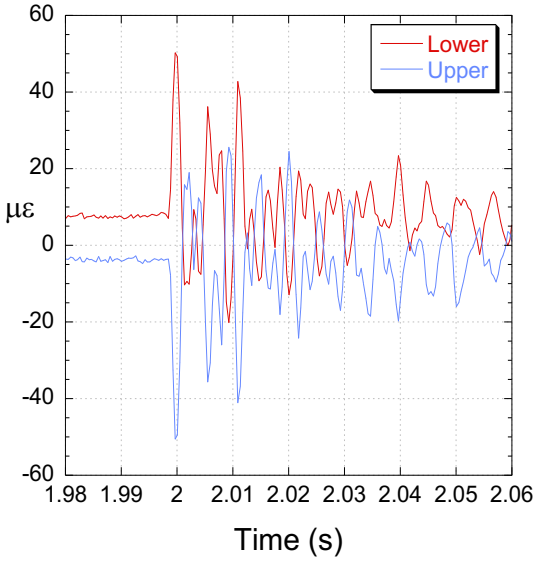

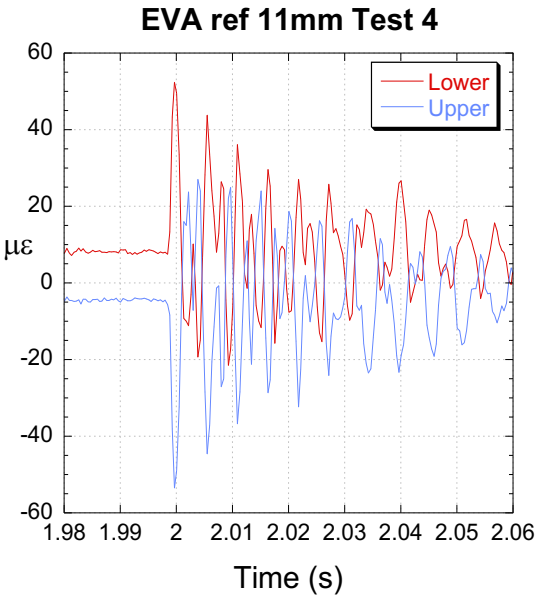

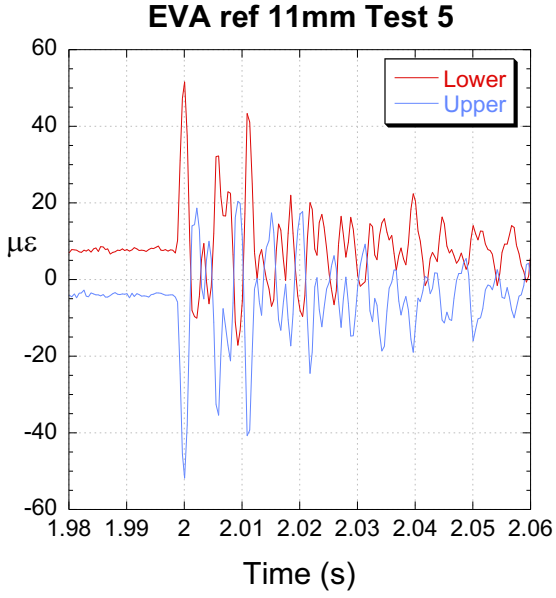

Studded EPDM 11 mm- 0 kN

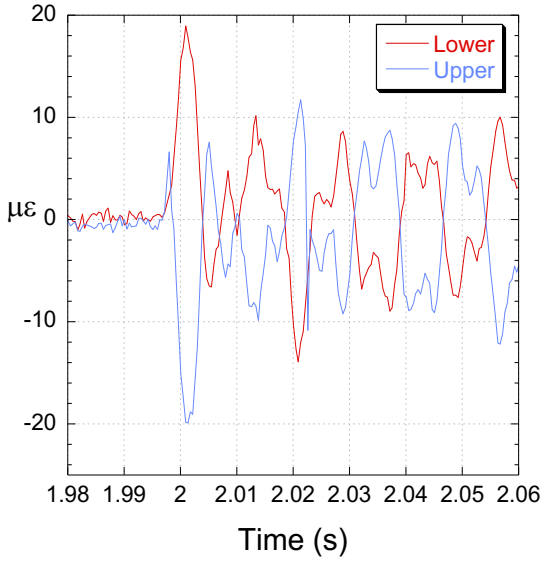

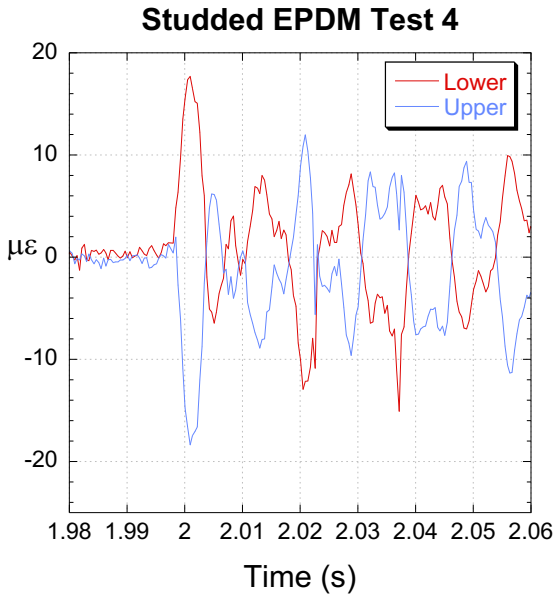

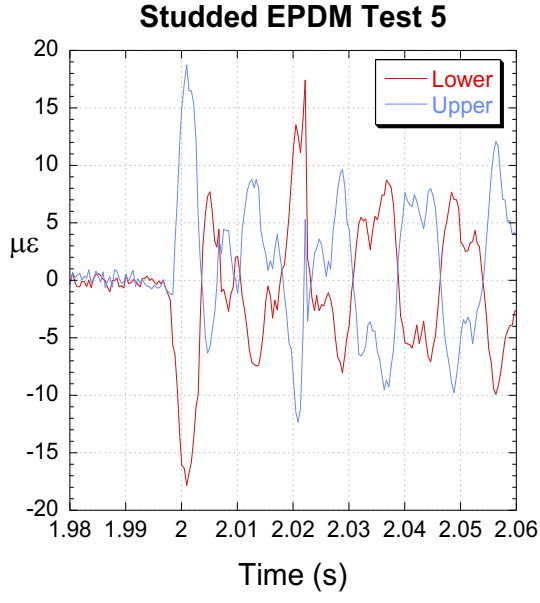

EVA REF 11 mm- 0 kN

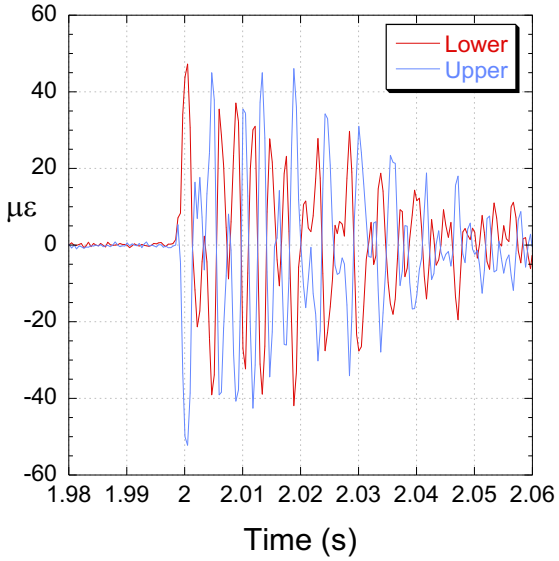

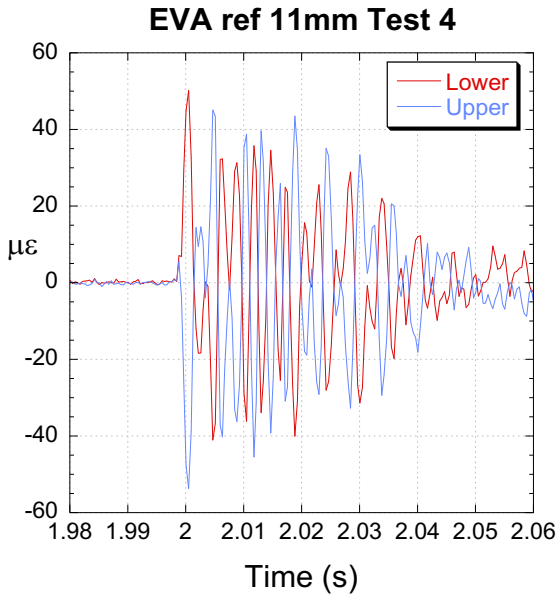

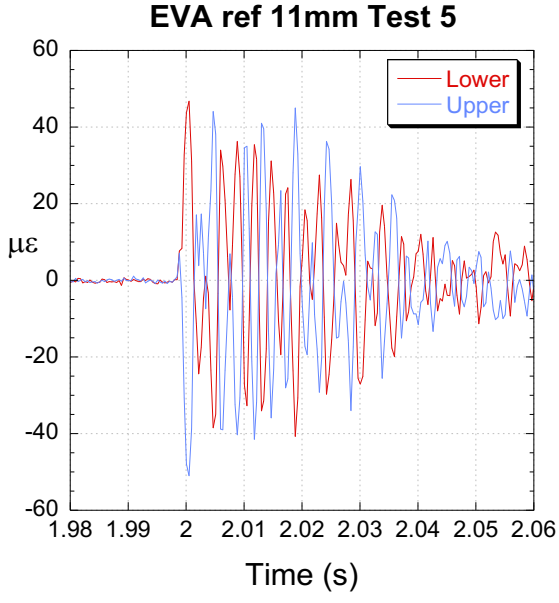

Microcellular rubber 11mm-50 kN

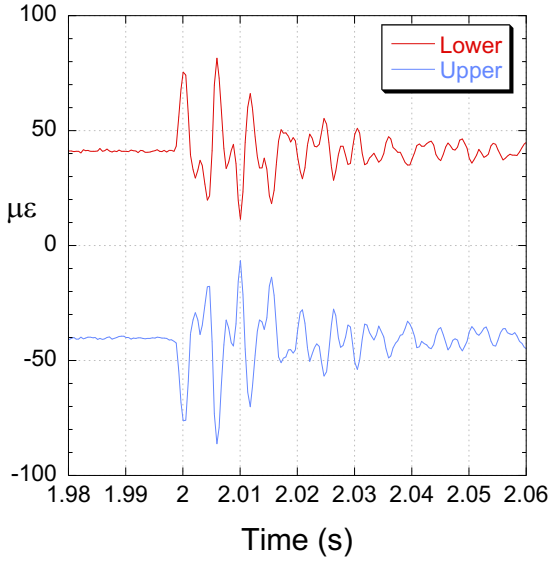

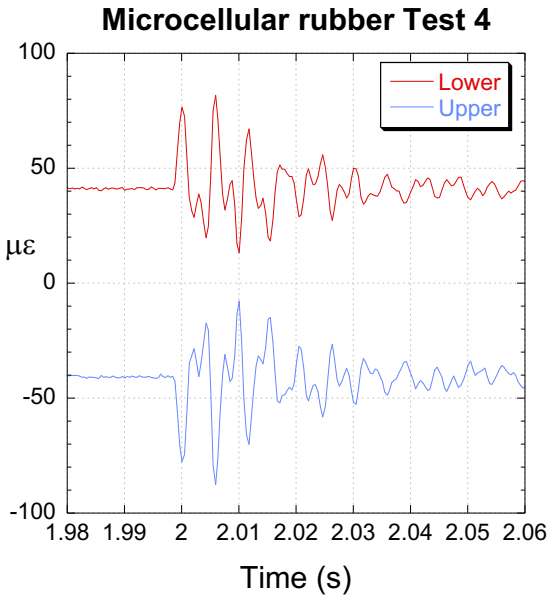

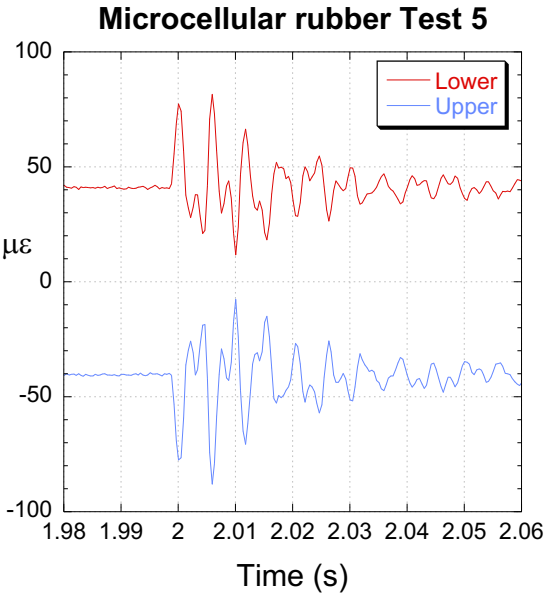

EVA REF 11 mm-50 kN

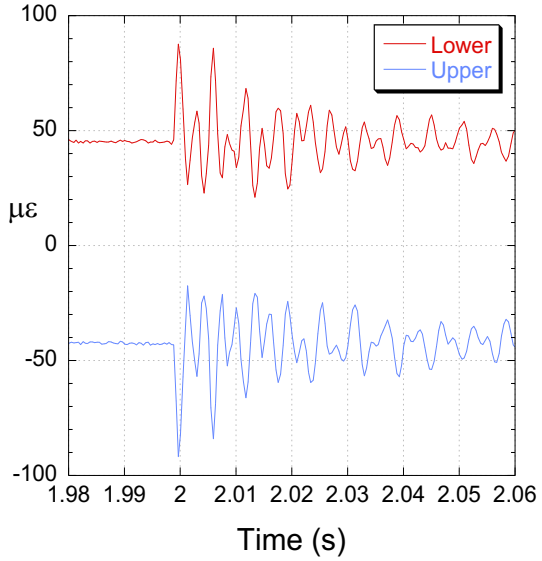

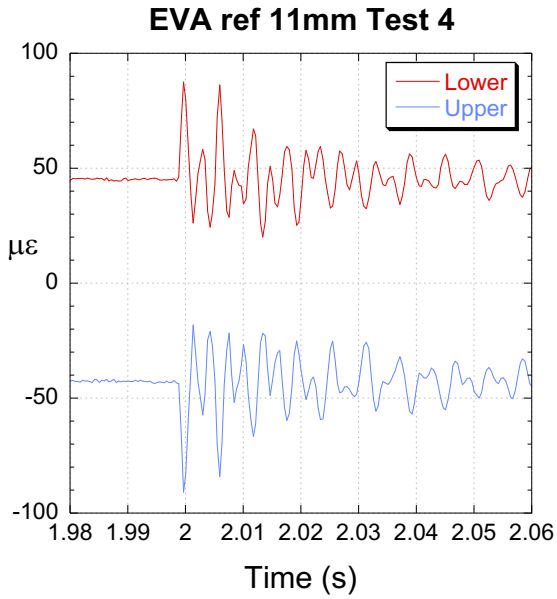

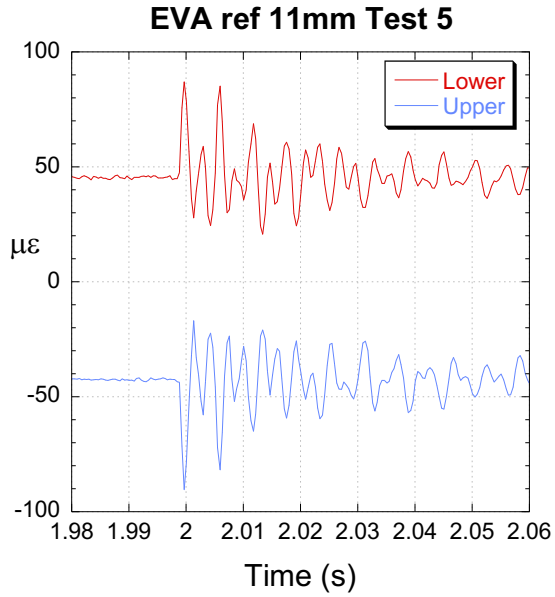

Microcellular rubber 11mm-25 kN

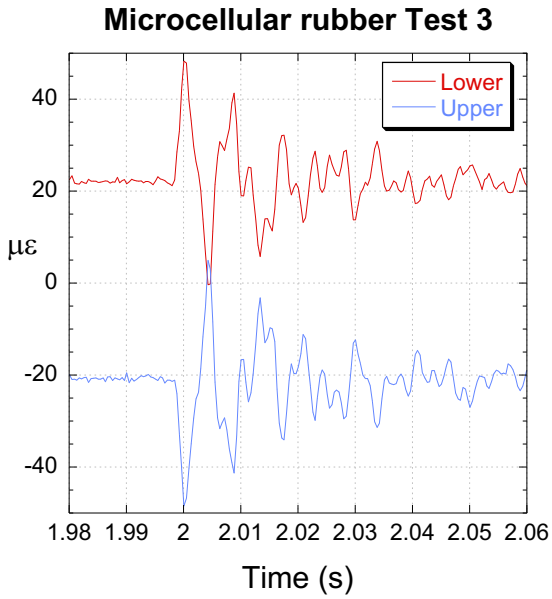

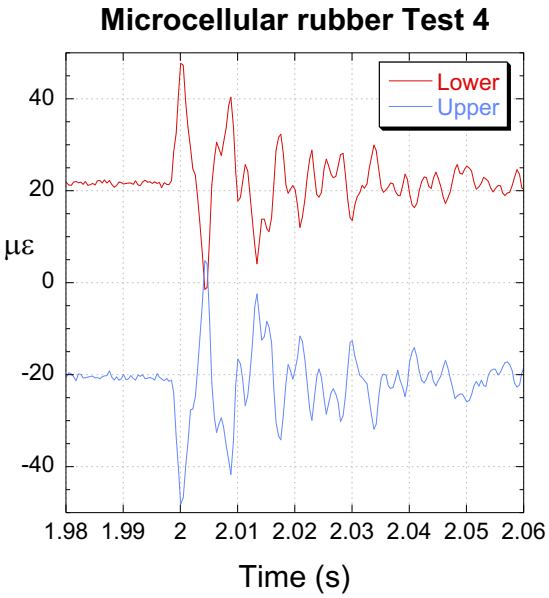

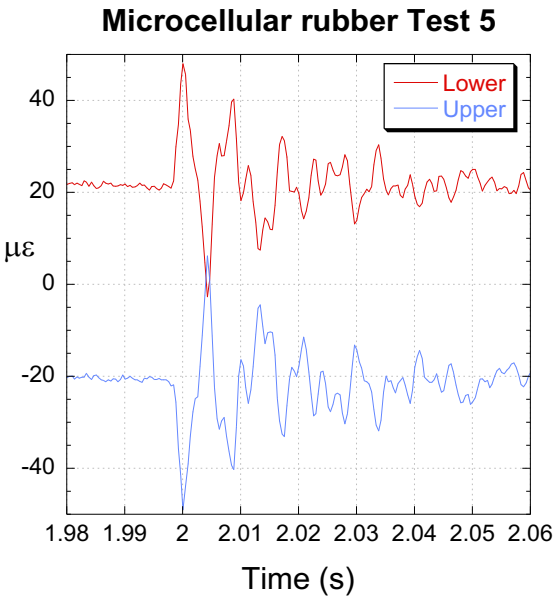

EVA REF 11 mm-25 kN

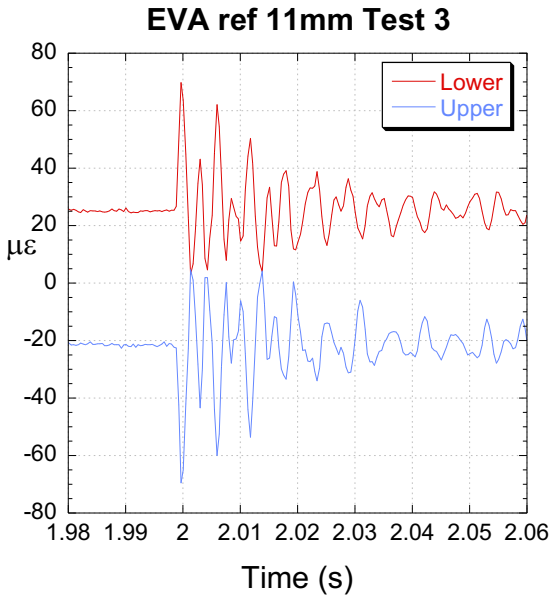

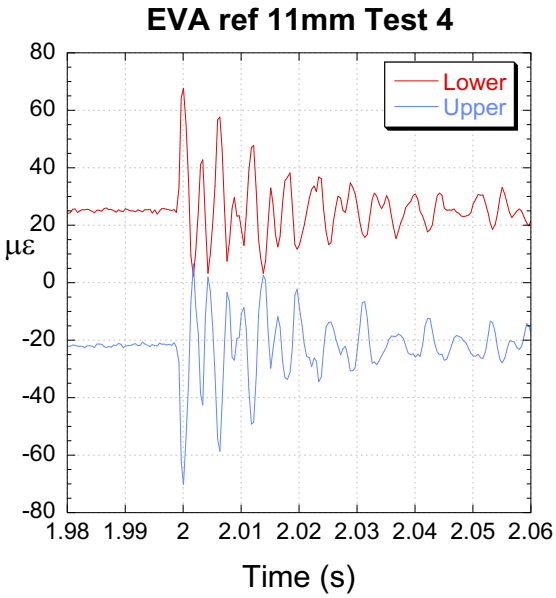

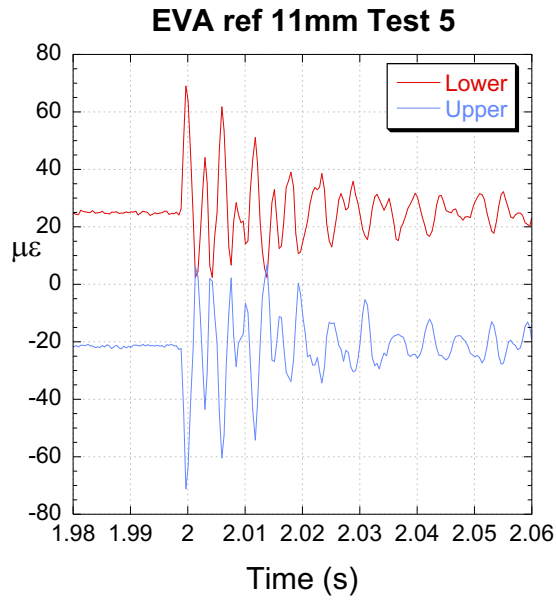

Microcellular rubber 11mm-10 kN

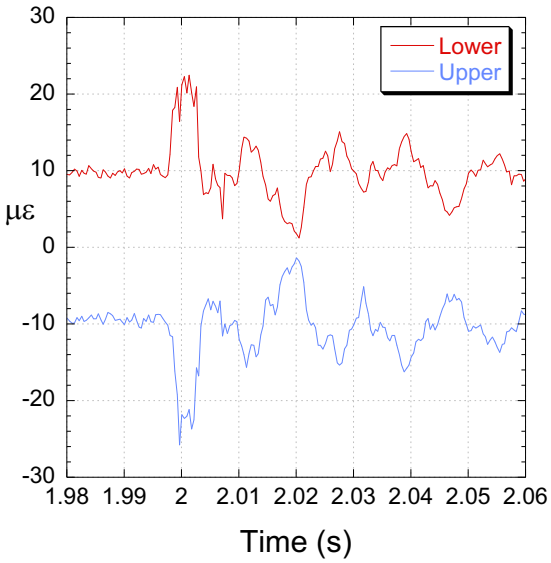

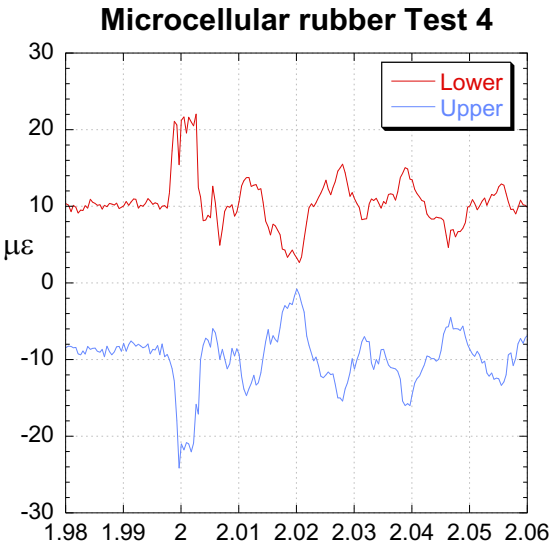

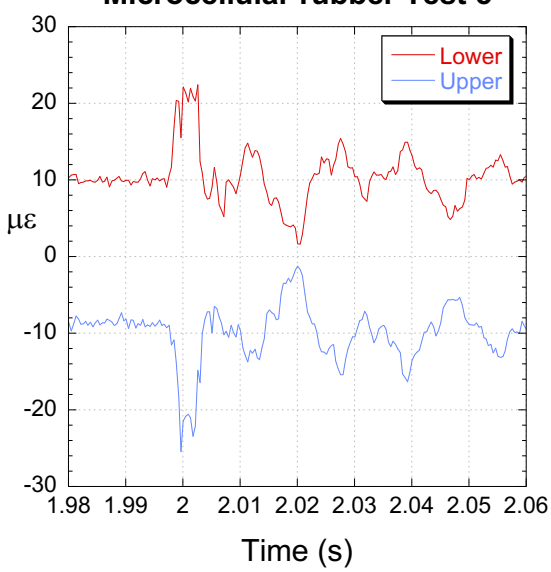

EVA REF 11 mm-10 kN

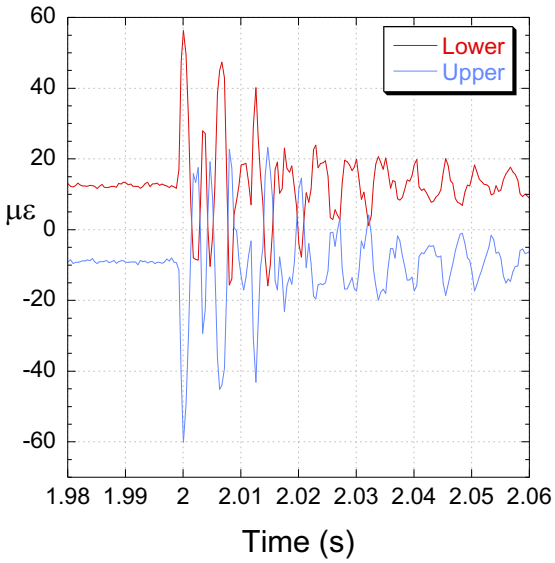

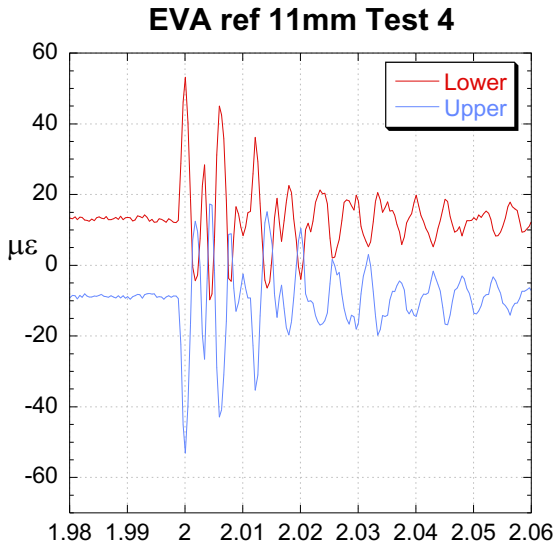

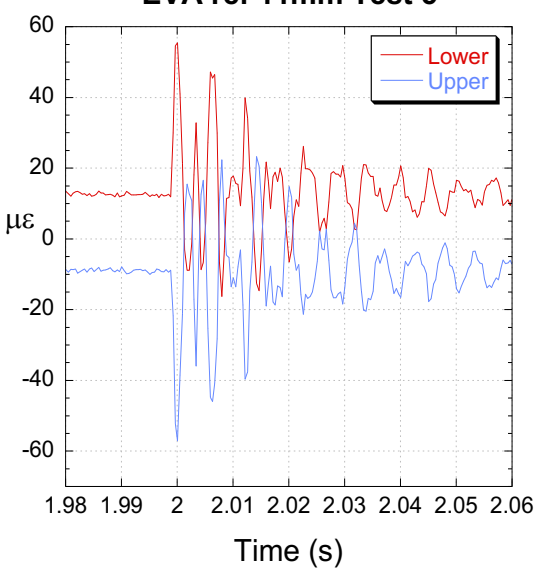

Microcellular rubber 11mm-5 kN

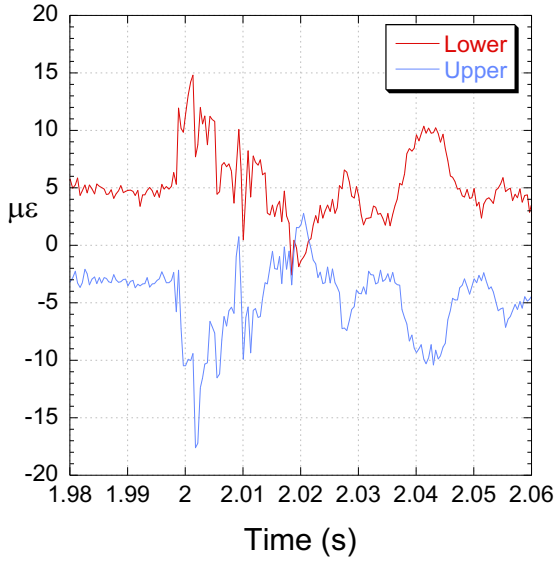

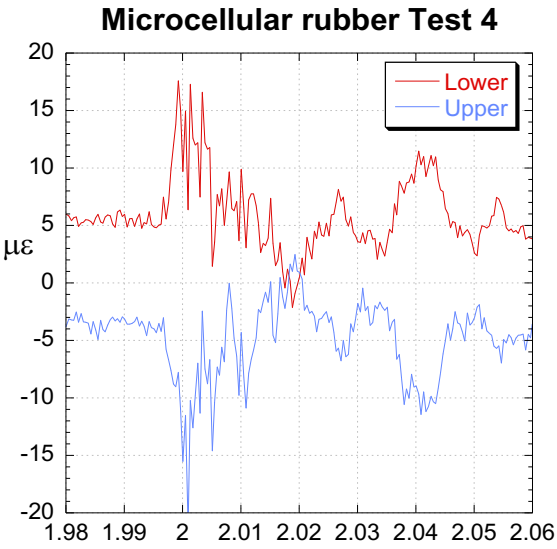

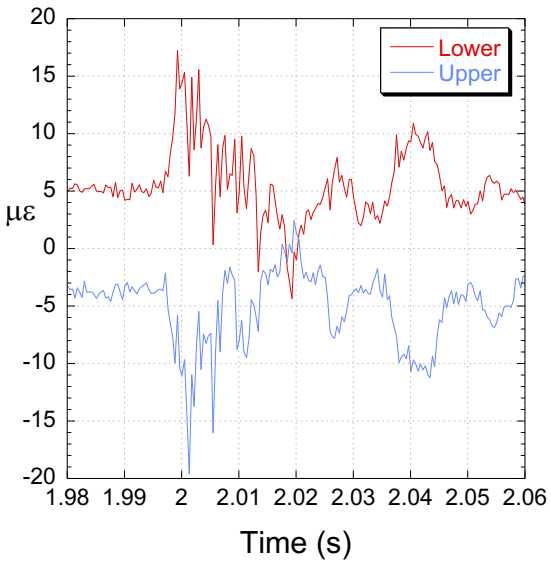

EVA REF 11 mm-5 kN

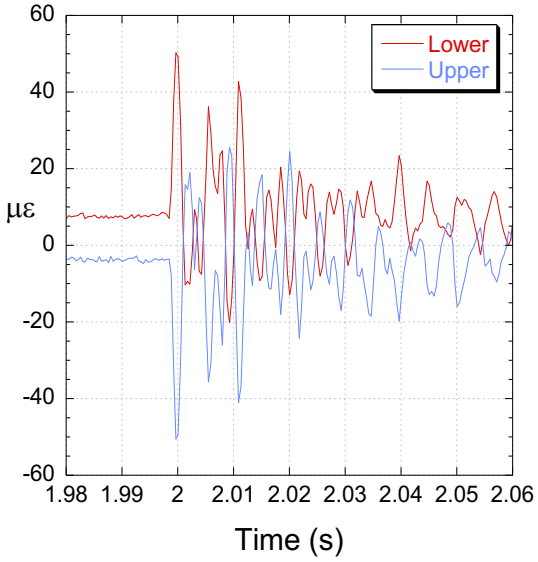

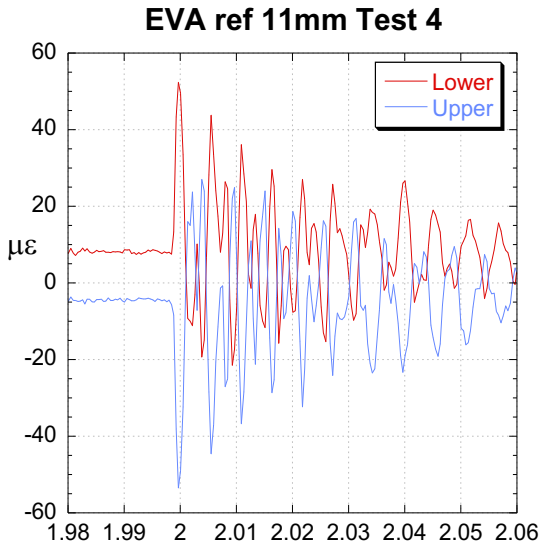

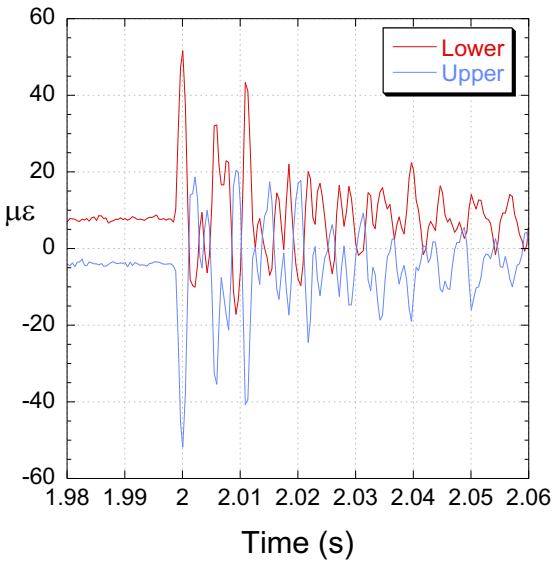

Microcellular rubber 11mm-0 kN

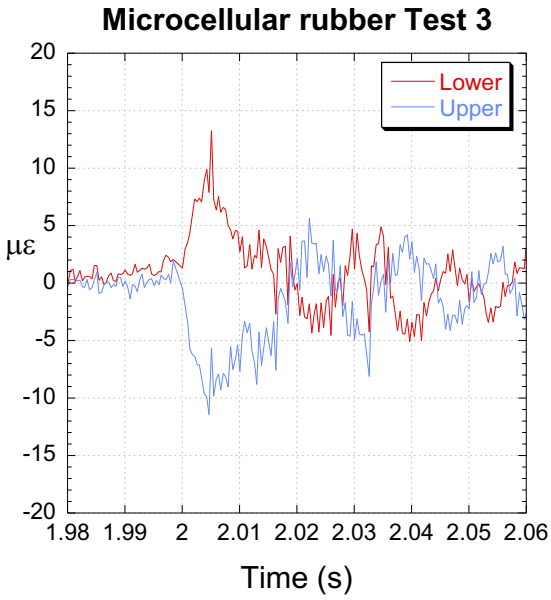

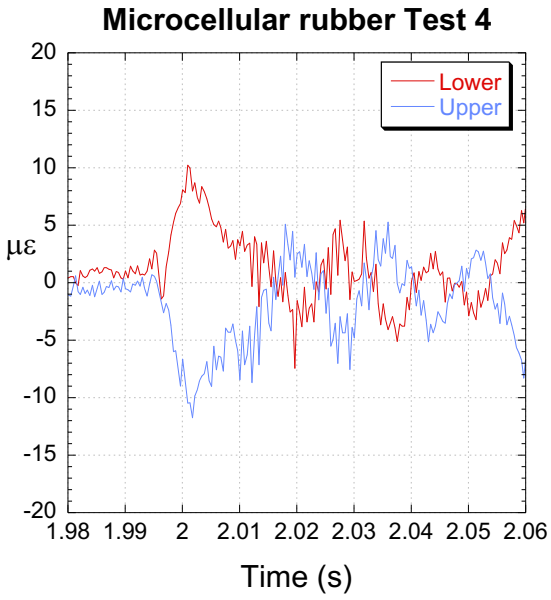

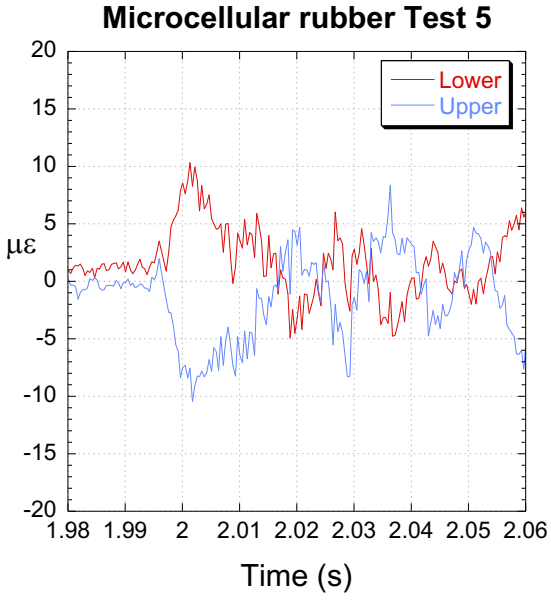

EVA REF 11 mm-0 kN

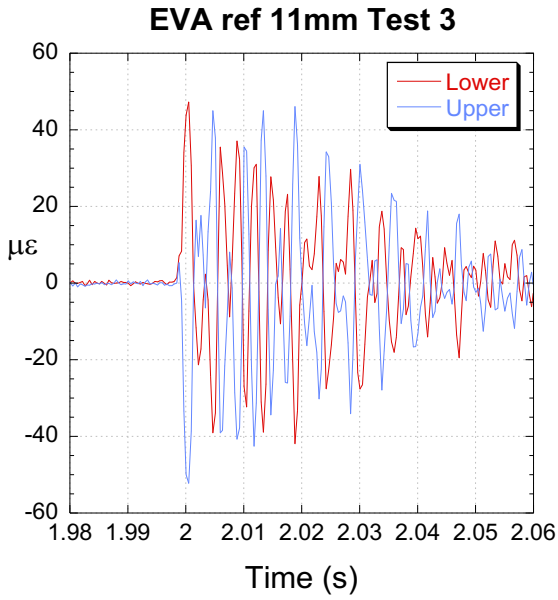

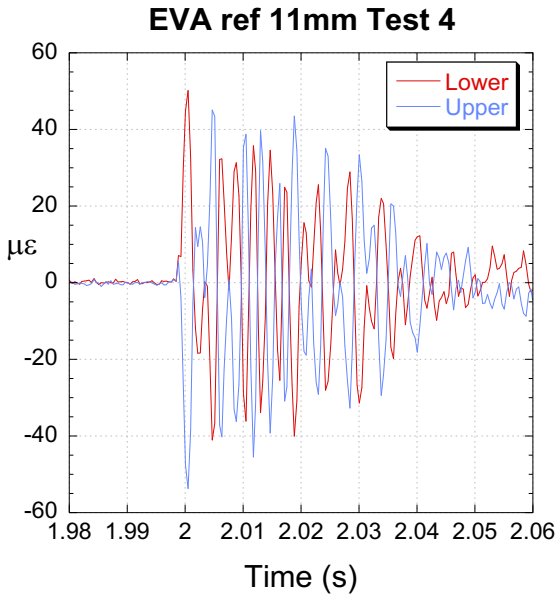

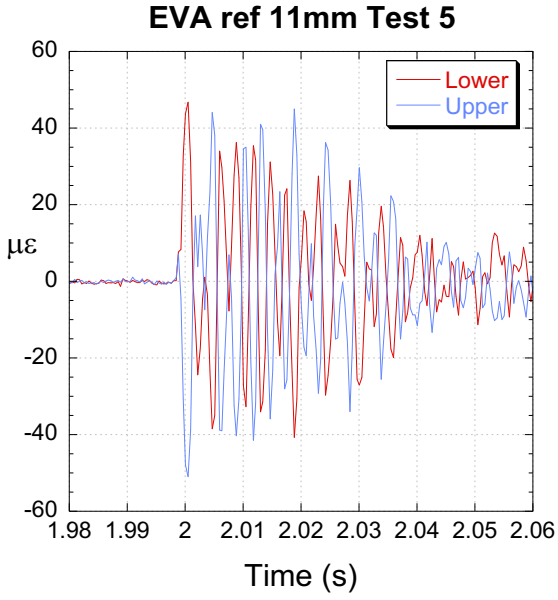

SOLID (REINFORCED RUBBER) 11mm

Solid reinforced rubber 11mm 50 kN

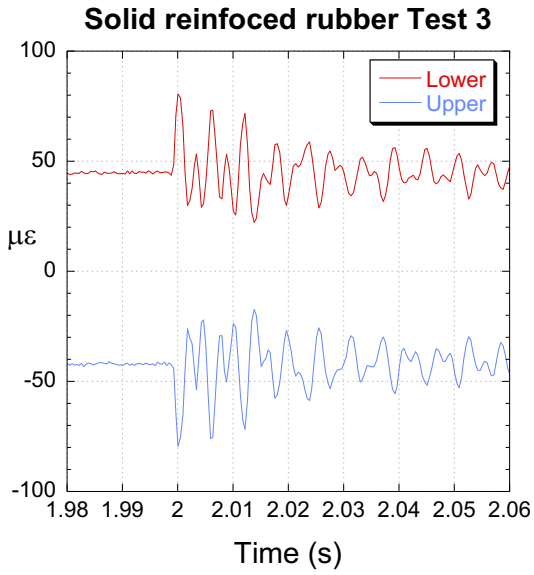

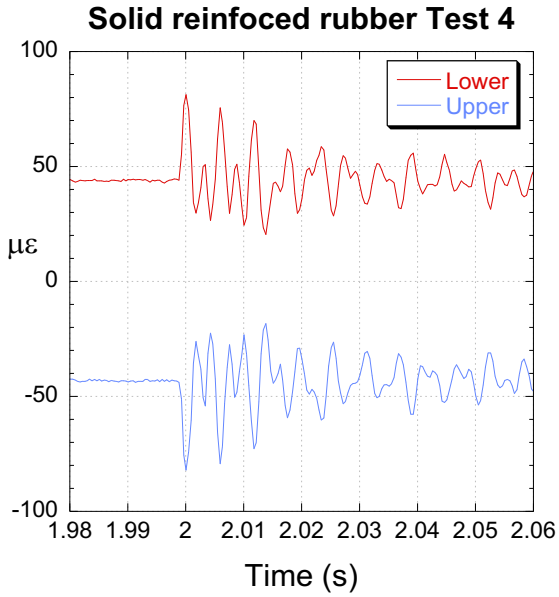

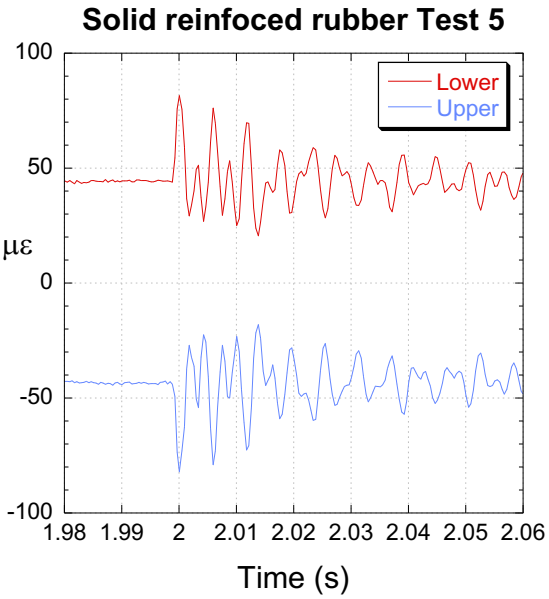

EVA REF 11 mm-50 kN

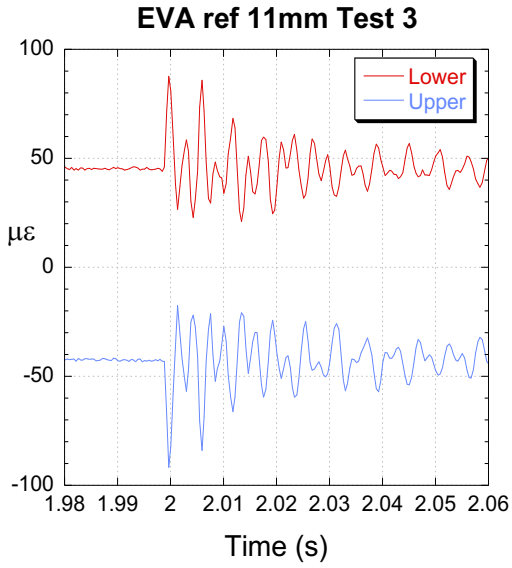

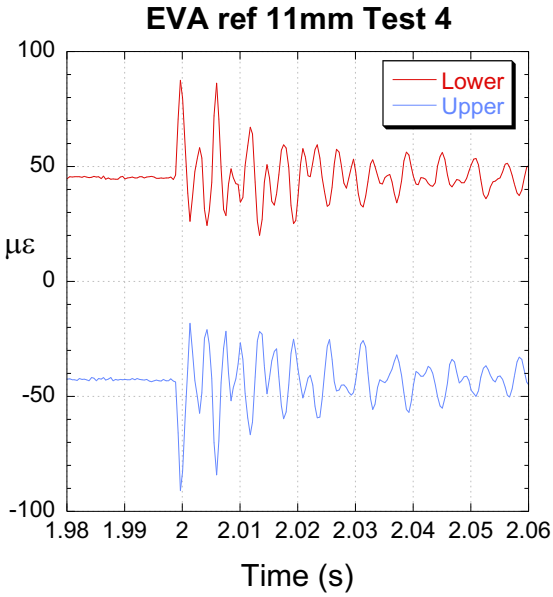

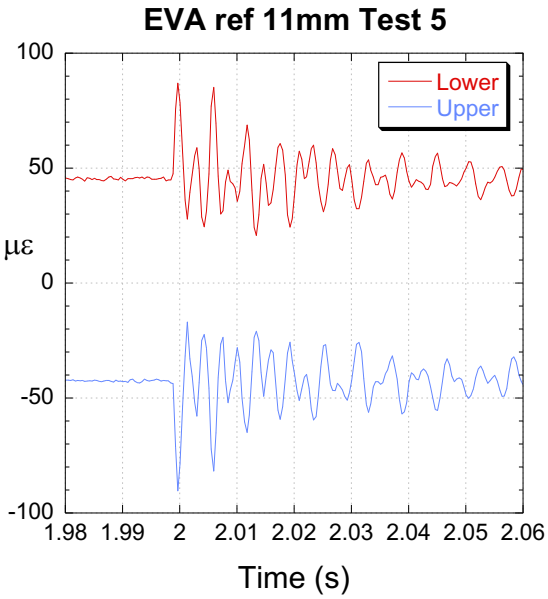

Solid reinforced rubber 11mm 25 kN

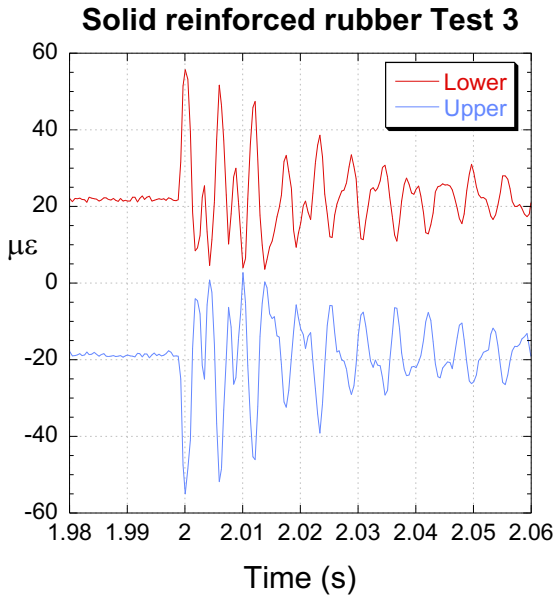

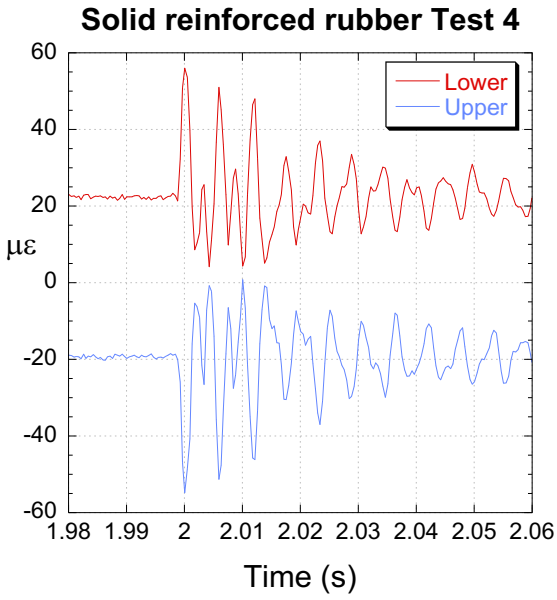

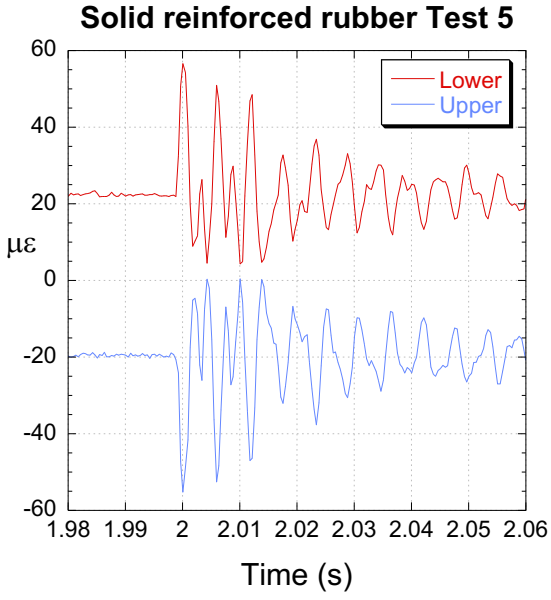

EVA REF 11 mm-25 kN

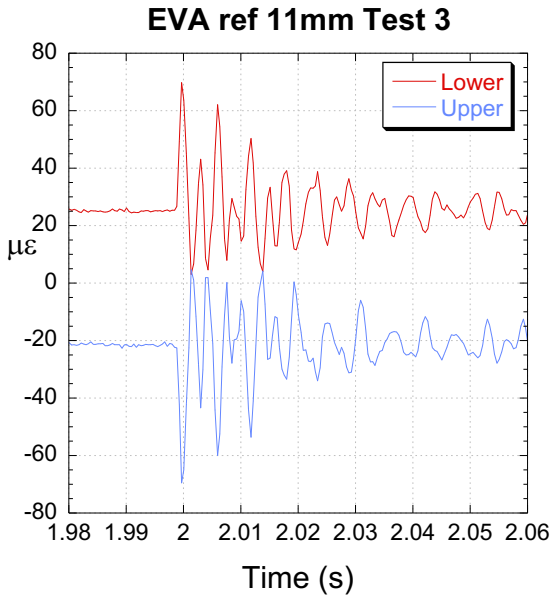

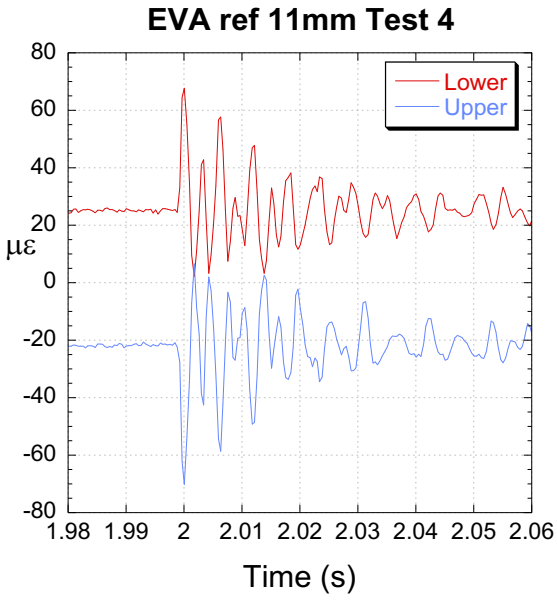

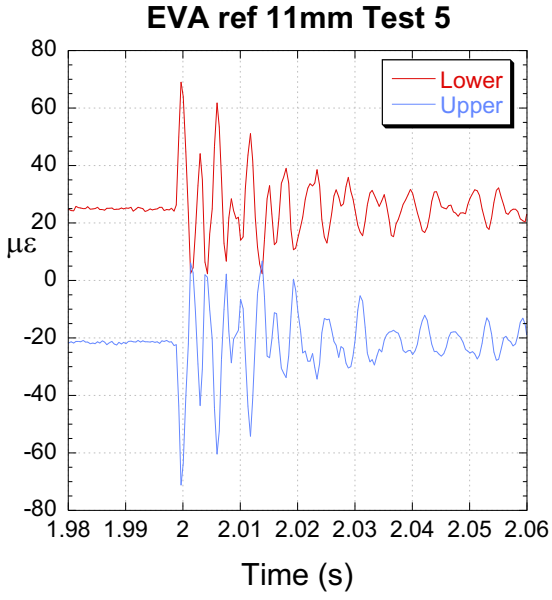

Solid reinforced rubber 11mm 10 kN

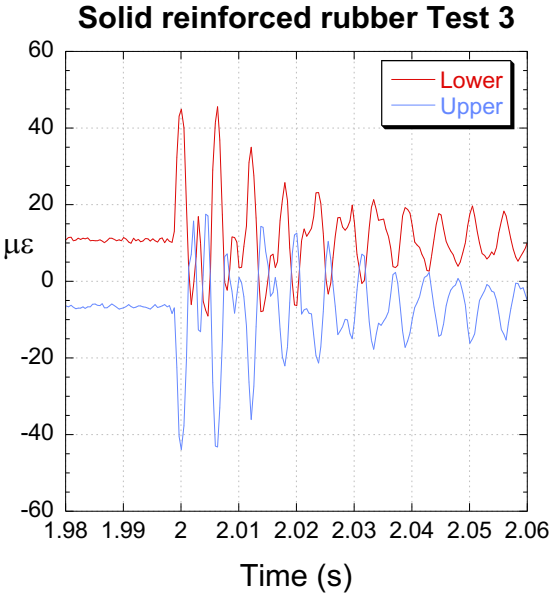

EVA REF 11 mm-10 kN

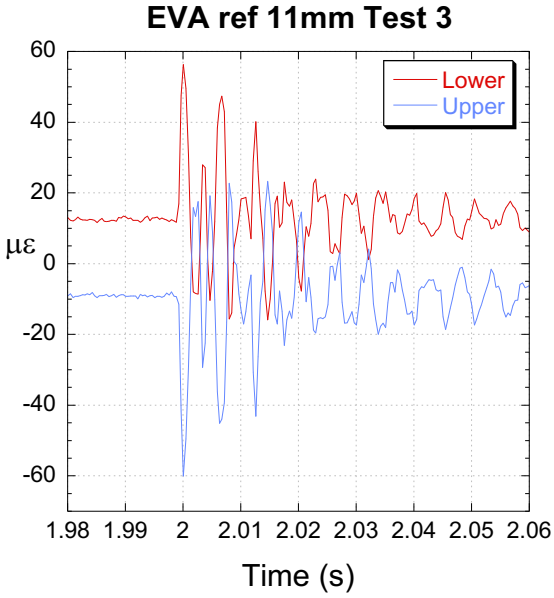

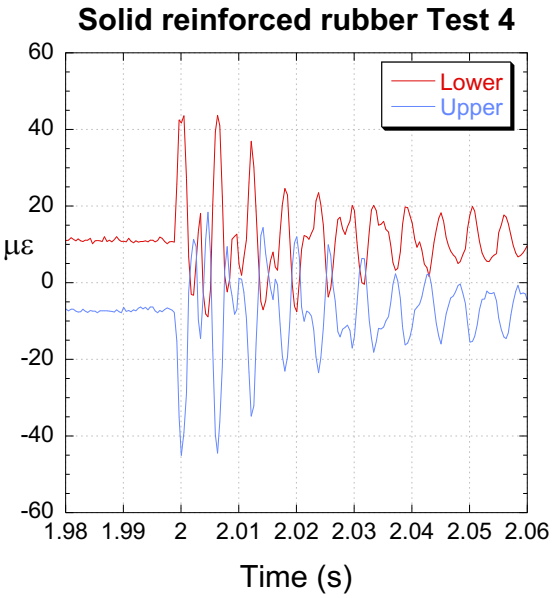

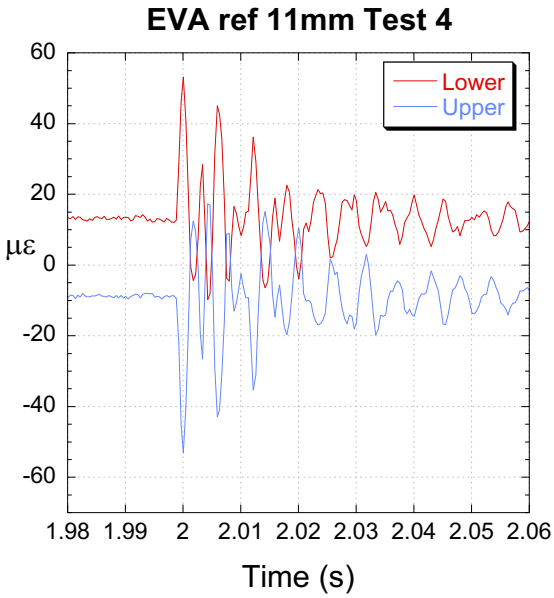

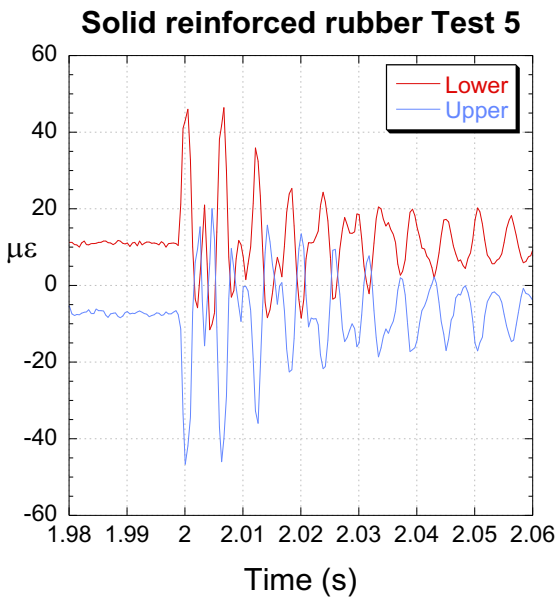

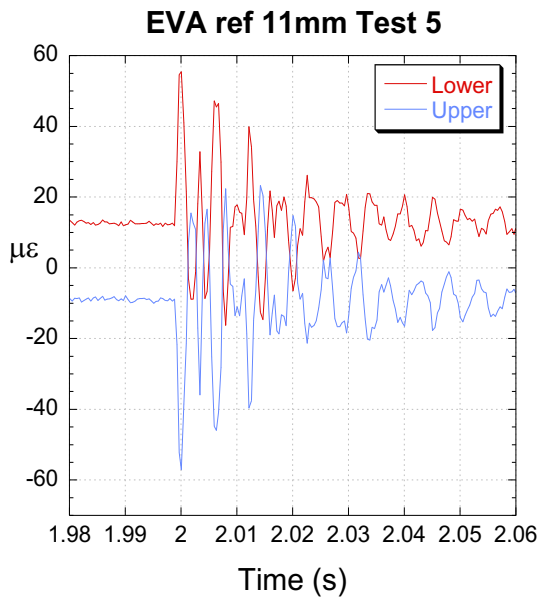

Solid reinforced rubber 11mm 5 kN

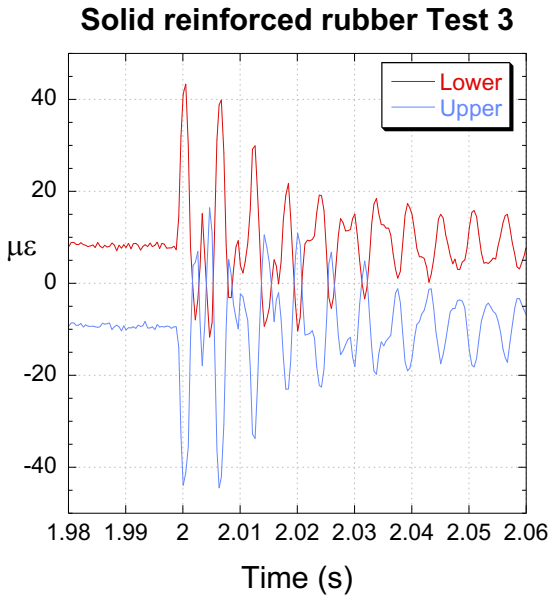

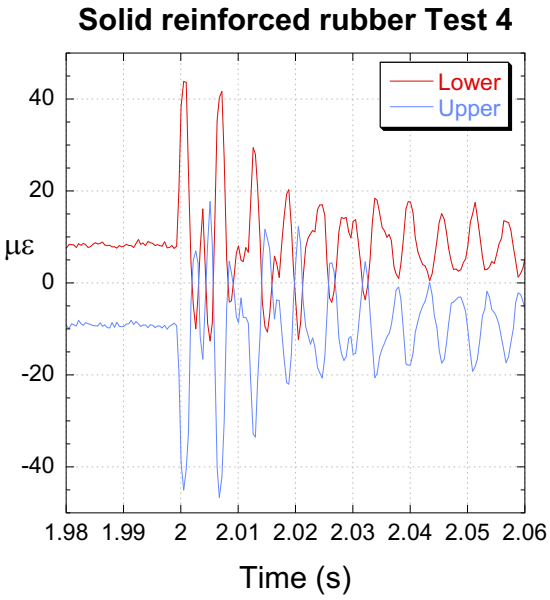

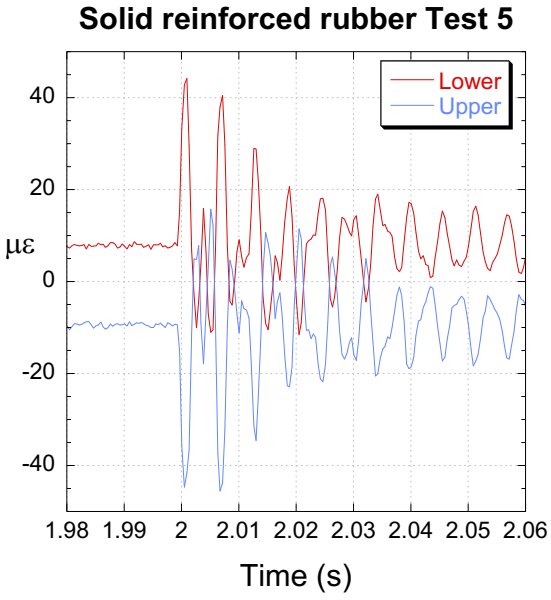

EVA REF 11 mm-5 kN

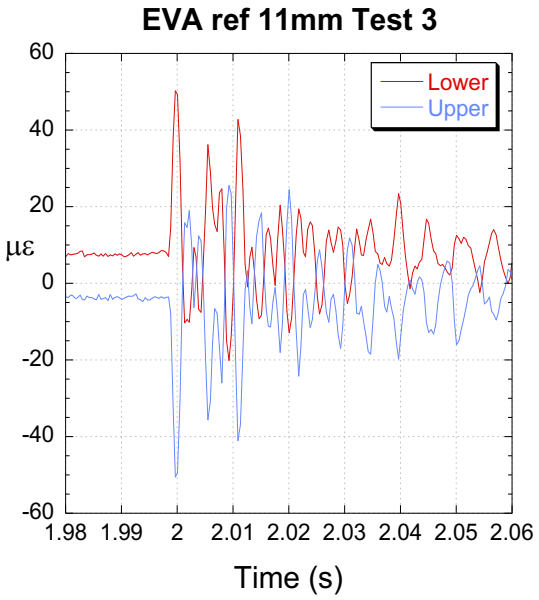

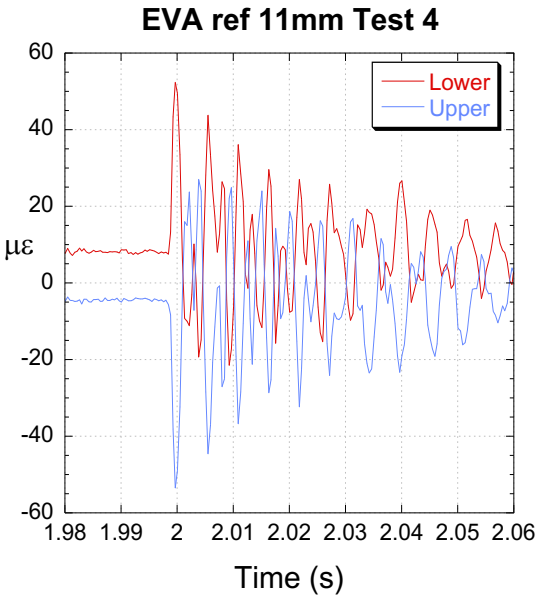

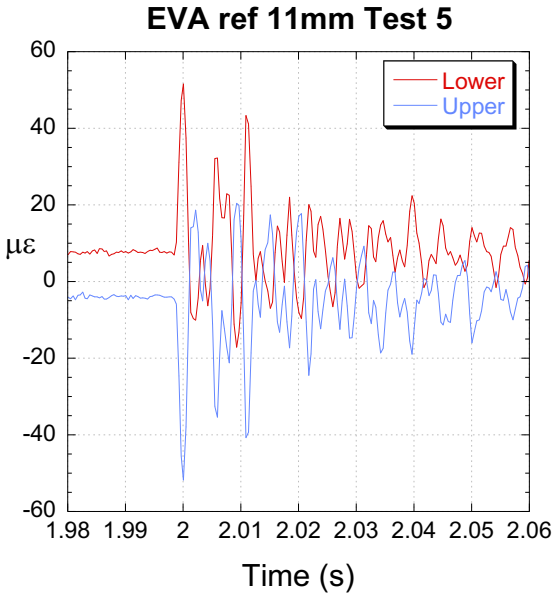

Solid reinforced rubber 11mm 0 kN

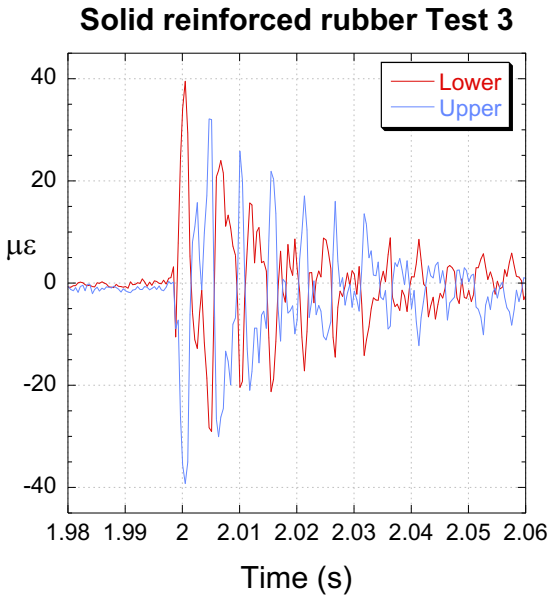

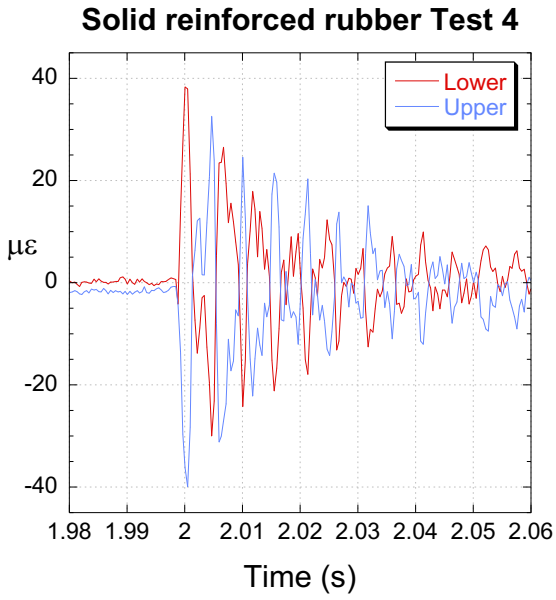

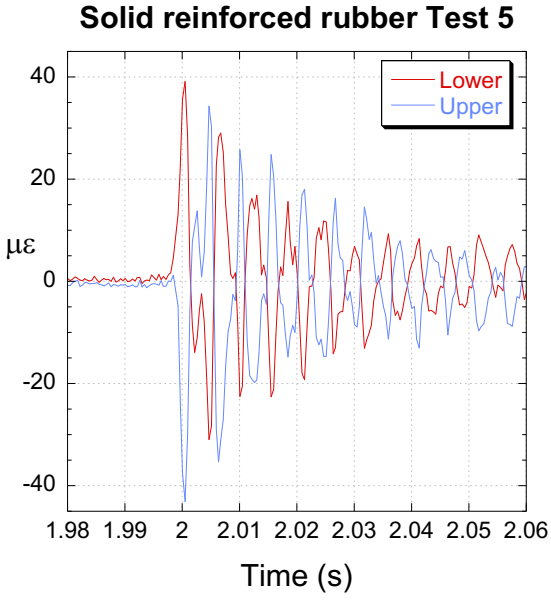

EVA REF 11 mm-0 kN

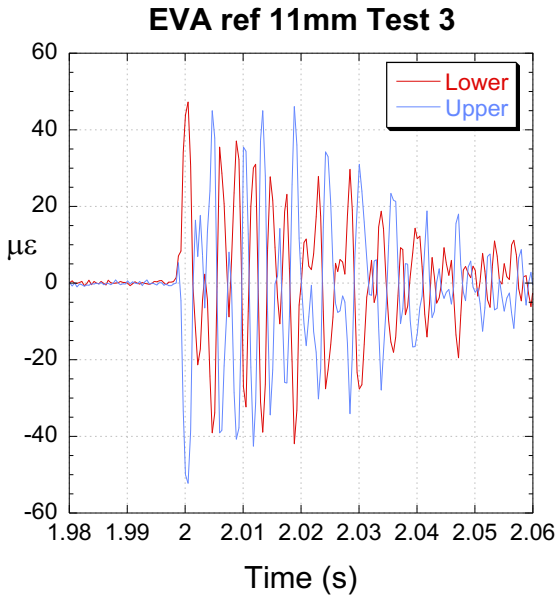

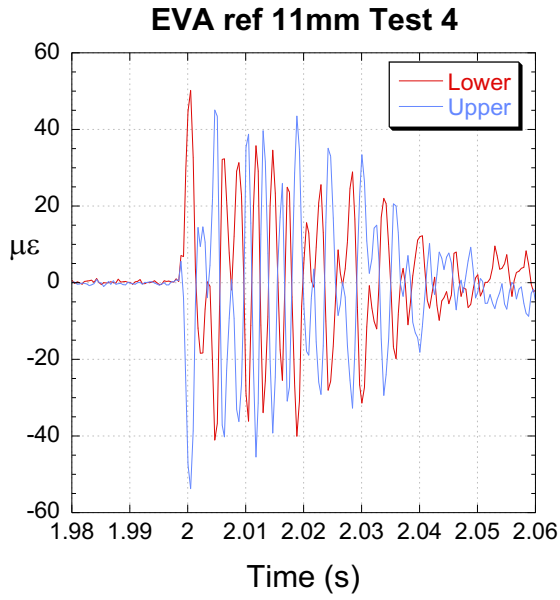

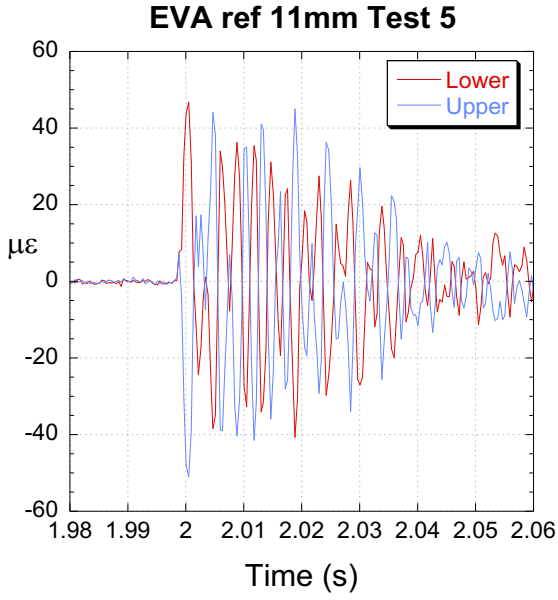

Studded TPE 7 mm 50 kN

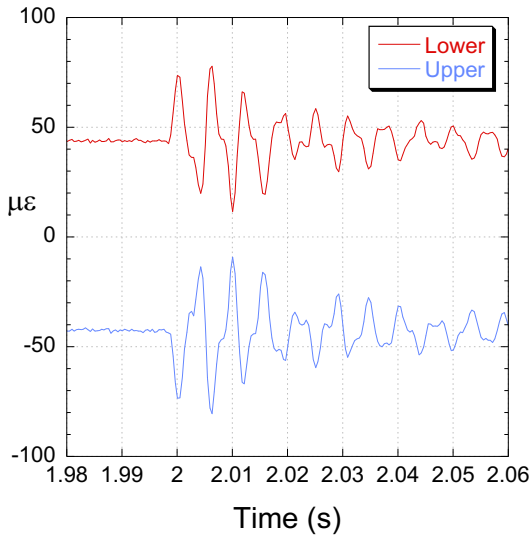

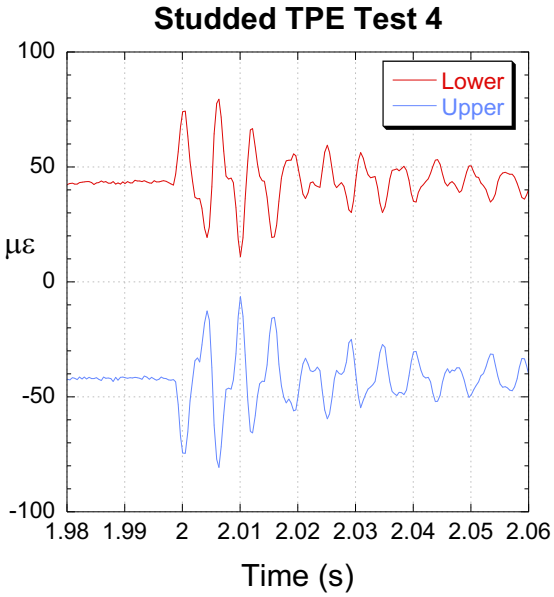

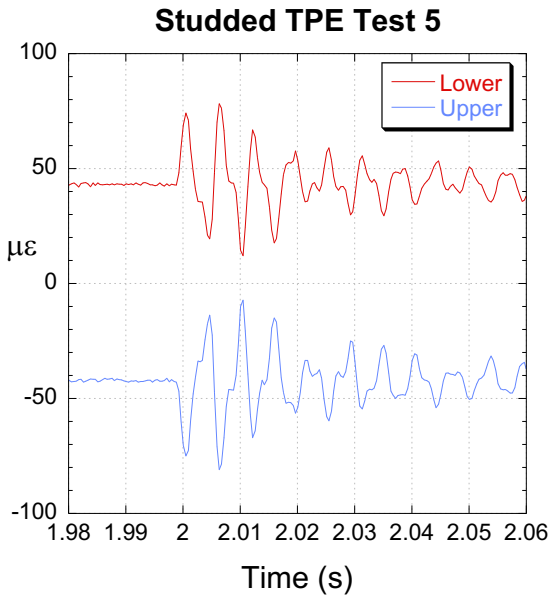

EVA REF 7 mm 50 kN

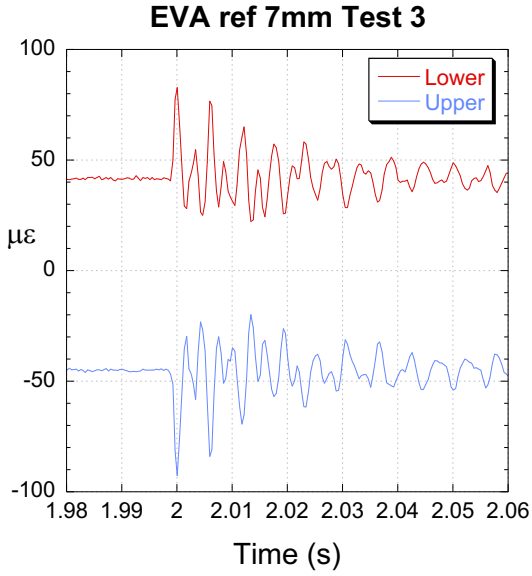

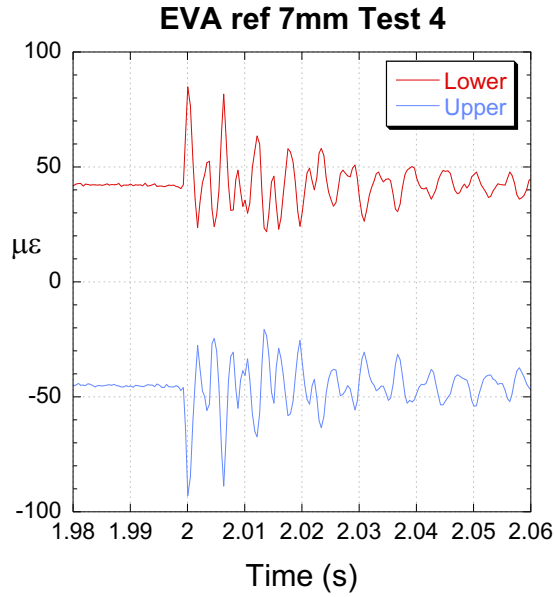

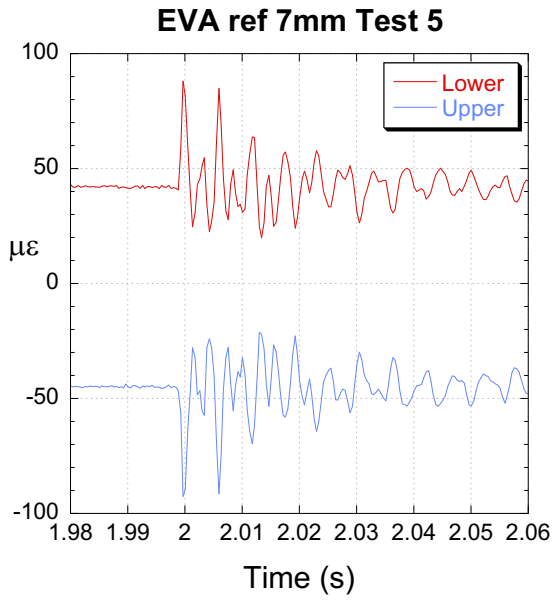

Studded TPE 7 mm 25 kN

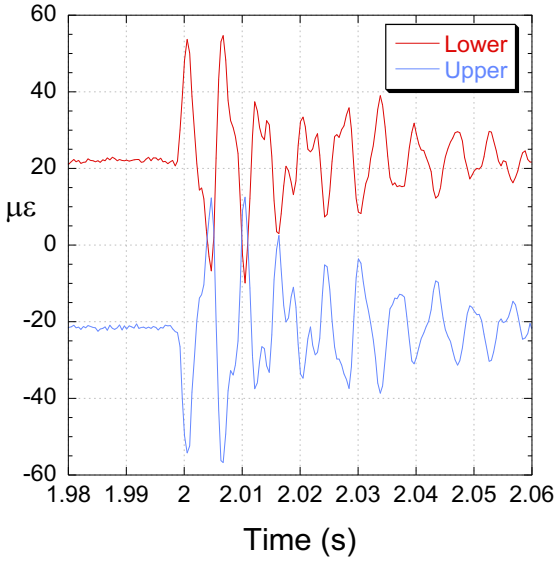

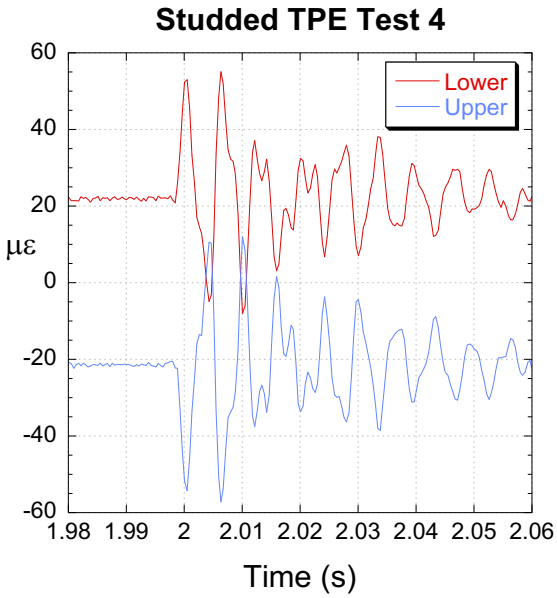

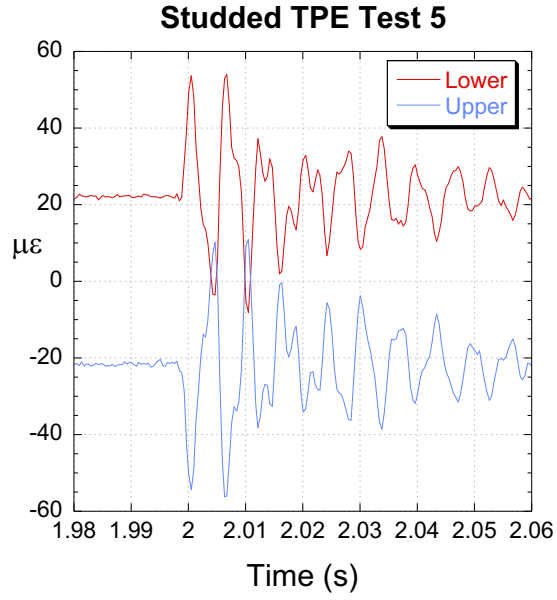

EVA REF 7 mm 25 kN

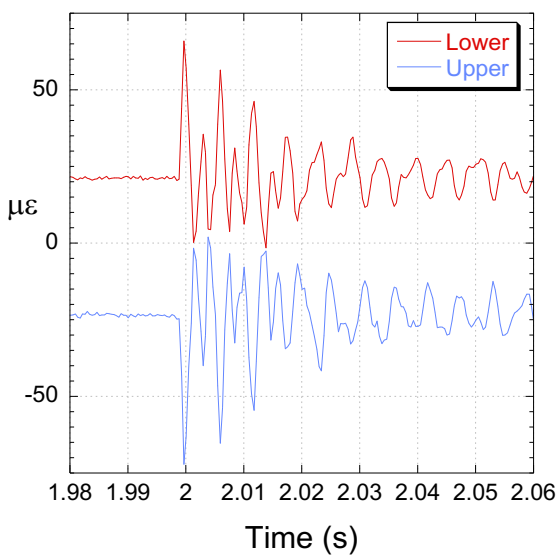

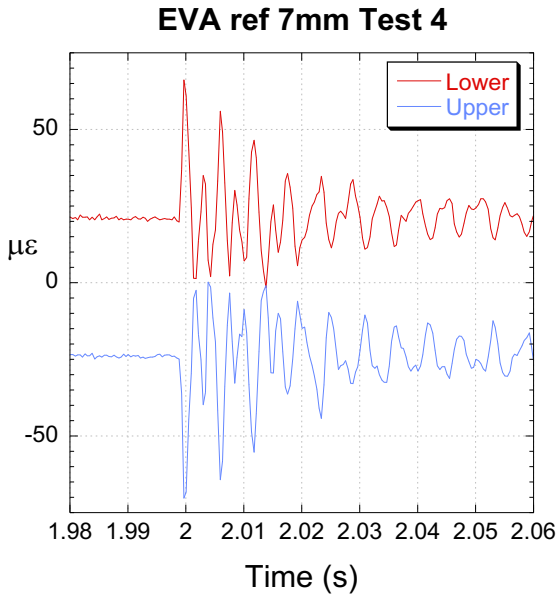

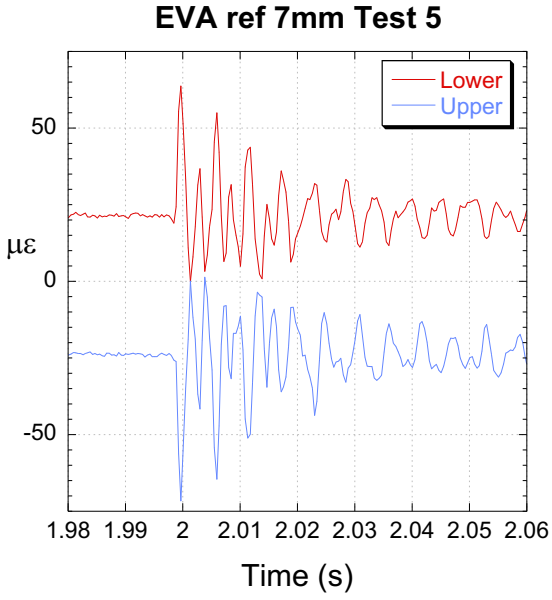

Studded TPE7 mm 10 kN

EVA REF 7 mm 10 kN

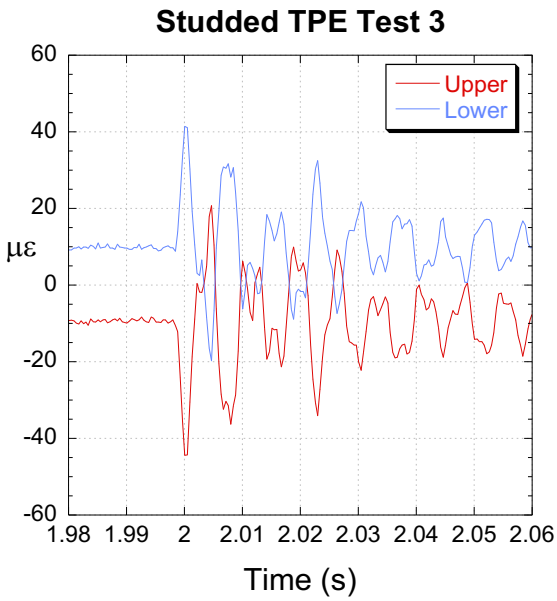

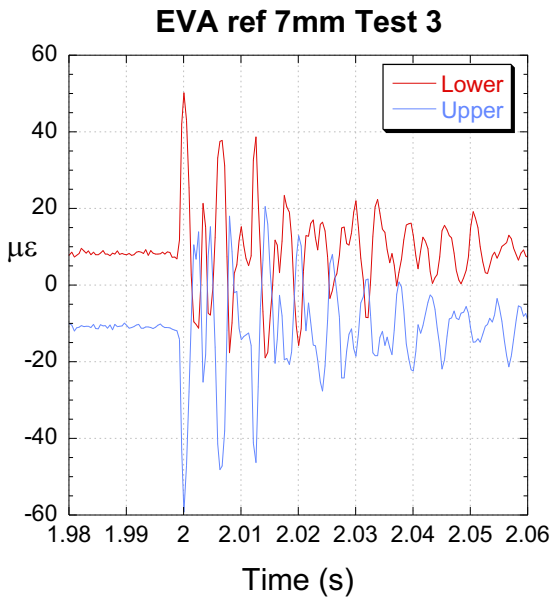

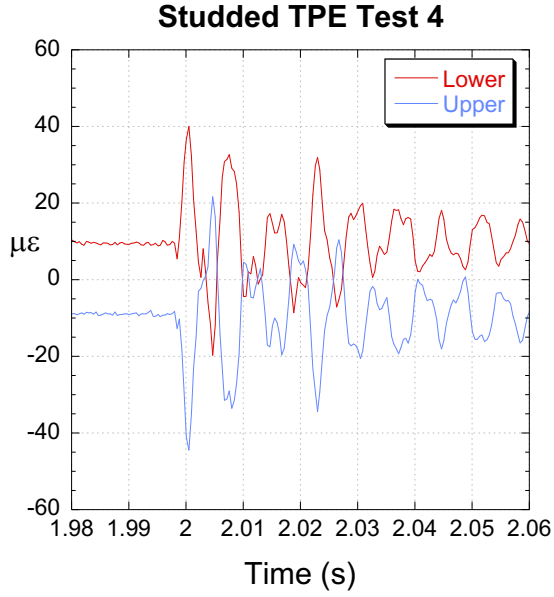

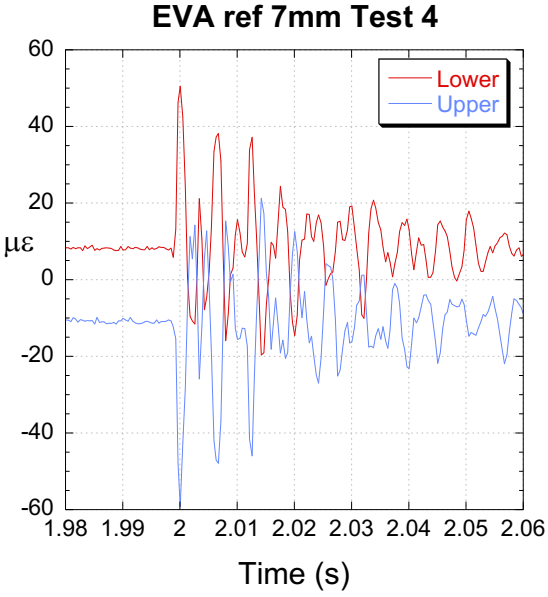

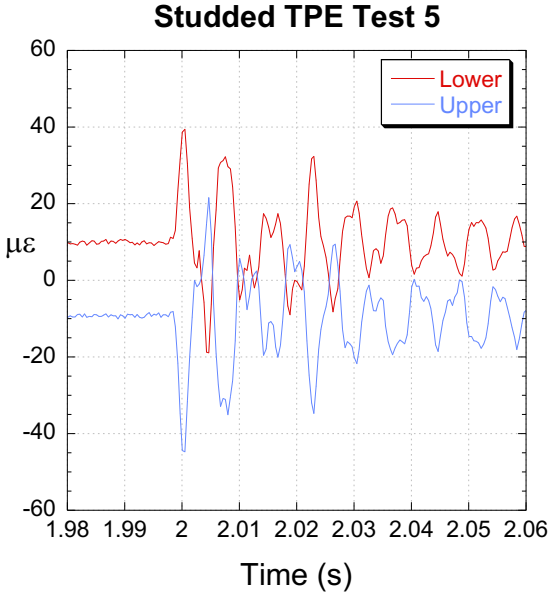

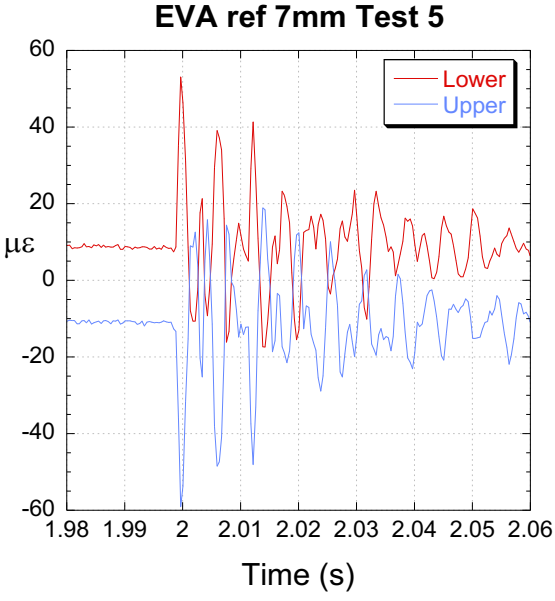

Solid EPDM (7mm)

Solid EPDM 7 mm 50 kN

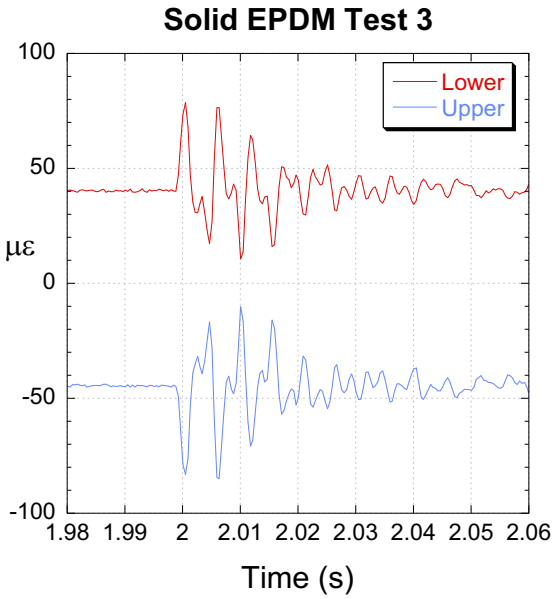

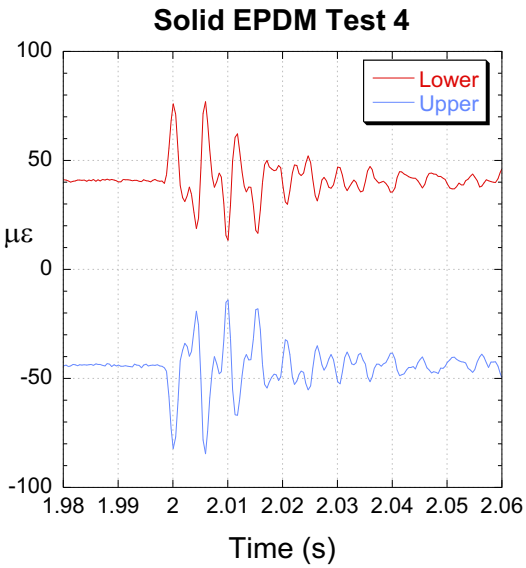

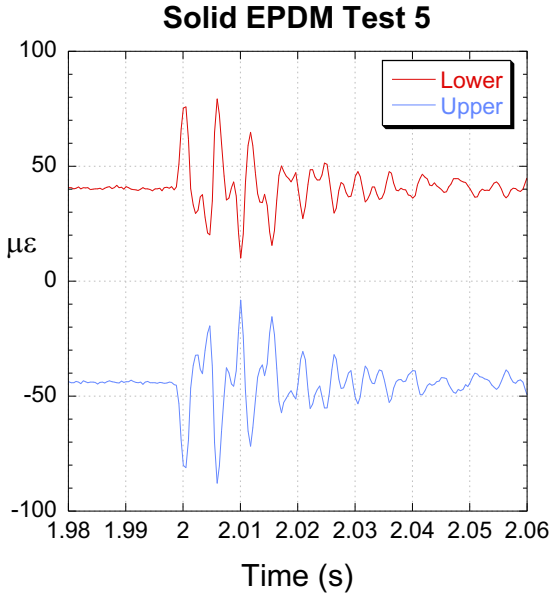

EVA REF 7 mm 50 kN

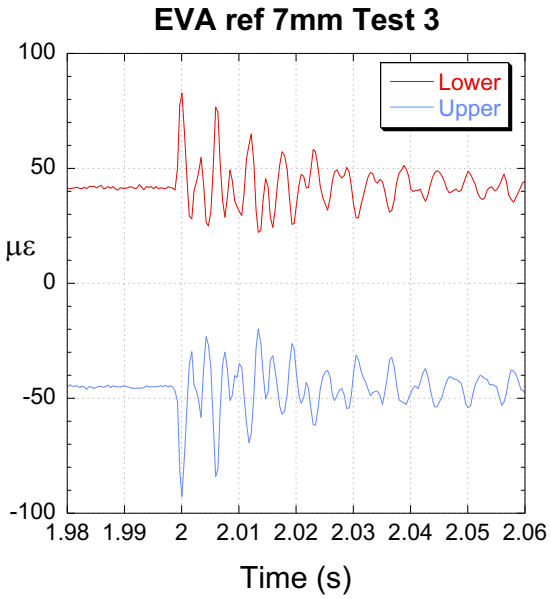

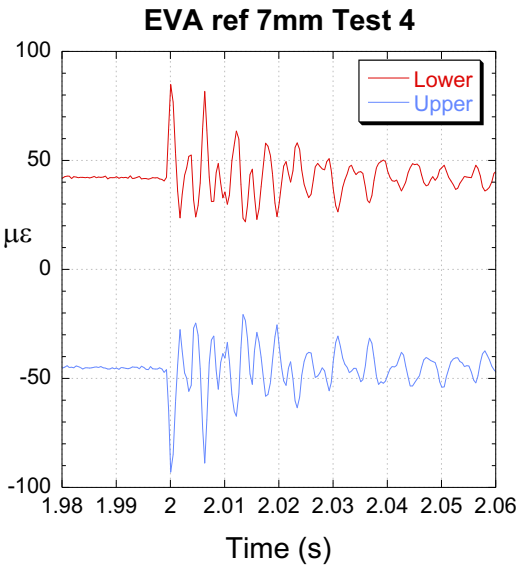

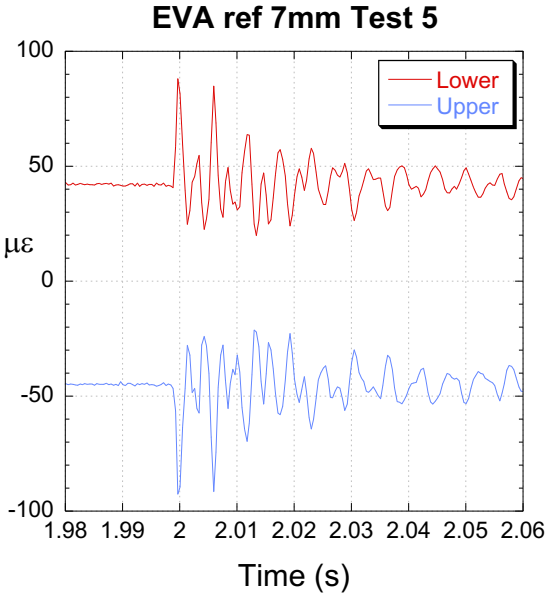

Solid EPDM 7 mm 25 kN

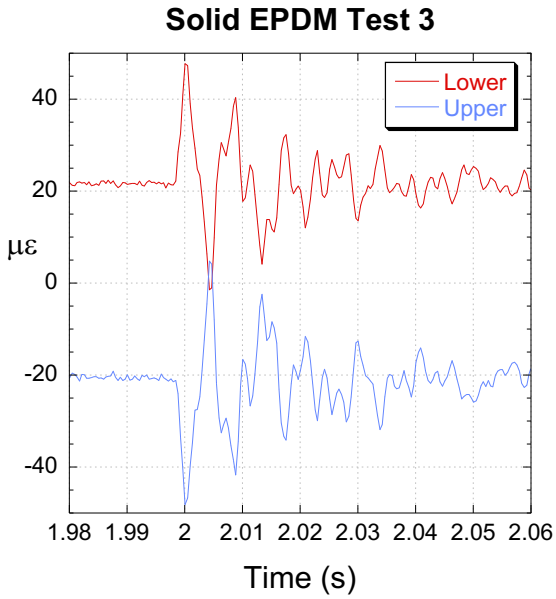

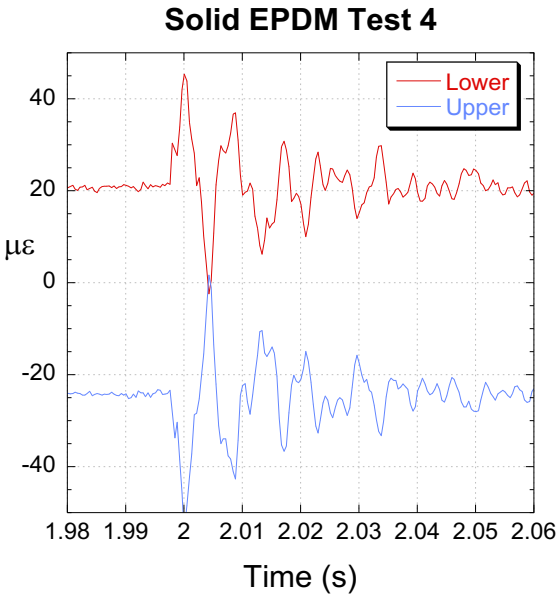

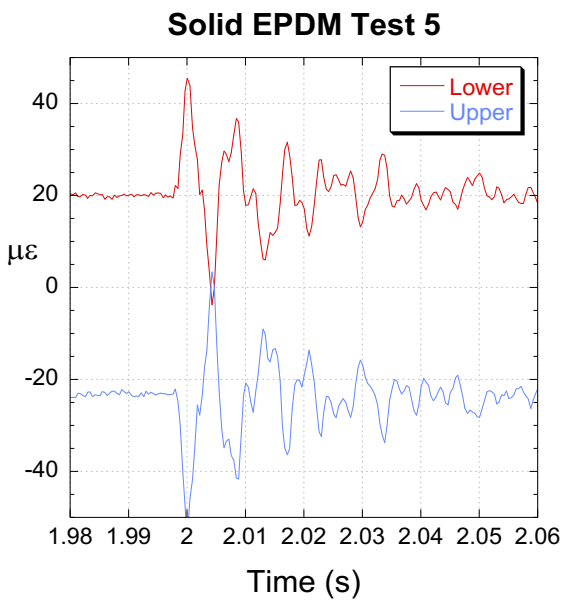

EVA REF 7 mm 25 kN

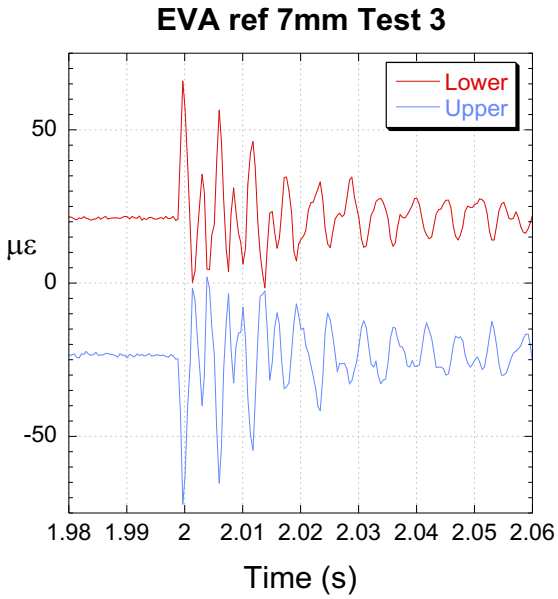

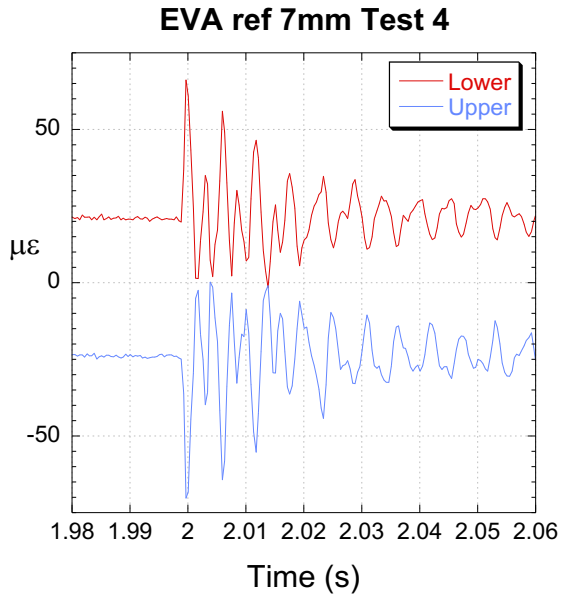

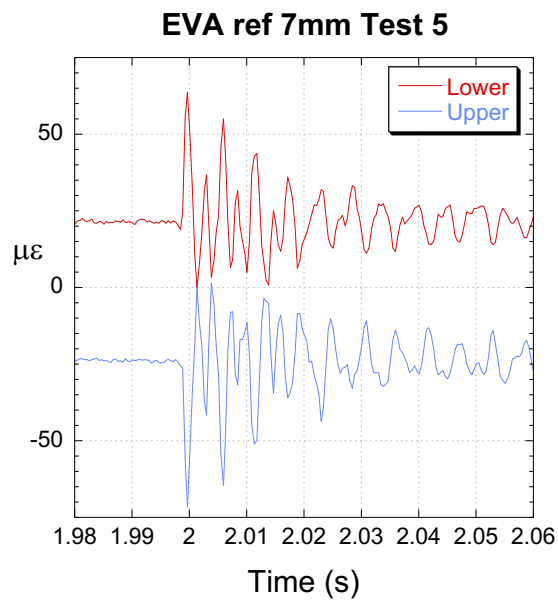

Solid EPDM 7 mm 10 kN

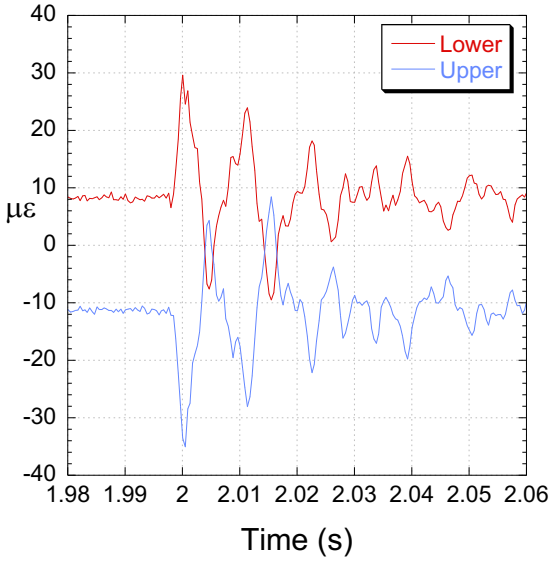

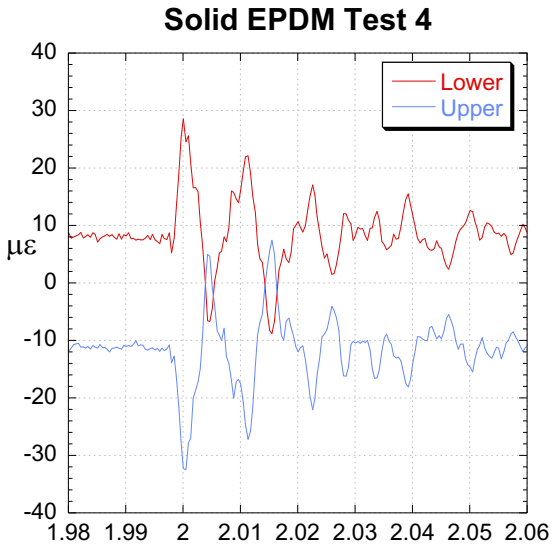

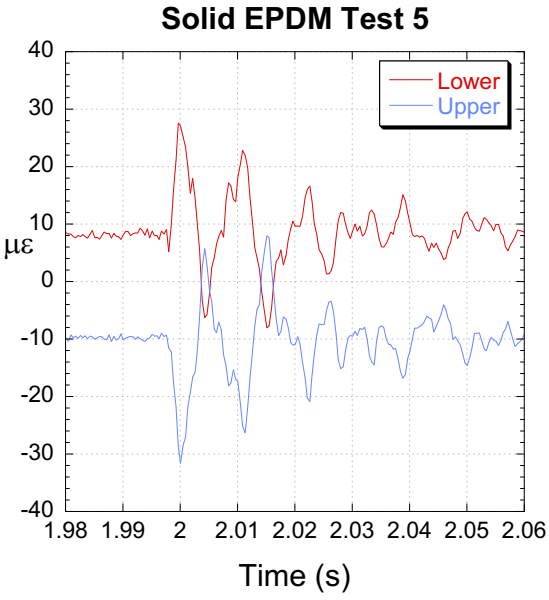

EVA REF 7 mm 10 kN

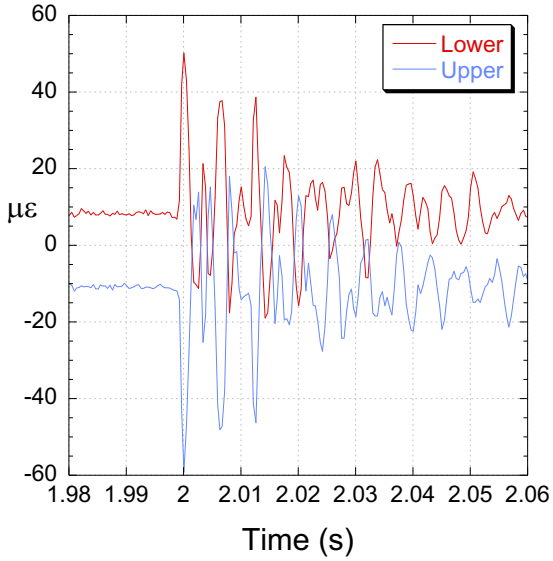

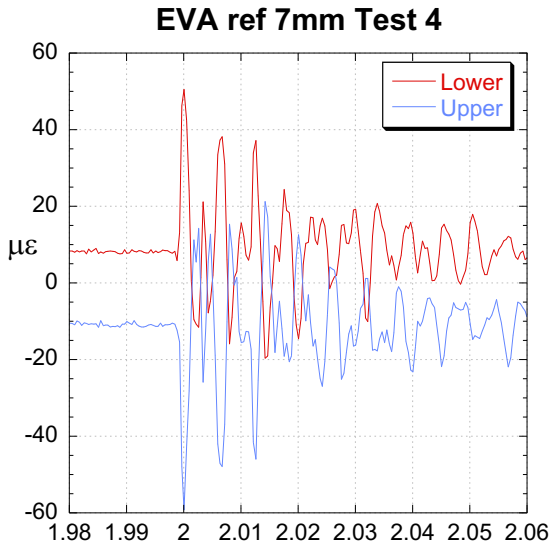

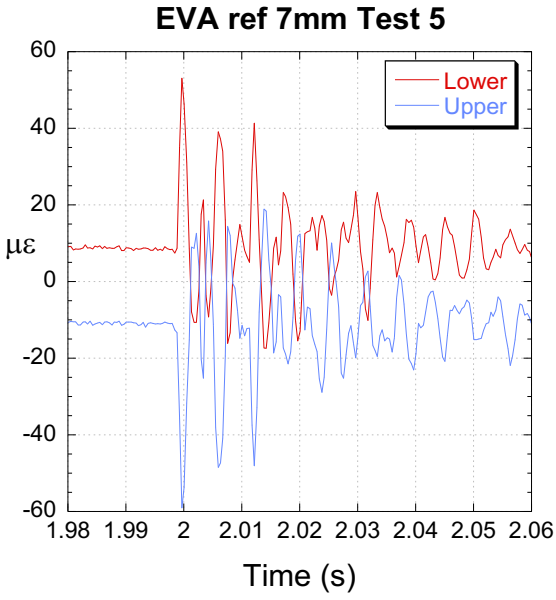

Solid NFU 11mm 50 kN

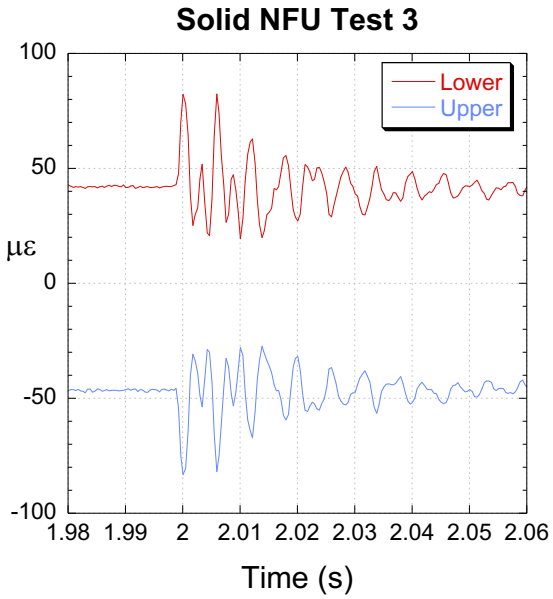

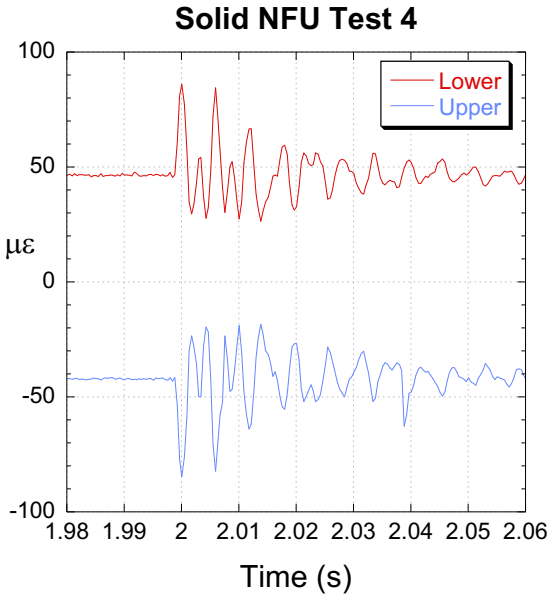

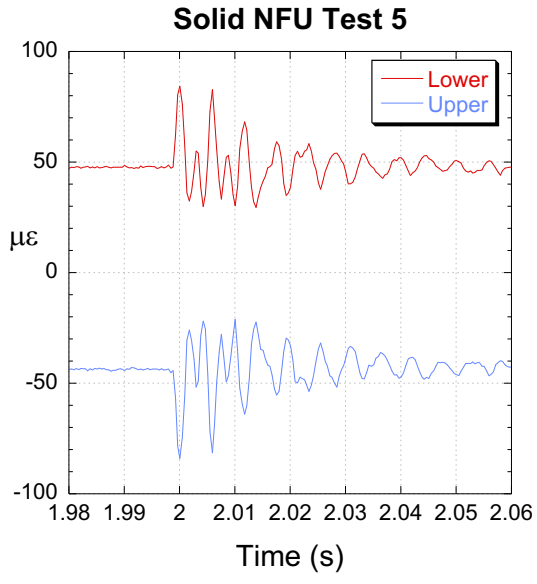

EVA REF 11 mm 50 kN

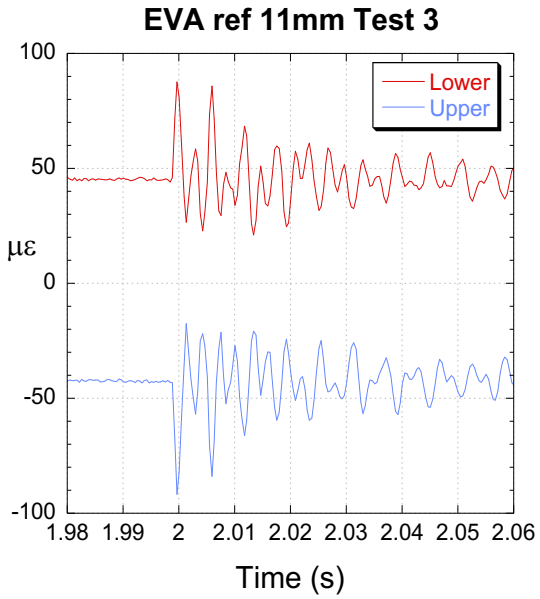

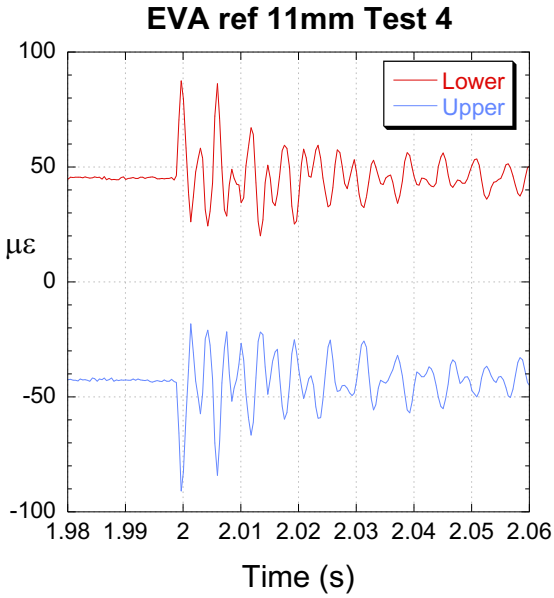

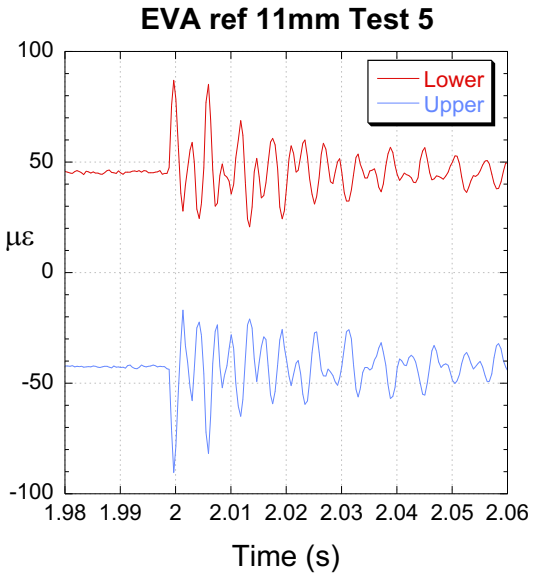

Solid NFU 11mm 25 kN

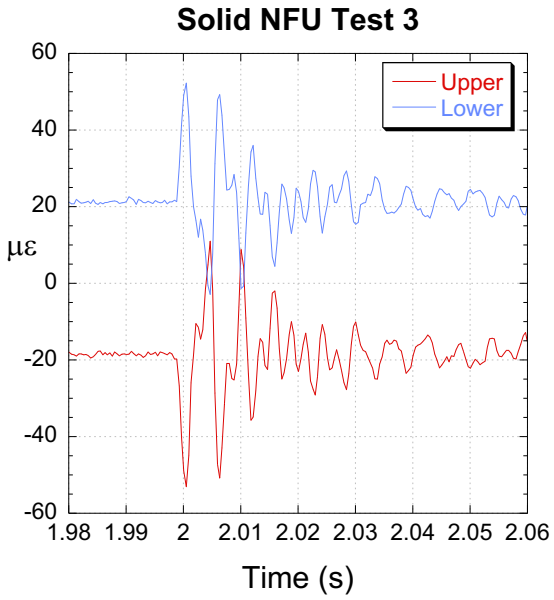

EVA REF 11 mm 25 kN

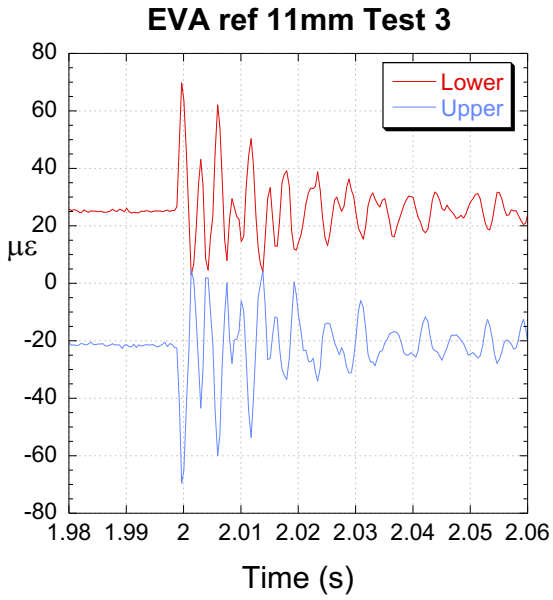

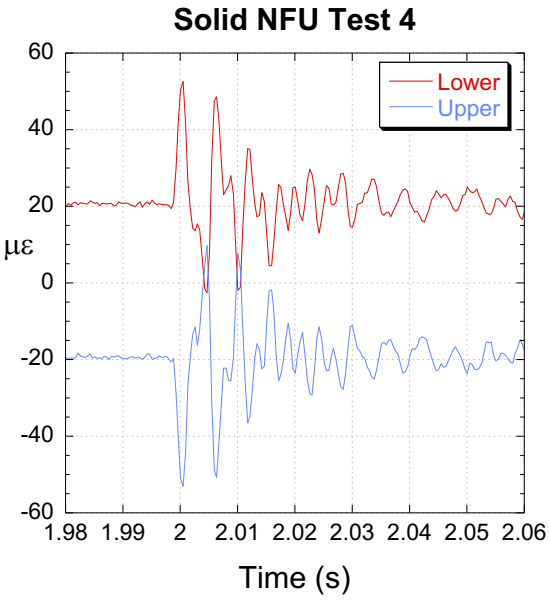

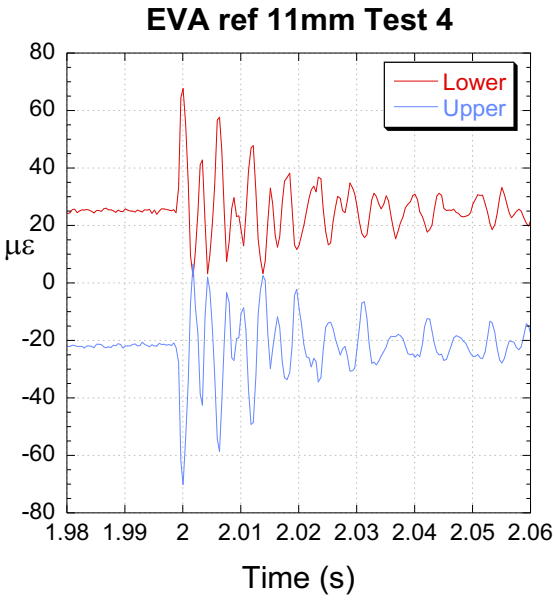

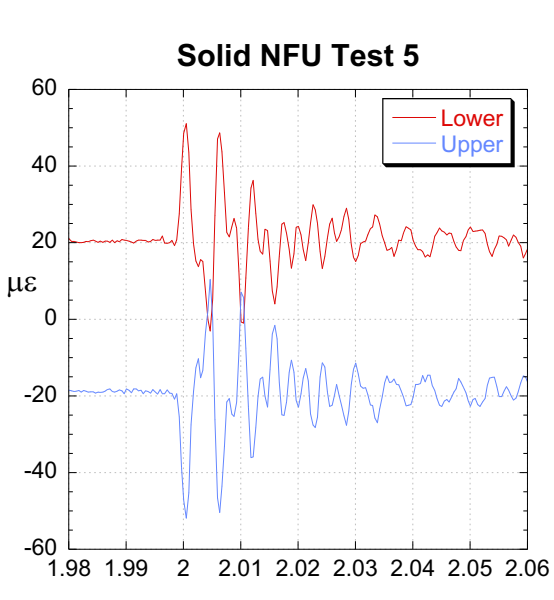

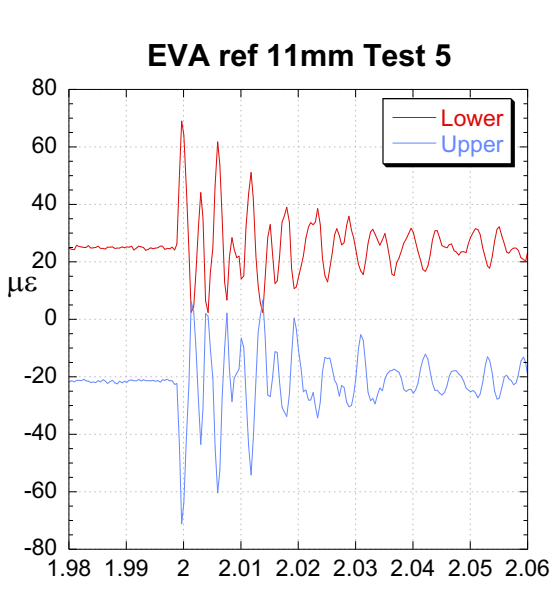

Solid NFU 11mm 10 kN

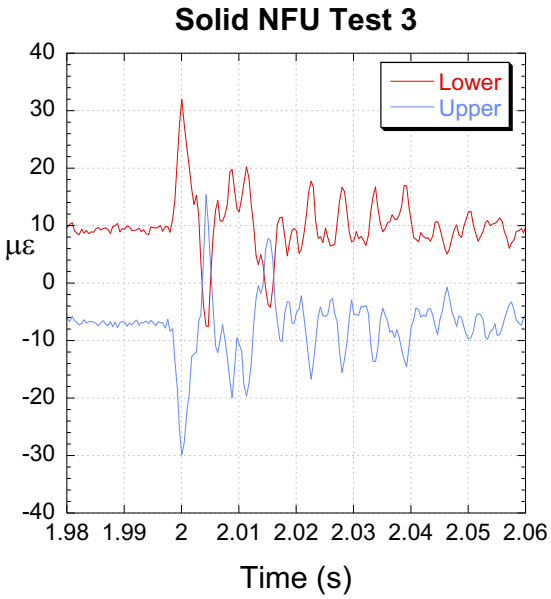

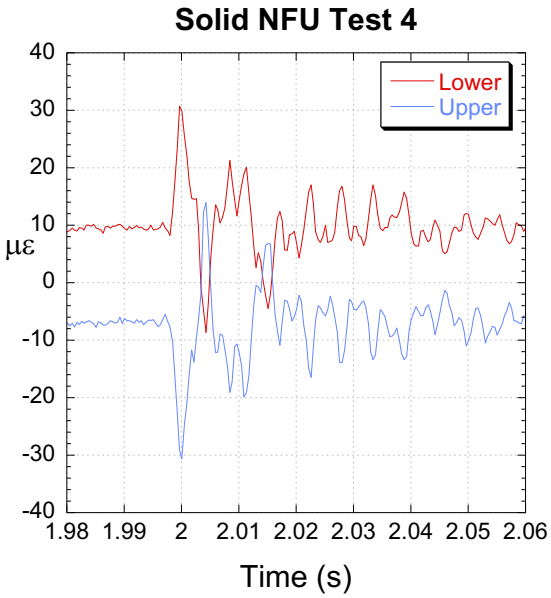

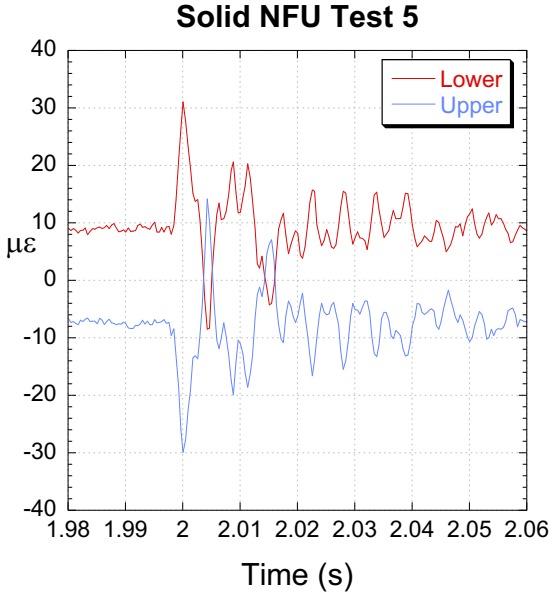

EVA REF 11 mm 10 kN

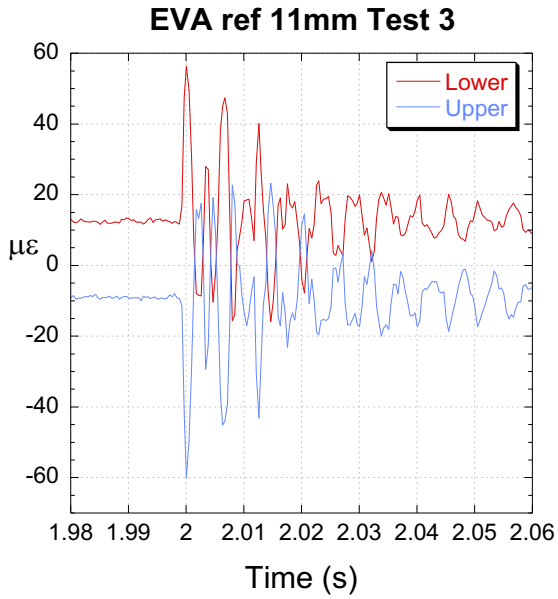

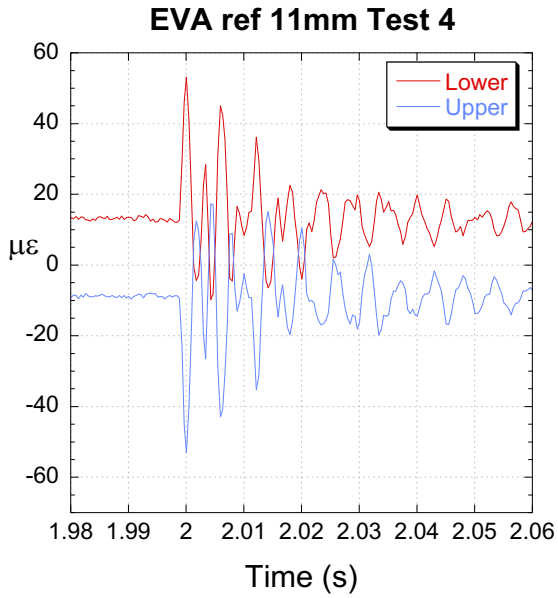

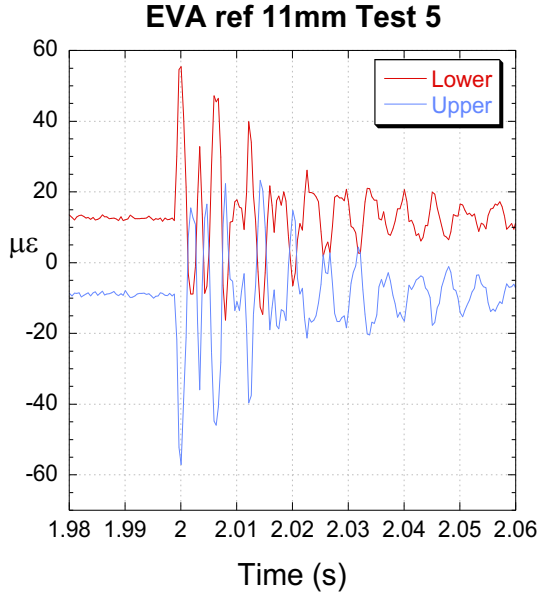

APPENDIX III: REFERENCE METHOD GRAPHS

Studded EPDM 11 mm

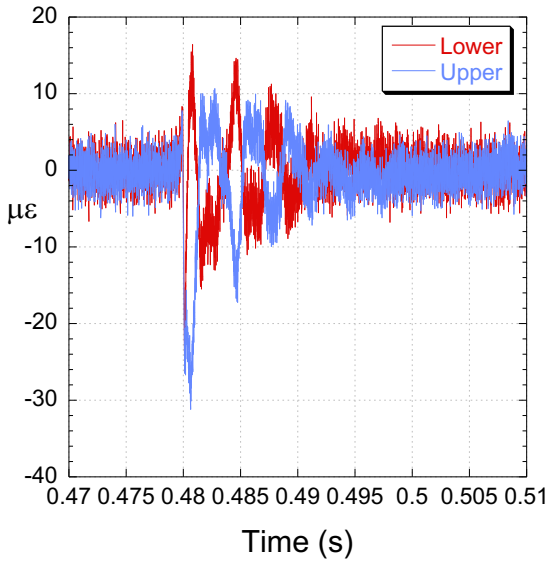

EVA ref 11 mm

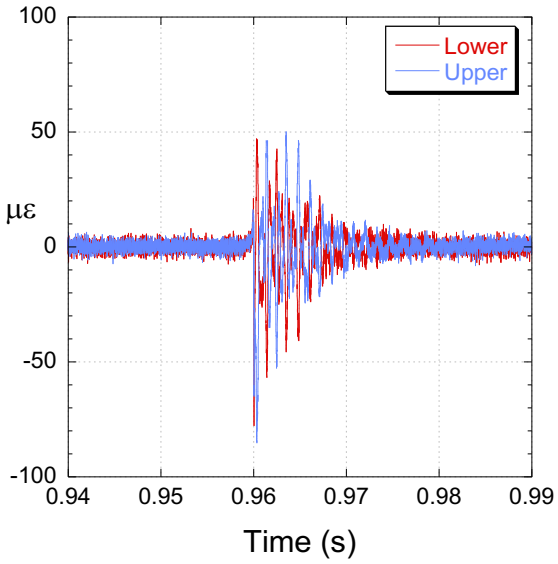

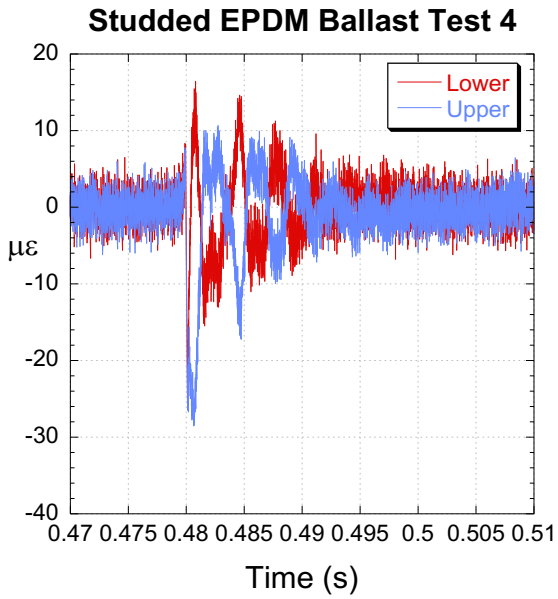

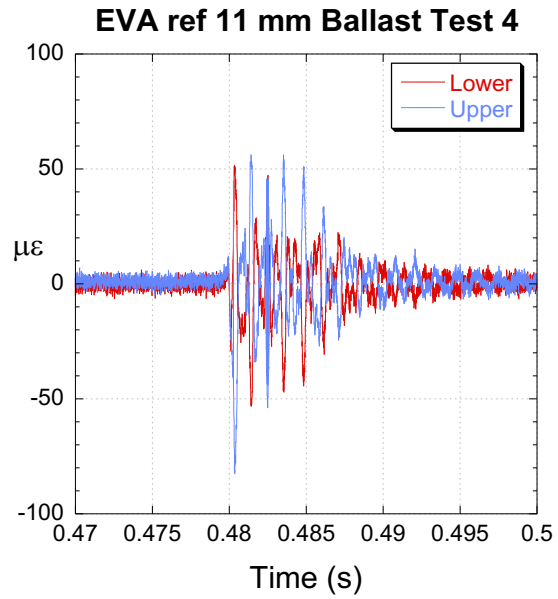

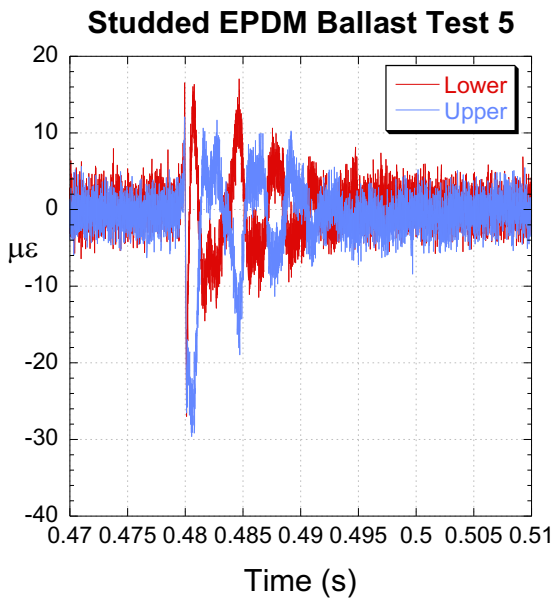

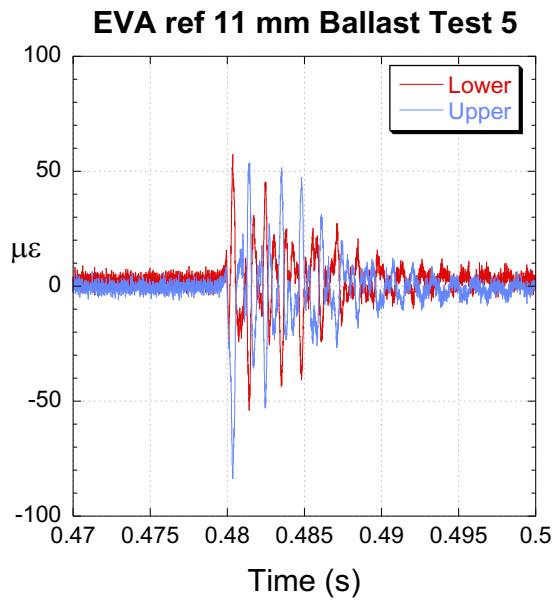

Studded EVA 10 mm

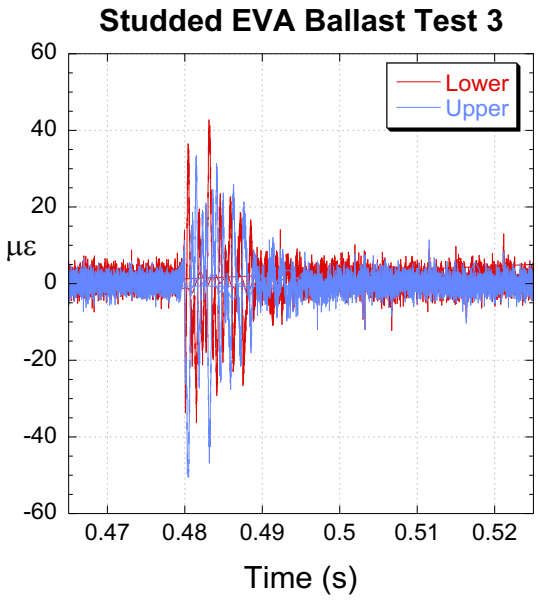

EVA ref 10 mm

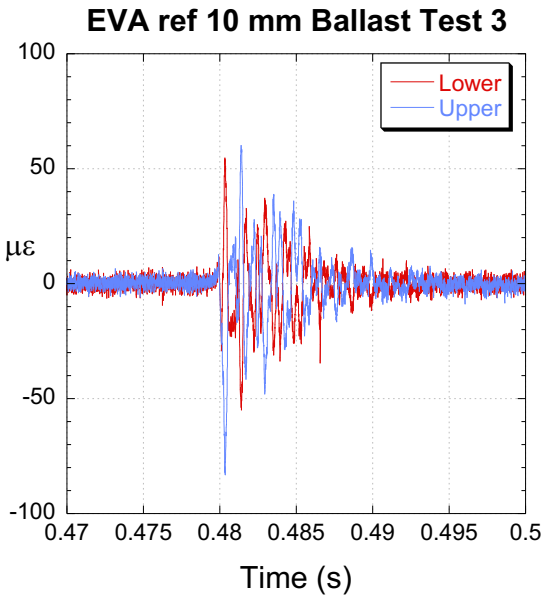

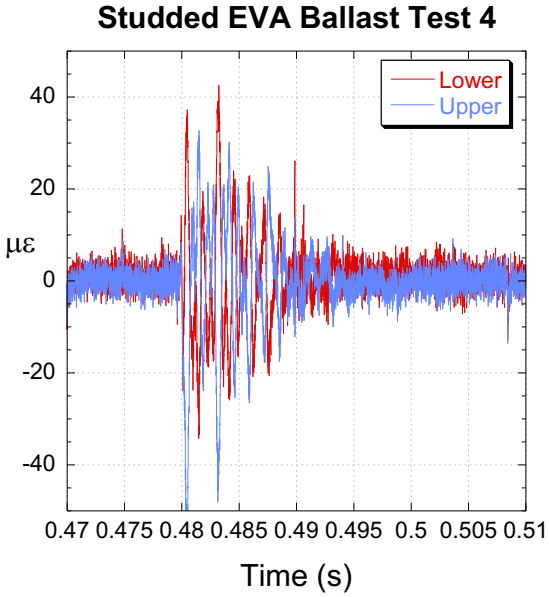

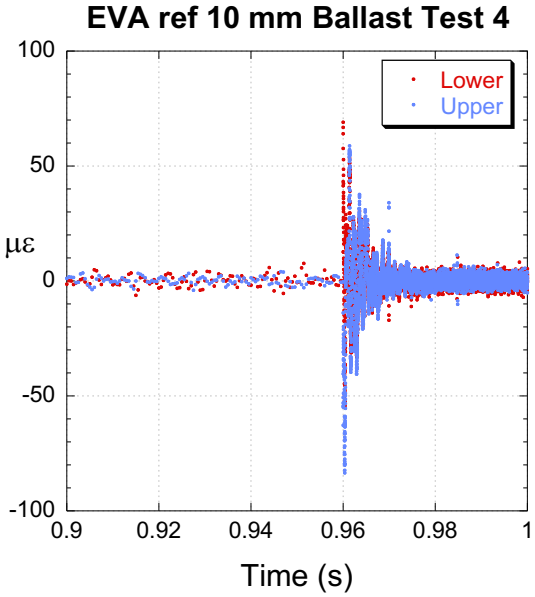

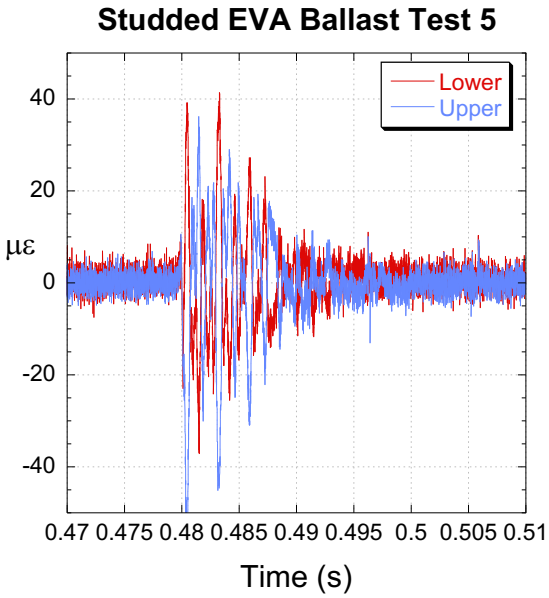

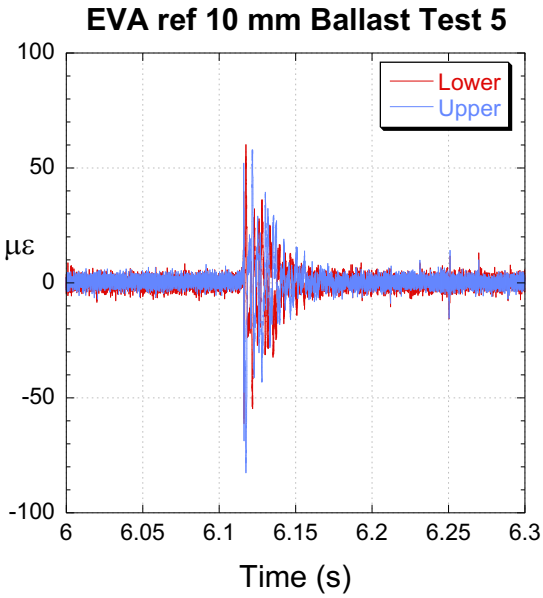

Solid reinforced rubber 11mm

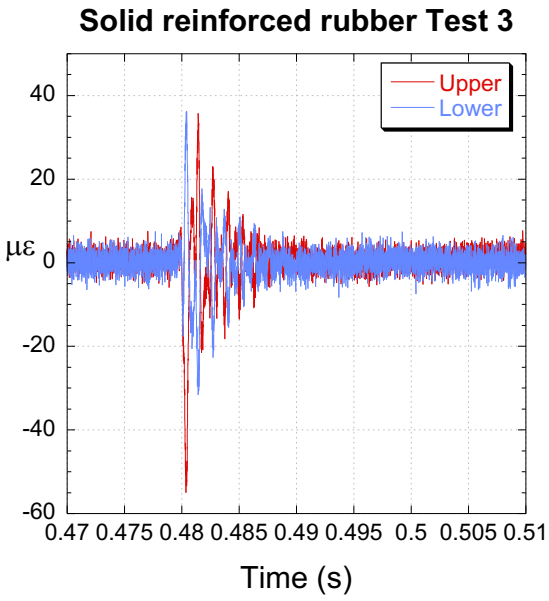

EVA ref 11 mm

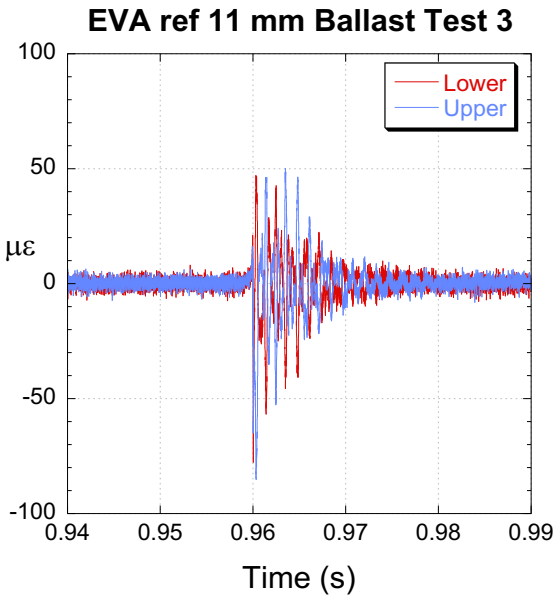

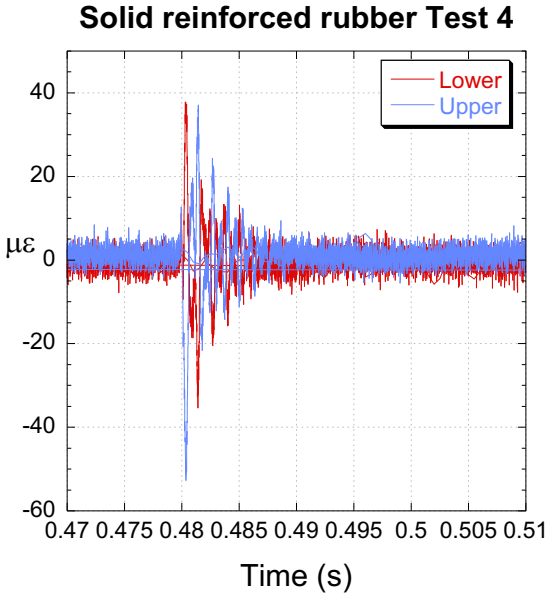

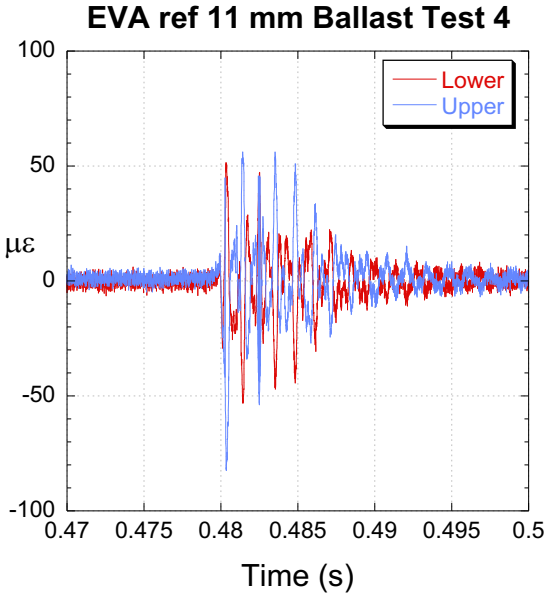

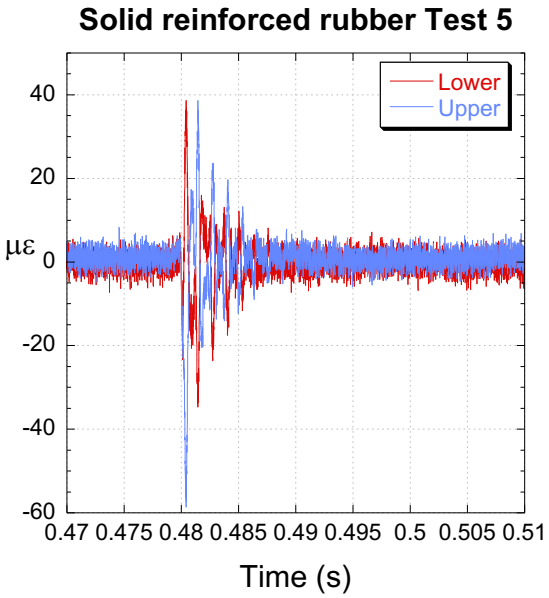

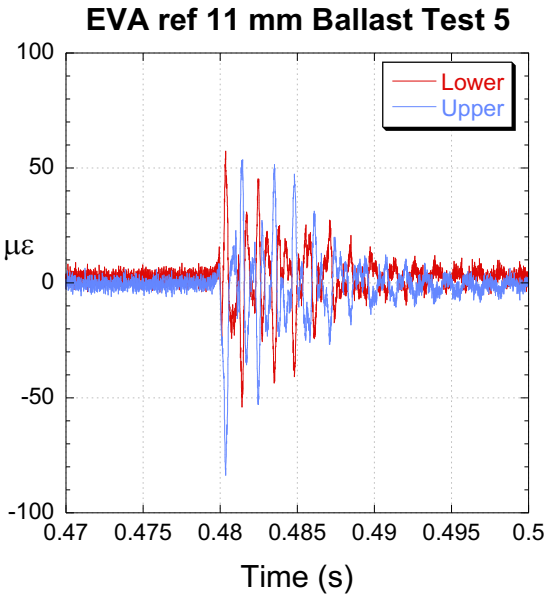

Solid EPDM 7 mm

EVA ref 7 mm

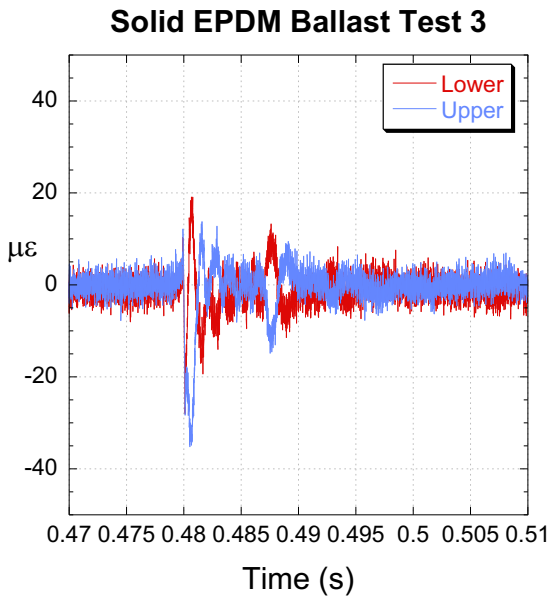

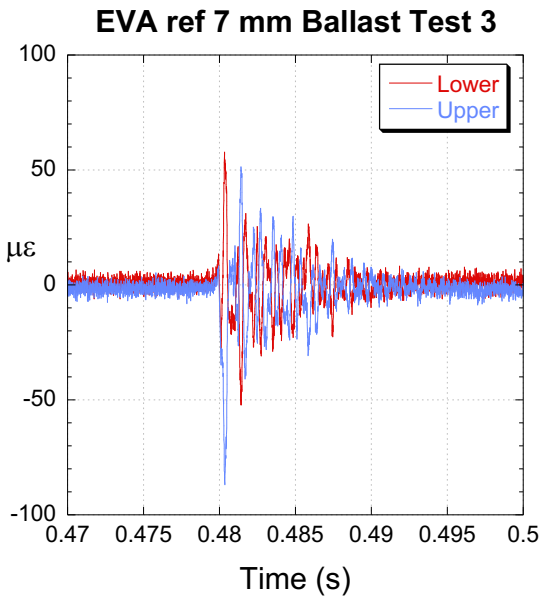

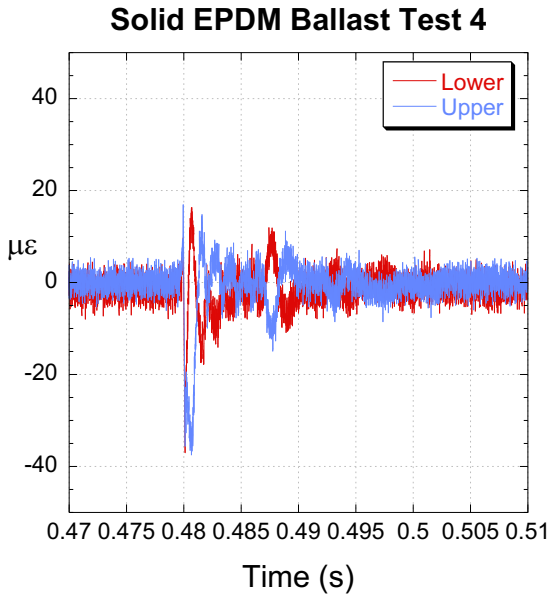

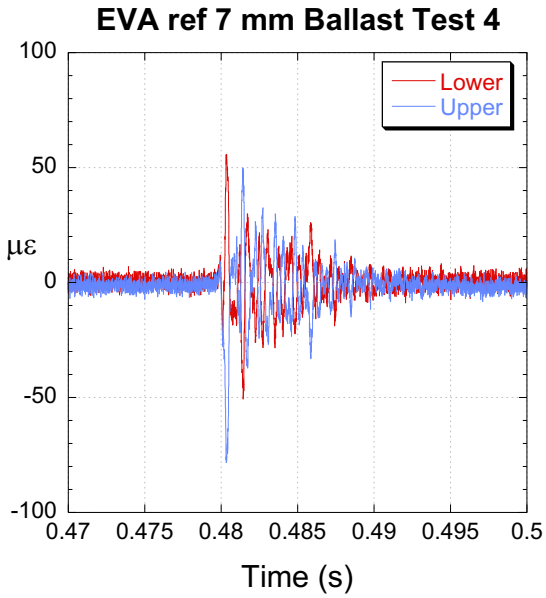

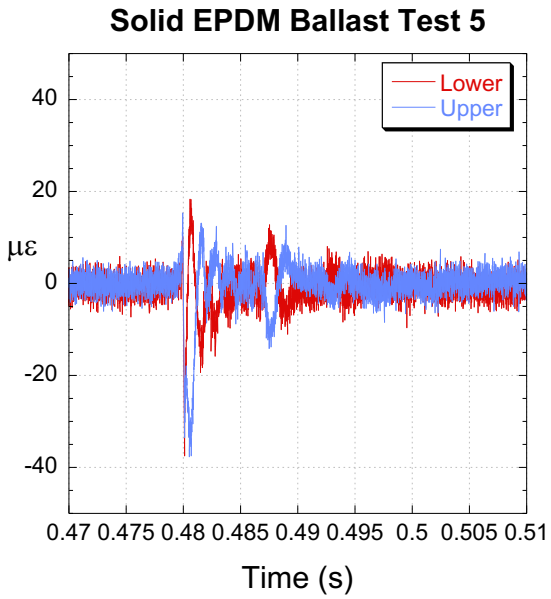

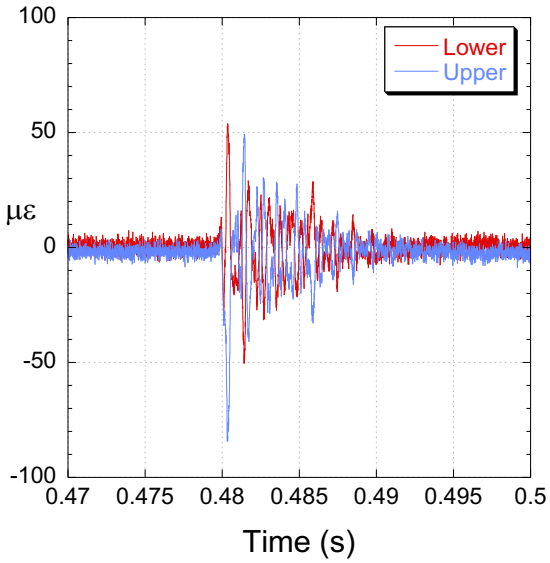

Studded TPE Ballast

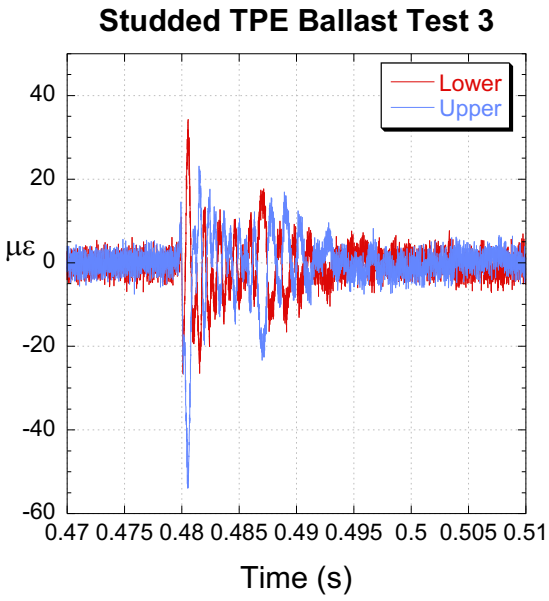

EVA ref 7 mm

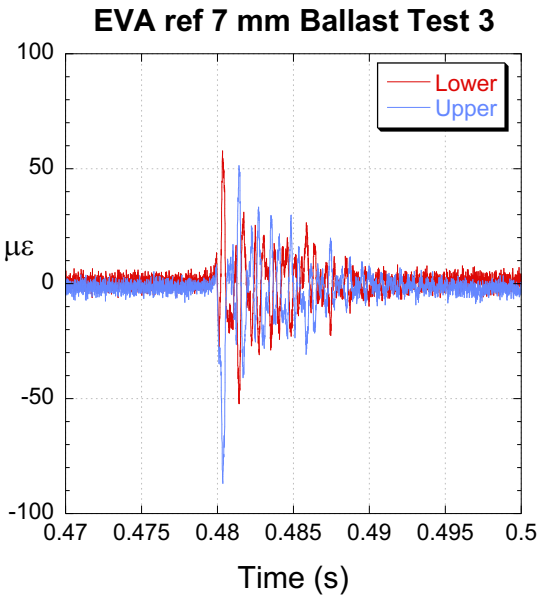

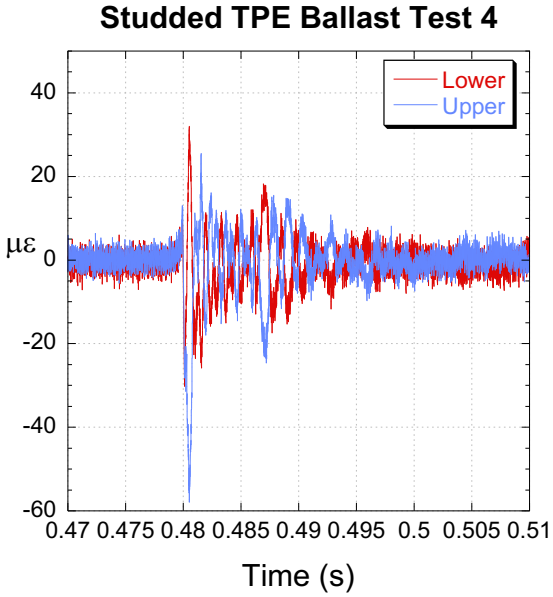

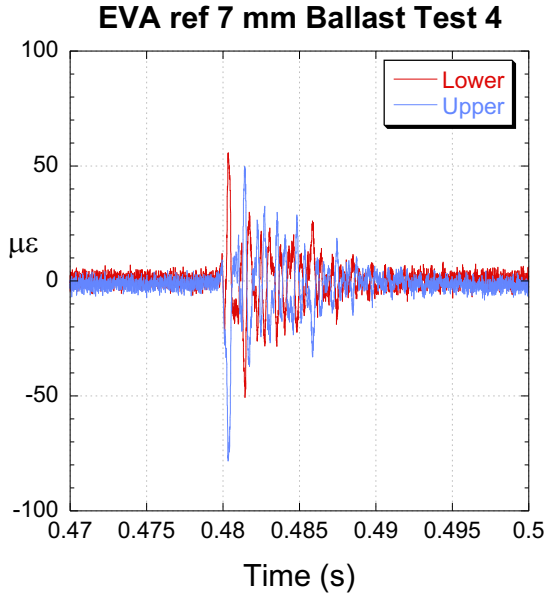

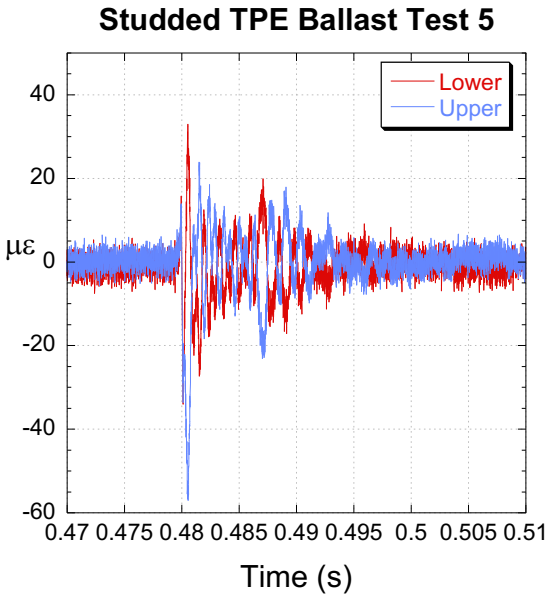

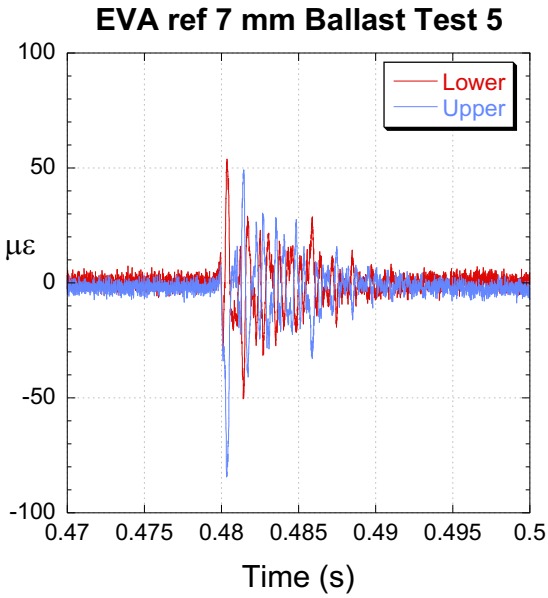

Solid NFU

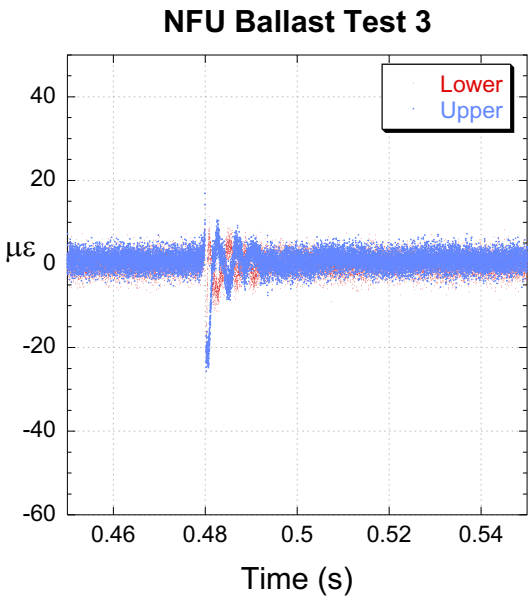

EVA ref 11 mm

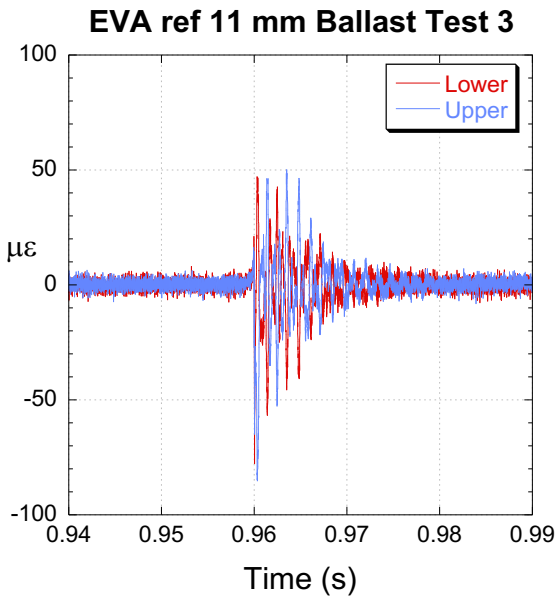

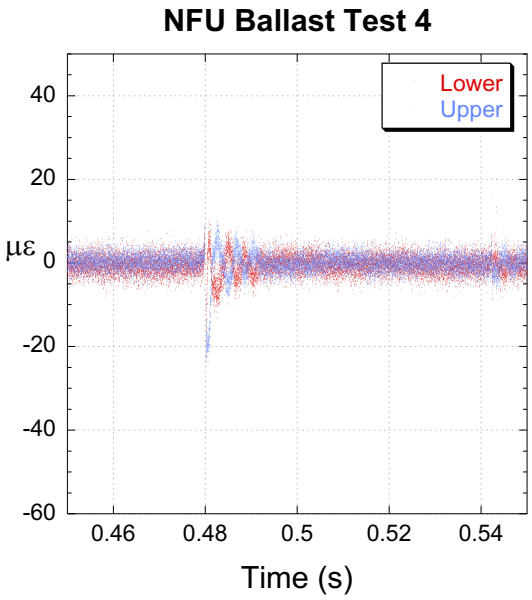

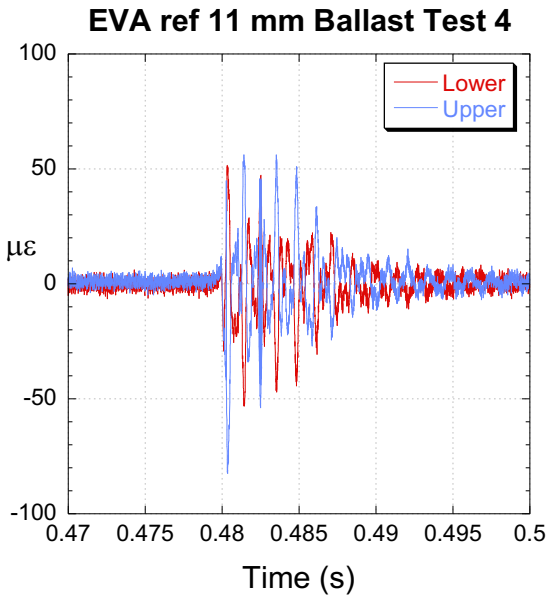

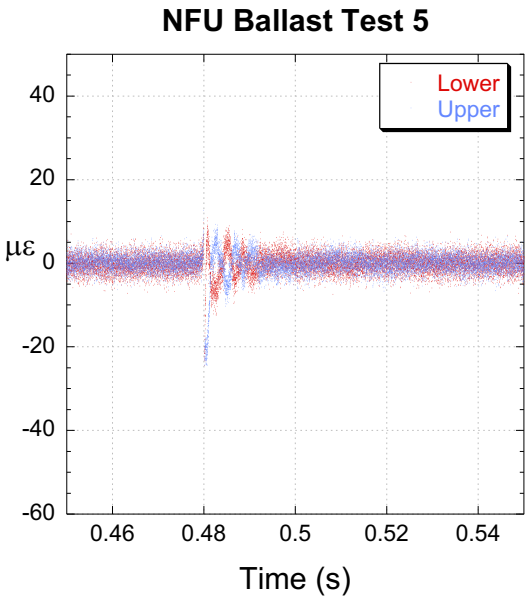

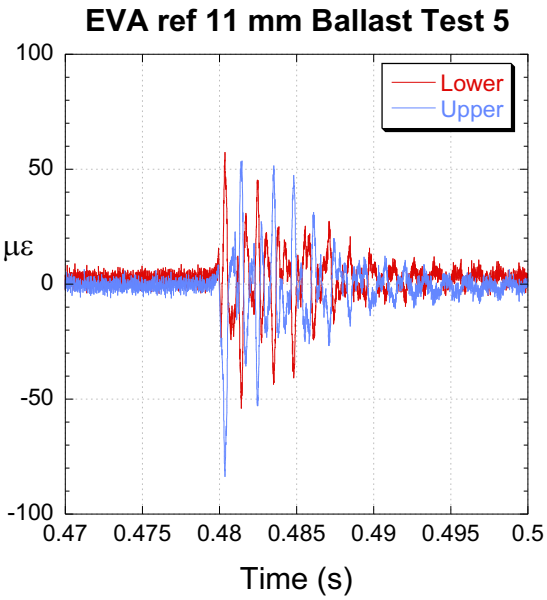

Microcellular rubber

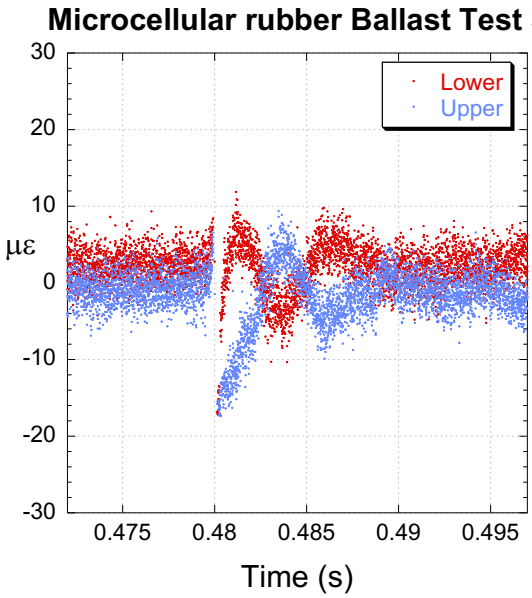

EVA ref 11 mm

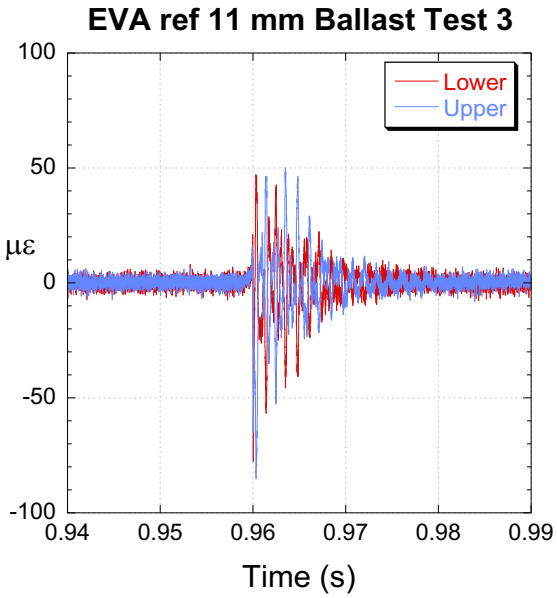

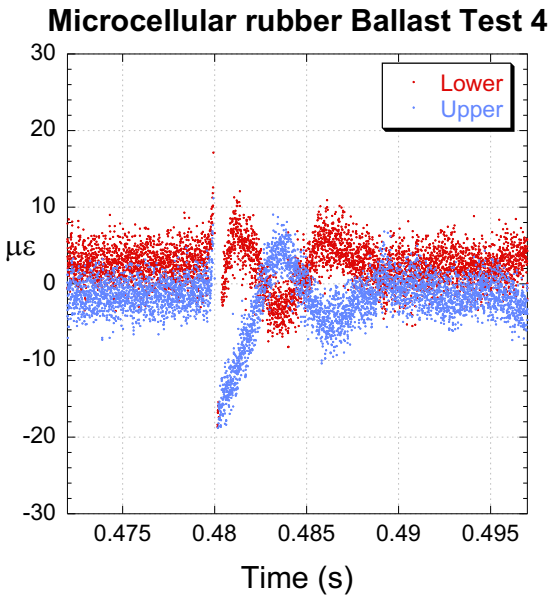

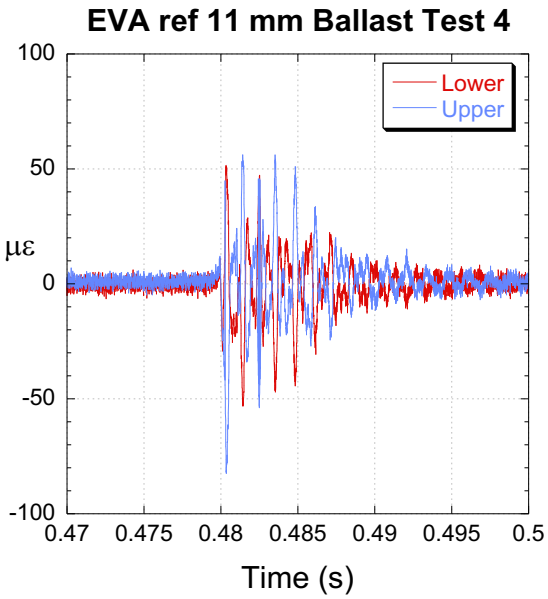

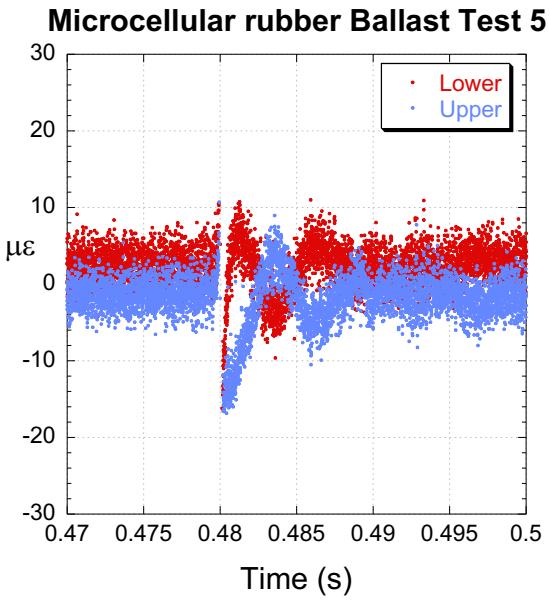

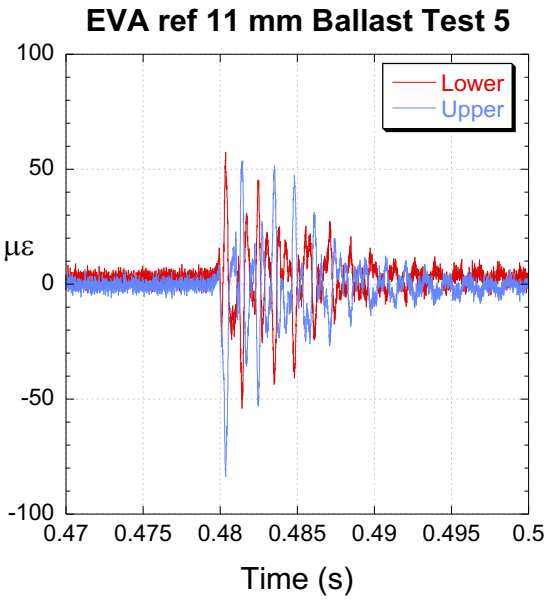

APPENDIX IV: COMPARISON BETWEEN METHODS

EXECUTION PERIOD	EXECUTED by	METHOD	Preloading Equipment	PRELOAD (kN)	ATTENUATION (%) Studded EVA (10 mm thick)	ATTENUATION (%) Studded EPDM (11 mm thick)	REMARKS
MAY - NOVEMBER 2017	LADICIM	Alternative. Spanish ET. Pendulum.	Rigid frame	50	Invalid	Invalid	Sleeper breakage
DECEMBER 2017-JANUARY 2018	LADICIM	Alternative Mass drop	Rigid frame	50	13.3	22.0	Sleeper ok
	LADICIM	Alternative Mass drop	Rigid frame	20	24.1	57.9	Sleeper ok
	LADICIM	Alternative Mass drop	Rigid frame	10	26.2	65.9	Sleeper ok
	LADICIM	Alternative Mass drop	Rigid frame with a set of springs	10	23.9	62.1	Sleeper ok
	LADICIM	Reference Mass drop	Ballast	no	34.8	71.9	Sleeper ok

SECOND SET OF TESTS						
Attenuation (%) with springs	Preload (kN)					
	50	25	10	5	0	
Microcellular rubber	3.61	41.13	68.35	70.67	69.17	
Studded EPDM	13.73	34.17	63.9	62.44	61.48	
Studded EVA	12.53	14.41	16.22	12.96	12.83	
Solid NFU	12.88	29.63	49.88			
Solid EPDM	12.65	40.99	53.08			
Studded TPE	18.92	26.34	27.66			
Solid reinforced rubber	17.06	24.59	20.07	19.53	21.7	